

The Effect of Welding Process of VIP Blocking Membrane on Its Heat Sealing Strength and Microstructure

Wang Shaogang, Chen Zhaofeng^{*}, Jin Shasha, Li Binbin, Wang Lei

College of Material Science and Technology, Nanjing University of Aeronautics and Astronautics, Nanjing, 210016, China

Abstract

Based on the blocking membrane PA/VMPET/Al/PE of vacuum insulation panel, heat sealing is carried out with different parameters including temperature, time and pressure. Combining with the test of heat sealing strength of blocking membrane, the welding parameters are optimized. Through the analysis of microstructure of films, the effect of various technology factors on heat sealing quality is investigated. Some ways are suggested to improve the heat sealing strength, which makes the blocking membrane welded well.

Keywords vacuum insulation panel; blocking membrane; welding process; heat sealing strength; microstructure.

1. Introduction

Vacuum Insulation Panel(VIP) is consisted of core material, getter and barrier, and its constituent is shown in Fig. 1. The blocking membrane is the barrier which can prevent the exchange of gas and moisture between VIP and atmosphere, and it is the key part which influences the service life of VIP[1 – 3]. The blocking membrane is usually composite films, mainly including heat sealing layer, gas resistance layer and reflection layer. In terms of the practical requirement of VIP, it also includes alkali resistance layer and surface reinforcement layer, etc. Because it is improved as greatly as possible the internal vacuum degree of VIP, the heat transfer caused by air convection can be effectively avoided, consequently, the thermal conductivity greatly decreases, and it lowers to $0.003 \text{ W}/(\text{m} \cdot \text{K})$ [4]. VIP is the most advanced material of high efficiency and heat preservation in the world, which is called super insulation material. At present, VIPs are widely used in many fields, such as aircraft, ships, refrigerator and construction, etc. It is of importance to energy-saving and emission-reduction.

During manufacturing VIP, the welding quality of blocking membrane is of importance to the property of

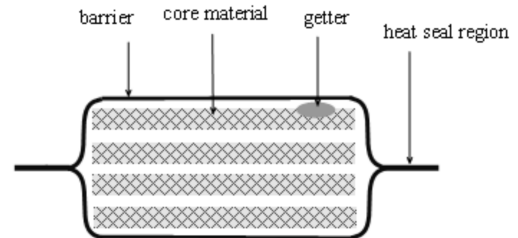


Fig. 1 Constituent of vacuum insulation panel

product. The heat sealing layer of blocking membrane is the weakest region of mechanical properties [5,6]. The weld defects such as air duct, lamination, wrinkle and degumming, etc, are easily generated in the heat sealing layer of blocking membrane. Studies show that the penetration of air and water vapor mainly occur to heat sealing layer, which results in the decrease of vacuum degree of VIP. Therefore, investigation on the welding process of blocking membrane and its interfacial microstructure, advantageous to improve the property and service life of VIP is of importance.

2. Experimental materials and procedure

The constituent of blocking membrane of VIP is successively PA/VMPET/Al/PE. The pattern of dry

^{*} Corresponding author, Tel : 86 - 25 - 5211 - 2909, E-mail: zhaofeng_chen@163.com

connection is used to bond each other, and its structure and thickness of each layer is shown in Fig. 2.

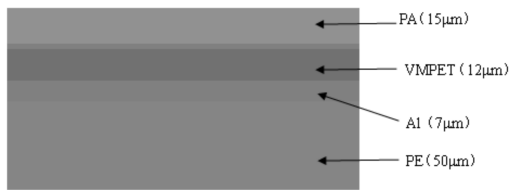


Fig. 2 Structure and thickness of each layer for blocking membrane

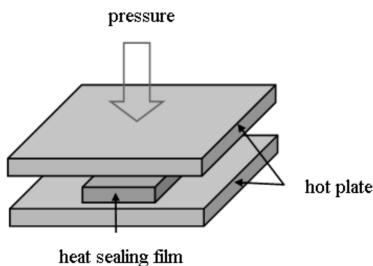


Fig. 3 Diagram of hot plate welding

The most common technology of film welding (namely heat sealing) is hot plate welding. The diagram is shown in Fig. 3. Under the action of pressure, the two layers films for welding and metal tool (hot plate or hot strip) directly contact to heat, and the surface of molten films bonds together, then cooling and solidification to form seal.

The heat sealing apparatus is used in the present work, and the heat sealing is carried out to blocking membrane with different welding parameters, including heat sealing temperature, pressure and time. In terms of standard QB/T 2358—1998, test method for heat sealing strength of plastic film packaging bag, the heat sealing strength of samples is tested, and the effect of different welding parameters on the property of blocking membrane is analyzed.

The S-4800 type cold field emission SEM is used to observe the interfacial microstructure of blocking membrane for heat sealing sample. The length of heat-affected zone (HAZ) for heat sealing region is measured by using TG (STA) Fourier transformation infrared spectrometer. The effect of various technology factors on heat sealing quality of blocking membrane is investigated, and the improving ways are also suggested.

3. Welding parameters and heat sealing strength

During the welding process of blocking membrane PA/VMPET/Al/PE, the heat sealing quality is mainly determined by the welding parameters, including heat sealing temperature, time and pressure, and the effect of temperature on heat sealing strength is the most obvious. Therefore, the heat sealing temperature is firstly determined during experiment. The differential scanning calorimetry (DSC) is used to measure the molten temperature range of PE, it is 117~122°C; the molten temperature of VMPET, 223°C; the molten temperature of PA, 254°C. The temperature of viscous fluid is 121.90°C, consequently, the heat sealing temperature can not be lower than 122°C. Because the heat sealing is practically the result of heat sealing layers melting by heating and diffusion bonding, and it needs a certain time for both of the temperature elevating and melting of heat sealing layer and the diffusion of macromolecule. According to the engineering practice, the range of heat sealing time is determined as 0.5~3.0s. Heat sealing pressure is generally limited by heat sealing apparatus, it has the variation range of 0.1~0.5MPa.

Results show that under the condition of heat sealing time 1.5s, and the heat sealing temperature 150°C, with the increase of heat sealing pressure, the heat sealing strength is lower than that of any value under the range of 160~170°C. Consequently, the heat sealing temperature should be over 150°C for the welding of PA/VMPET/Al/PE. When the heat sealing pressure is 0.1 and 0.5MPa respectively, the heat sealing strength is lower than that of any value under the heat sealing pressure 0.2, 0.3 and 0.4MPa respectively. Therefore, in order to make PA/VMPET/Al/PE bonded well, the heat sealing pressure should be in the range of 0.2~0.4MPa.

Under the condition of heat sealing pressure 0.2MPa, the welding experiment is carried out with the welding parameters of heat sealing temperature 150, 160, 170, 180 and 190°C, and heat sealing time 0.5, 1.0, 1.5, 2.0 and 2.5s respectively. Results show that when the heat sealing temperature is at the range of 150~170°C, with the increase of heat sealing time, heat sealing is completed. When the heat sealing temperature

is 180°C or 190°C, the heat sealing strength is lower than that of any value at the range of 150~170°C. This is because, with the increase of heat sealing temperature, it will result in decomposition of partial high polymer and the decrease of heat sealing strength. So the heat sealing temperature should be lower than 180°C. Under the condition of heat sealing temperature 170°C and time 1.5s, the heat sealing strength arrives to the maximum value.

Keeping the heat sealing time 1.5s, the heat sealing temperature 150, 160 and 170°C, and the heat sealing pressure 0.2, 0.3, 0.4MPa respectively are further selected to conduct technology experiment. Results show that when the range of heat sealing temperature is 150 ~ 170°C, and if the heat sealing pressure is lower than 0.3MPa, the degree of interdiffusion among PE particles increases, which results in improving heat sealing strength. While the heat sealing pressure is higher than 0.3MPa, the phenomenon of melting and extrusion occurs to PE particles, thus the thickness of heat sealing layer decreases and it leads to heterogeneity of the thickness of heat sealing layer. As a result, the heat sealing layer is damaged and the heat sealing strength decreases. Under the condition of heat sealing temperature 170°C, pressure 0.3MPa and time 1.5s, the heat sealing strength raise up to the maximum value, 57.44 N/15mm. Consequently, it is the optimized welding parameters under the experimental condition.

The heat sealing strength of blocking membrane under heat sealing pressure 0.3MPa, with different heat sealing temperature and time is given in Tab. 1.

Tab. 1 When $P=0.3\text{MPa}$, the heat sealing strength of blocking membrane with different parameters (N/15mm)

$T/^\circ\text{C}$ t/s	150	160	170	180	190
0.5	51.17	51.56	52.90	43.57	43.78
1.0	52.51	54.66	57.08	36.62	42.42
1.5	53.12	55.78	57.44	31.64	35.21
2.0	55.80	54.37	52.79	36.82	35.04
2.5	52.98	52.31	52.81	32.06	38.36

The macro-photograph of VIP with the optimized welding parameters is shown in Fig. 4. From Fig. 4, it

can be seen that the shape of heat sealing layer is good, and seal region distributes uniformly and presents smoothly, it demonstrates that the heat sealing quality is well.

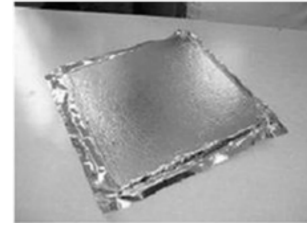


Fig. 4 Photograph of vacuum insulation panel

4 Results and discussions

4.1 Interfacial microstructure of blocking membrane

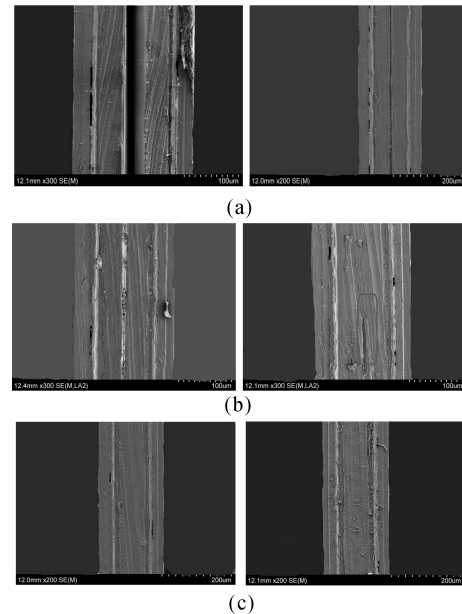


Fig. 5 Interfacial morphologies of seal region between two layers PE with different heat sealing temperature

(a)123°C, not bonded basically; (b)127°C, bonded partially
(c)150°C, bonded completely

In order to investigate further the effect of heat sealing temperature on microstructure of heat sealing region of PA/VMPET/Al/PE sample, it is necessary to observe and analyse the interfacial microstructure of heat sealing layer of blocking membrane. As mentioned above, the effective heat sealing temperature can not be lower than 122°C, so the heat sealing samples are prepared under the heat sealing temperature 123°C, 127°C and 150°C, then the SEM photographs of transverse are observed. The morphology photographs of seal interface of two layers PE with different heat

sealing temperature are shown in Fig. 5. At 123°C, there is obvious crevice between two layers PE in heat sealing region, it is not bonded basically, as shown in Fig. 5(a). At 127°C, two layers PE bonds partially, there still exists some crevice, and the boundary between two layers PE is still quite distinct, as shown in Fig. 5(b). At 150°C, two layers PE bonds completely, and no boundary can be seen, the original two layers PE have molten to form a new layer PE, as shown in Fig. 5(c). Consequently, the lower limit of heat sealing temperature is determined as 150°C, which coincides with the selection of welding parameters above.

During the welding of VIP, with the action of heat source on heat sealing layers, a certain region near the two sides of heat sealing layers whose microstructure and properties changed is named HAZ. Consequently, investigation on that if the microstructure of HAZ in heat sealing layer will be influenced by the heat sealing process, it is of great importance to improve the heat sealing quality. Taking the sample of blocking membrane with the condition of heat sealing temperature 160°C and pressure 0.3MPa, SEM is used to observe its microstructure, as shown in Fig. 6. From Fig. 6, it can be seen that the microstructure of HAZ in heat sealing layer is not changed during welding.

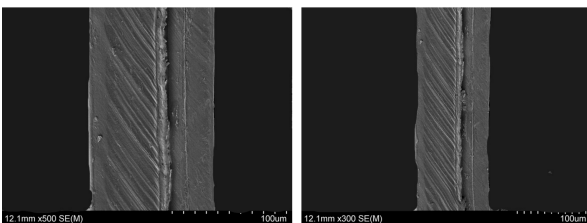


Fig. 6 Microstructure of blocking membrane

4.2 The effect of micro-defects on heat sealing quality

During the welding of blocking membrane, if the welding parameters are not properly determined, the weld defects such as inclusions, HAZ becoming wider and weld charring, etc, will be generated in heat sealing layer, and it will cause detrimental effect to heat sealing layer of blocking membrane, thus it will result in the decrease of the property of VIP.

The weld inclusion mainly indicates that residual non-metallic inclusions in weldment after heat sealing. During welding, it usually occurs to that the inclusions

such as glass fiber yarn, dust, particle, etc, remained in heat sealing layer. The existence of weld inclusion is not only to decrease the toughness of weld and cause low temperature brittlement, but also leads to the trend of hot cracking and lamellar tearing of weld. SEM photographs of weld inclusions generated by glass fiber are shown in Fig. 7.

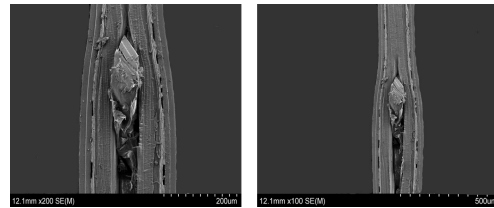


Fig. 7 Photographs of weld inclusion generated by glass fiber

The glass fiber inclusion remained in heat sealing layer will decrease the vacuum degree of VIP and the integrity of heat sealing layer, and the thermal conductivity increases. As a result, it accelerates the failure of VIP and decreases its service life. Consequently, during welding, the probability of occurrence of weld inclusion should be decreased as little as possible. Some technology ways should be taken such as keeping workshop clean, powder is added to core material, so as to decrease the elastic resilience of core material, and core material is soaked films, etc.

Moreover, in order to guarantee the heat sealing quality, the property of weld and HAZ should be simultaneously met requirements. Usually, it is expected to decrease the dimension of HAZ. During welding, the heat sealing region is comprehensively determined by various factors such as heat sealing time, pressure and temperature, etc. Therefore, the problems occurred to HAZ will become more complex, and it is the weak region of weldment. The photograph of HAZ in heat sealing layer is shown in Fig. 8. From Fig. 8, the distinct compact strip in the center is weld, and the wrinkle at both sides of weld is HAZ.

In order to measure accurately the length of HAZ in heat sealing layer, the Fourier transformation infrared spectrometer (FTIR) is used, taking the position that distance from heat sealing layer in heat seal region 0.5mm as reference point, and the FTIR spectrum of this point of internal Polyethylene (PE) in heat sealing layer is measured. The infrared spectrums of PE with

heating and without heating are shown in Fig. 9. From Fig. 9, it can be seen that, when the curve of PE in HAZ moves backward to the position of 12.9mm, the FTIR spectrum of internal PE in heat sealing layer (as shown in Fig. 9) is as the same as the standard infrared spectrum of PE. Consequently, it can be concluded that the length of HAZ in heat sealing layer is 12.9mm.

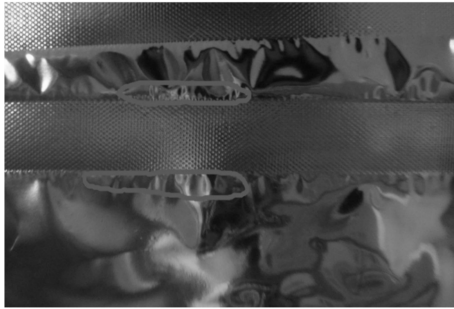


Fig. 8 HAZ in heat sealing layer of blocking membrane

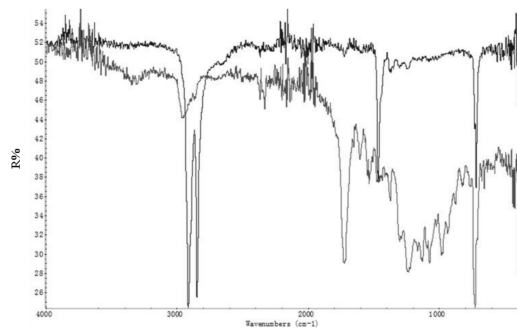


Fig. 9 The infrared spectrums of PE with heating and without heating

From the variation of the infrared spectrums of PE with heating and without heating (the blue curve represents infrared spectrums of PE without heating, and the red with heating), it can be seen that, the decomposition of internal PE occurred to heat sealing layer of blocking membrane during heating, will influence the properties of PE, such as crystallinity and barrier, etc, and thus the quality of heat sealing layer

decreased to a certain extent. Consequently, during the welding of blocking membrane, the welding parameters should be optimized, and the width of HAZ should be decreased as little as possible, so as to ensure the heat sealing quality can satisfy the practical application.

5. Conclusions and outlook

Under the condition of heat sealing temperature 170°C, time 1.5s and pressure 0.3MPa, the heat sealing strength of blocking membrane of VIP achieves maximum, and the microstructure is not changed in HAZ of blocking membrane of heat sealing layer.

The weld inclusions of glass fibers will decrease the integrity of heat sealing layer, which results in the increase of thermal conductivity of VIP, and it accelerates the failure process of VIP.

In order to obtain good welding quality for blocking membrane, the heat sealing parameters should be optimized and the weld defects should be decreased as little as possible.

Acknowledgements

The authors appreciate Suzhou VIP New Material Corp., Ltd providing with experiment apparatus and materials. For the financial support: BA2013097 from Jiangsu Project and 2015DFI53000 from National Project.

References

- [1] H. Schwab et al. *Journal of Thermal Envelope and Building Science* 28 (2005) 357 – 374.
- [2] Y. G. Wen et al. *Cryogenics* 6 (2008) 35-39. (In Chinese)
- [3] N. Zhang et al. *Vacuum* 47 (2010) 19-22. (In Chinese)
- [4] B. P. Jelle. *Energy and buildings* 43 (2011) 2549 – 2563.
- [5] S. Brunner et al. *Surface and Coatings Technology* 200 (2006) 5908 – 5914.
- [6] S. Brunner et al. *Surface and Coatings Technology* 202 (2008) 6054 – 6063.

Research on the Barrier Development of Vacuum Insulation Panels Using Thermoplastic Polyurethane Material: with Features of Good Wear and Puncture Resistance

Wang Lu^{a,b}, Chen Zhaofeng^{a*}, Cao Yun^b, Wu Jinhua^b

a. College of Material Science and Technology, Nanjing University of Aeronautics and Astronautics, Nanjing, 210016, P. R. China

b. The 55th Institute of China Electronics Technology Group, Nanjing, 211100, P. R. China

Abstract

To improve the wear resistance and puncture resistance behavior of Vacuum Insulation Panel (VIP) barrier envelopes, this research prepared Thermoplastic Polyurethanes (TPU) coating on the surface of Aluminum Foil (AF) multilayer composite membrane which was one of the present typical barrier envelopes of VIP using dry compound technology. Three-factors and three-levels orthogonal experiment on the combination technology of TPU coating was designed according to the three major control conditions, namely roll temperature, roll pressure and TPU coating thickness before the barrier envelopes and VIP samples coated with TPU were made. Results of some relevant performance tests and comparisons proved that the wear resistance and puncture resistance of those barrier envelopes coated with TPU improved significantly compared with AF at nearly no risk of degrading thermal insulation property. Additionally, MATLAB neural network was utilized for separately optimization of the wear resistance and puncture resistance performances, correspondingly achieving the most appropriate technological parameters' values. On this basis, a balance of wear resistance, puncture resistance and thermal insulation performance of those samples was reached with the help of multipurpose optimal method. It turned out that when the roll temperature, roll pressure and TPU coating thickness was 160 °C, 413 KPa and 47 μm respectively, the integrated performance of samples was the best with the minimum quality loss being 963.26 μg/cm², the maximum puncture strength of TPU coating being 12.047 MPa and the minimum thermal conductivity of TPU VIP being 1.92 mW/(m · K) correspondingly.

Keywords vacuum insulation panel, thermoplastic polyurethanes, wear resistance, puncture resistance, optimization

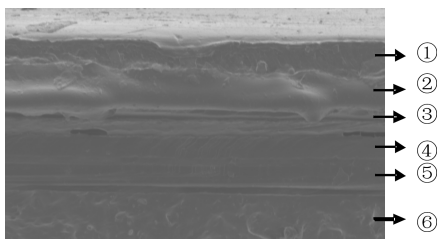


Fig. 1 Microscope image of AF envelope structure with TPU coating

- ①→Polyethylene (PE),
- ②→Aluminum Foil (Al),
- ③→Aluminum Metallized Polyethylene Terephthalate (VMPET),
- ④→Aluminum Metallized Polyethylene Terephthalate (VMPET),
- ⑤→Polyamides (PA),
- ⑥→Thermoplastic Polyurethanes (TPU)



Fig. 2 Photo of VIP coated with TPU

* Corresponding author, Tel :86 - 25 - 52112909, E-mail: zhaofeng_chen@163.com

Numerical Prediction of Thickness of Thermal Insulation Material for Different Structures

Chen Xianhui, Chen Zhaofeng^{*}, Liu Weilan

College of Material Science and Technology, Nanjing University of Aeronautics and Astronautics, Nanjing, 210016, P. R. China.

Abstract

Selection and determination of optimum thickness of insulation is of prime interest for many engineering applications. In the present paper, a finite element analysis method is applied to help to predict the required thickness of thermal insulation materials covering around the different structures made of steel at a specified heat flow and surface temperature. A circle pipe and a T branch pipe with a circle section are used in this paper. The method is based on basic fundamentals of heat transfer and reliable data. The finite element method is a simple easy way for the engineers to estimate the thickness of thermal insulation for applications.

Keywords glass wool mat, finite element analysis, heat transfer, pipe structures

1. Introduction

Energy consumption is rapidly increasing due to increasing population, urbanization, migration to large cities and improvement in standard of living. Because of the limited energy-sources and environmental pollution arising from the use of fuels, energy saving has become mandatory[1]. Thermal insulation is a key factor to increase energy efficiency of buildings because space heating and cooling of buildings take a major portion of total energy consumption[2].

As the thermal conductivity of thermal insulation materials is a function of temperature, it's hard for engineers to calculate the thickness of thermal insulation material directly in prior. Therefore, many computational tools are widely used to help the researchers and engineers to numerical estimate the thickness of thermal insulation material, or further study of mechanism of heat transfer of thermal insulation materials[3-6].

Herein, a finite element model is developed to numerically analyses the heat transfer of different structures covered by thermal insulation material. It's also used to predict the thickness of thermal insulation

material.

2. Modeling

In this section, the finite element method is used to establish the heat transfer model via Abaqus/Explicit package to numerical predict the thickness of the thermal insulation material for the structures. 3D models of circle pipe and T branch pipe are modeled in CATIA V5 R21 (Fig. 1), and then are imported to the finite element package of Abaqus for the following heat transfer modeling.

The steel pipes have same diameters as 20cm and thickness as 1 cm. The thermal insulation materials are covered or stacked closely on the outer surface of steel pipes, so that a tie constraint are applied to define the interaction properties between the steel pipe and the thermal insulation materials.

Before the heat transfer begins, the outer surface of the steel pipe is heat up to 200°C. Therefore, a predefined temperature field of 200°C is applied to the outer surface in prior. Then the initial temperature boundary of 650°C is defined to the inner surface of steel pipe of the structures, while the ambient temperature is 25°C and the radial emissivity of air is defined as 1, as

* Corresponding author, Tel: 86 - 18651860691, E-mail: zhaofeng_chen@163.com

well as the film coefficient as $10 \text{ W}/(\text{m}^{-2} \cdot \text{K})$.

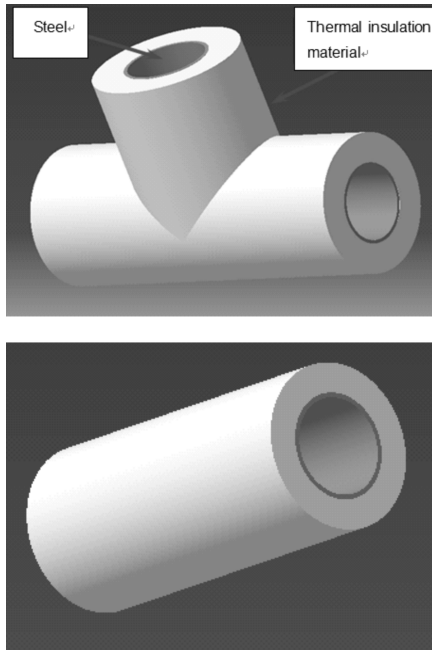


Fig. 1 3D structure models (Top : T branch pipe, bottom; circle pipe)

In this work, the glass wool mat is used as the thermal insulation material which is stacked on the outer surface of the steel pipe. The material parameters of different materials used in the modeling are listed in Tab.1 and Tab.2.

Tab. 1 Basic material parameters of steel

Material	Thermal conductivity $\text{W}/(\text{m} \cdot \text{K})$	Density kg/m^3	Specific heat $\text{J}/(\text{kg} \cdot \text{K})$
Steel	70	7800	448

Tab. 2 Thermal conductivity of glass wool mat

Temperature/ $^{\circ}\text{C}$	Thermal conductivity/ $(\text{W}/(\text{m} \cdot \text{K}))$
0	0.05187
50	0.04877
100	0.04664
200	0.04499
300	0.04642
400	0.05045
500	0.05657
600	0.06429
650	0.06859

3. Results and discussions

Based on the finite element analysis, a thickness

value of 150 mm for the circle pipe is achieved to satisfy the requirement which the outer surface temperature is less than 40°C . It can be seen from Fig. 2(a) that the temperature decreases along the radial direction, and the temperatures at different locations which have same distance from the axis of the pipe are still same to each other.

As for the T branch pipe, on the basis of the numerical prediction of circle pipe, the same thickness of glass wool mat is stacked on the outer surface of steel pipe. It is worth noting that the temperature at different locations of the outer skin of the thermal insulation materials varies.

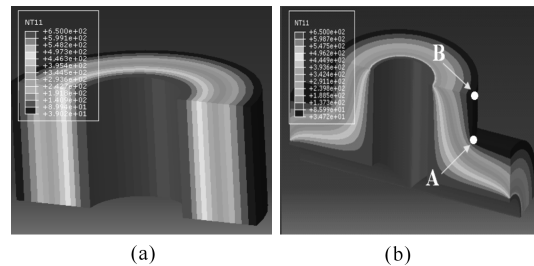


Fig. 2 Temperature distribution of the structures, circle pipe (a), T branch pipe (b)

Fig. 3 shows the variation of temperature at A and B locations (shown Fig. 2(b)) on the outer skin of thermal insulation material. It is obviously observed that the temperature at A location is higher than that at B location when the temperature comes to stable, which may because heat flux from the branches interact and strengthen at the intersection region of the T branch pipe. Thus, the thickness of thermal insulation material at the intersection region should be thicker to meet the requirement.

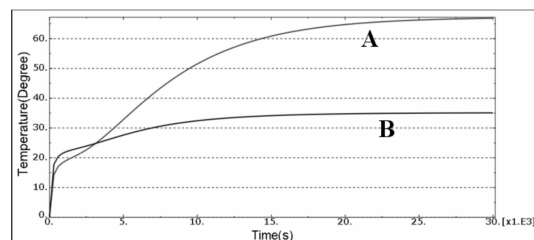


Fig. 3 Temperature vs. time curves at different location of the outer skin of T branch pipe

Therefore, finite element analysis method can be useful to numerical predict the thickness of insulation

materials applied to different structures.

4. Conclusions and outlook

In the present work, the finite element analysis method is used to predict the thickness of thermal insulation materials for different kind of pipe structures. It's shown that the FEA method is simple and useful for the engineers to predict the reliable thickness of thermal insulation materials in application in prior.

Acknowledgement

The authors would like to thanks the Jingsu Project BA2013097 and National Project 2015DFI53000.

References

- [1] Dombayci ÖA, Gölcü M, Pancar Y. Optimization of insulation thickness for external walls using different energy-sources[J]. *Appl Energy*. 2006,83:921 – 8.
- [2] Wakili Karim Ghazi. The world energy crisis—Part 2: Some more vacuum-based solutions[J]. *Vacuum*. 2008,82:679.
- [3] Coquard R, Baillis D, Grigorova V, et al. Modelling of the conductive heat transfer through nano-structured porous silica materials [J]. *Journal of Non-Crystalline Solids*, 2013, 363(3):103 – 115.
- [4] Yuan J, Sundén B. On continuum models for heat transfer in micro/nano-scale porous structures relevant for fuel cells[J]. *International Journal of Heat & Mass Transfer*, 2013, 58(1-2):441 – 456.
- [5] M Bouquerel, T Duforestel, D Baillis, et al. Heat transfer modeling in vacuum insulation panels containing nanoporous silicas—A review [J]. *Energy and Buildings*, 2012, 54: 320 – 36.
- [6] R. Coquard, D. Quénard, Modeling of heat transfert in nanoporous silica - influence of moisture, in: *Proceedings of the 8th International Vacuum Insulation Symposium, Würzburg, Germany, 2007*.
- [7] Wang J, Carson J K, North M F, et al. A new approach to modelling the effective thermal conductivity of heterogeneous materials[J]. *International Journal of Heat & Mass Transfer*, 2006, 49(17-18):3075 – 3083.

New Metallized Laminates with Al Foil-like Air Permeation

Yoash Carmi, Eddie Shufer^{*}, Liat Suari

Hanita Coatings RCA, Ltd. Hanita, 2288500, Israel

Abstract

The rate of air permeation (Permeability) through the envelope almost solely determines the degradation rate of fiberglass VIPs. It also has a critical effect on the degradation rate of fumed silica panels in building applications. In order to ensure a much slower degradation rate for both applications, a new generation of ultra high barrier laminates has recently been developed. These are based on the synergistic effect between EVOH films and advanced types of vacuum deposited Al layers. The Permeability of the new laminates at ambient were found to be as low as 1.6cc/m² year, which is 4 to 6 times lower than the best standard metallized films. The corresponding pressure increase rate for a 12mm thick panel is as low as 0.1mbar/year, similar to the annual pressure increase when Al foil laminates are used. The article describes these new films and also contains a description of several new techniques for measuring the degradation rates of panels with a large spectrum of laminates and core materials. These new techniques allow very easy, fast and accurate determination of the $\lambda - P$ curve of any core material. Using these advanced techniques the air permeation rate as function of temperature and relative humidity of many types of films was measured and the results are shown in the article. All films showed Arrhenius-like dependence of the permeability on temperature with different values for the activation energy. The results of this permeation measurement were used to create useful life-time Excel calculators that accurately predict the increasing values of the thermal conductivity of fiberglass cores installed in refrigerators. It was found that by using the new Al foil-like films, the effective thermal conductivity of installed panels can be kept below 7mW/(m • K) for more than 15 years.

Keywords vacuum insulation panels, high barrier laminates, permeability, life time calculator

1. Introduction

The thermal conductivity of typical closed cell PU foam used for refrigerator insulation is $\lambda = 18\text{mW}/(\text{m} \cdot \text{K})$, while with VIPs the thermal conductivity can be lowered to less than $2\text{mW}/(\text{m} \cdot \text{K})$. In spite of this huge performance advantage, only a small percentage of newly produced refrigerators use VIPs. The main reason is cost; PU foams are much cheaper than VIPs. The most effective way to make VIPs cheaper is to use a fiberglass (FG) core instead of the more expensive fumed silica (FS) core.

Typical FG cores have an average pore size of around 50 μ , while the average pore size of FS cores is around 0.33 μ — 150 times smaller. The thermal conductivity of cores with an average pore size of tens of microns increases quickly even at pressure lower than

1mb. In order to avoid rapid performance degradation when using FG cores, it is necessary to use envelopes that allow a very slow permeation rate of atmospheric gases into the inner space of the panels. This is why laminates with Al foils are so popular amongst Asian VIP manufacturers despite the fact that VIPs with Al foil based envelopes have very poor insulation performance due to the thermal bridge effect. In addition, Al foil based VIPs create a very high risk of condensation along the VIP edges where local thermal conductivity is extremely high due to the presence of the Al foil.

Consequently, the entire industry is moving rapidly towards using envelopes containing metallized films, or to the hybrid solution whereby bags are formed from

^{*} Corresponding author, Tel :972-525-73918, E-mail:yoash@hanitacoatings.com

two different laminates; metallized laminate on one side, and Al foil based laminate on the other side. In order to achieve the required longevity for refrigerator insulation with FG VIPs, the annual pressure increase due to air permeation should be around 0.2 mbar/year or less. Up to now, such low levels of air permeation rate were beyond the capability of standard commercially used metallized laminates.

Using EVOH films and sophisticated vacuum metallization processes, Hanita Coatings has succeeded in developing a new type of metallized laminate that meets this demanding barrier performance. These new METEVOH laminates ensure that the annual pressure increase rate of 10mm thick panels reach less than 0.2mbar/year inside the refrigerator walls.

The following paragraphs contain a description of those Al foil-like laminates, together with results of wide-reaching evaluation tests made at different temperatures and levels of relative humidity.

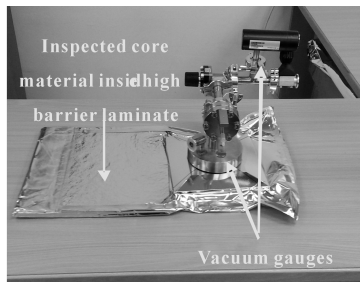


Fig. 1 Picture of the $\lambda - P$ measurement system. The flat part of the panel on the left is used for thermal conductivity measurements. The leak-tight connector on the right side of the panel allows quick and controlled changes of the internal pressure together with accurate measurement of the pressure while the thermal conductivity readings are taken

2. Accurate determination of air permeation rate

The air permeation rate through VIP envelopes can be determined by measuring the change of thermal conductivity of a FG VIP using the laminate under consideration. The accuracy of the calculated values of the internal pressure along the storage period of time is critically dependent on precise knowledge of the exact relation between the internal pressure and the thermal conductivity of the FG core used-known as the $\lambda - P$ curve.

Recently, Hanita managed to develop a very fast and easy-to-operate technique for producing very accurate $\lambda - P$ curves of any known core materials. A picture of the $\lambda - P$ device can be seen in Fig. 1. The idea is very simple: a leak-tight connector is mounted on the right side of the panel while the left side of the panel is kept flat for hot plate thermal conductivity measurements. The connector on the right allows a deliberate change of internal pressure by letting in a small dose of air, and also accurately measures the internal pressure level while the hot plate device takes thermal conductivity readings. It takes about 24 hours to plot the entire $\lambda - P$ curve of a core. Fig. 2 and Fig. 3 show the curves of several FG and FS cores measured this way. It can be seen that each of the curves can be described very accurately by the function[1].

$$\lambda(P) = \lambda_0 + \frac{25.5}{1 + \frac{P_{1/2}}{P}}$$

which describes the relation between the thermal conductivity of gases trapped in porous media and the pressure. 25.5mW/(m · K) is the thermal conductivity of free air. It can be seen that any of the curves can be characterized by two parameters: λ_0 is the contribution of the heat conducted by the fibers (powder) plus the IR radiation contribution; $P_{1/2}$ is pressure (in mbars) where the contribution of the gas to λ equals 12.75mW/(m · K) (half of the thermal conductivity of free air). Comparison between the curves of the different core types clearly shows that cores with larger $P_{1/2}$ value ensure improved longevity for the panels. When FG cores are used it is always highly advantageous to choose cores with the highest possible $P_{1/2}$ in order to achieve a longer life time for the panel.

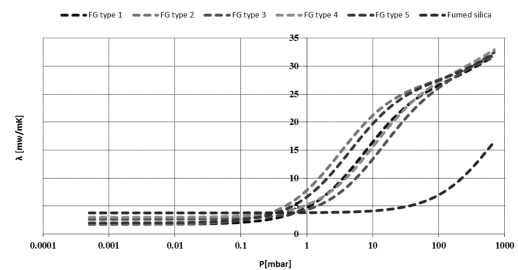


Fig. 2 $\lambda - P$ curves of five FG and a FS core created with the system shown in Fig. 1— Logarithmic pressure scale

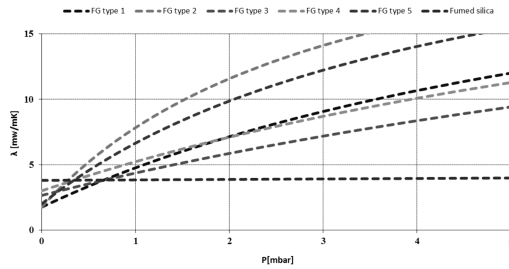


Fig. 3 The graph of Fig. 2 is drawn with a linear pressure scale. Using linear scale emphasizes the big effect of the value of $P_{1/2}$ on the degradation rate of the different types of core materials

Tab. 1 Summary of the values of $P_{1/2}$ and λ_0 related to the different core materials presented in Fig. 2 and Fig. 3

Core	$\lambda_0 / (\text{mW}/\text{m} \cdot \text{K})$	$P_{1/2} / \text{mbar}$
FG type 1	1.75	7.5
FG type 2	1.75	3.2
FG type 3	2.65	14
FG type 4	3	10.5
FG type 5	2	4.5
Fumed silica	3.8	700

Definition of Permeability

Permeability is a useful unit for characterizing the air permeation rate through a laminate. It is defined as the amount of air (cm^3) permeating through the entire envelope of a $1\text{m} \times 1\text{m}$ panel in a year ($\text{cc}/\text{m}^2 \text{ year}$). Knowing the Permeability of a laminate makes it very easy to calculate the annual pressure increase inside a panel (in mbar) independent of its surface area. The annual pressure increase rate (mbar) due to air permeation equals the Permeability of the envelope divided by the panel thickness in mm. For example, the annual pressure increase of a 10mm thick panel with an envelope having Permeability of $2\text{cc}/\text{m}^2 \text{ year}$ is equal to 0.2mbar/year.

3. Test results: Metallized EVOH films allow Permeability at ambient similar to Al foils

The best known metallized laminates based on metallized PET films have a permeability level of around $6\text{cc}/\text{m}^2 \text{ day}$. In order to reach this low level of permeability, it is necessary to laminate at least 3

PETMET films. These films have extremely low MVTR levels. With standard laminates based on metallized EVOH film, Permeability levels of $3\text{cc}/\text{m}^2 \text{ year}$ to $4\text{cc}/\text{m}^2 \text{ year}$ can be reached at ambient, but these films are very sensitive to higher humidity levels and elevated temperatures. The Permeability and the MVTR levels of these films show a very strong dependence on either temperature or humidity levels.

Over the past year, Hanita has managed to develop advanced vacuum metallization processes specially adjusted to EVOH films, resulting in improved Permeability and much lower sensitivity to elevated temperatures and exposure to humidity. These new high barrier laminates contain one metallized PET film in addition to the metallized EVOH film and 50μ thick PE seal layer (36μ PETMET / 12μ METEVOH / 50μ PE).

The Permeability of these new METEVOH laminates at ambient was measured to be lower than $2\text{cc}/\text{m}^2 \text{ year}$, with a much lower MVTR level and lower sensitivity to elevated temperatures than standard existing METEVOH laminates. Taking into account that the Permeability measured also included the contribution from the side air permeation through the seals, it is not hard to show that the Permeability due to skin air permeation was about $1\text{cc}/\text{m}^2 \text{ year}$ or smaller. Knowing the Permeability of these newly developed METEVOH laminates, it would be quite easy to calculate how the thermal conductivity of FG panel with this laminate will increase along their service life inside refrigerator walls. For this purpose, Hanita developed the already well known, Excel based tool, Life Time Calculator (LTC).

Fig. 4 presents the evolution of the calculated effective thermal conductivity (including thermal bridge) of a 11mm thick FG panel having $P_{1/2} = 7$ mbar and $\lambda_0 = 2\text{mW}/(\text{m} \cdot \text{K})$. The calculations were performed for a hybrid envelope - METEVOH laminate on one side, and Al foil based laminate on the other side of the bag. The graph in Fig. 4 reveals excellent performance of such panels along the entire life time of the refrigerator. The effective thermal conductivity stays below $6\text{mW}/(\text{m} \cdot \text{K})$, even when the refrigerators reach the age of 10 years.

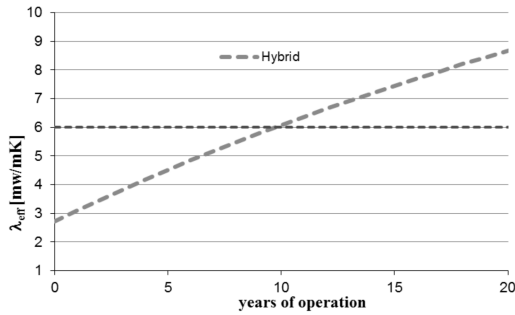


Fig. 4 The effective thermal conductivity of 11mm thick panel as function of the refrigerator life time as calculated by the Life Time Calculator. Hybrid envelope with one side new METEVOH laminate and Al foil laminate on the other side. FG with $P_{1/2} = 7\text{mbar}$ and $\lambda_0 = 2\text{mW}/(\text{m} \cdot \text{K})$

4. The dependence of permeability on temperature

The dependence of the air Permeability of high barrier laminates on temperature can be very different from one laminate to another. To verify this assumption, we ran comprehensive comparison tests between many types of VIP envelopes. In these tests, FG panels with the different envelopes were stored at different temperatures long enough to reach a steady state situation (constant pressure increase rate). Thermal conductivity measurements were taken every few weeks along the storage period of time. The steady state permeability levels were calculated then using the previously measured $\lambda - P$ curve of the FG core used.

Tab. 2 summarizes the results of this large comparison test. In Fig. 5 below, the same results are presented graphically, fitted to Arrhenius-like functions. The constant A represents the Permeability at very high temperatures, and E_a is a fitting parameter resembling the role of activation energy. Because of the complexity of the systems (many layers of different films, adhesive layers and Al layers) the actual physical meaning of the E_a constants is not clear.

At all temperatures, the relative humidity was at ambient level (other than at $T = 50^\circ\text{C}$, where the relative humidity was 70%). It can easily be seen that the standard METEVOH laminates have stronger dependence on temperature compared to the PETMET laminates. The new METEVOH laminates developed

by Hanita have very low Permeability at ambient, together with a relatively moderate effect of elevated temperatures. As a result their Permeability levels stayed relatively low even at quite extreme high temperatures.

It is important to note that data collected in such tests can be very useful when there is a need to convert the degradation rate measured in accelerated ageing tests to the actual degradation rate during the service life where the panels can be exposed to very different environmental conditions

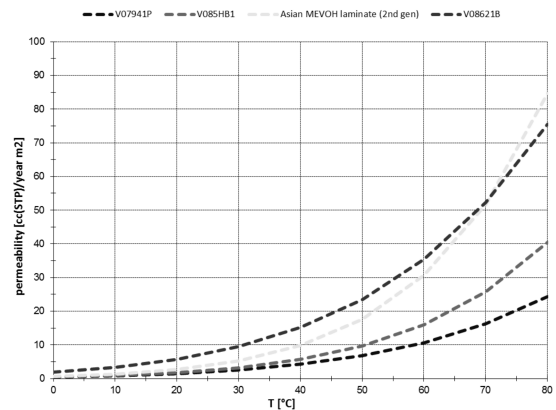


Fig. 5 Plot of the steady state Permeability of several types of laminates as a function of the storage temperature. The continuous lines represent best fitting of the data points to Arrhenius-like functions $P(T) = A \exp\left(\frac{E_a}{RT}\right)$

Tab. 2 Summary of the values of the A and the E_a best fitted constant related to the different laminates shown in Fig. 5

Laminate	E_a	A
V07941P (Al foil laminate)	4.0E+04	2.4E+07
V085HB1-New METEVOH laminate	4.5E+04	2.1E+08
Asian METVOH laminate (2nd gen)	5.0E+04	1.9E+09
V08621B (PETMET tri-laminate)	3.7E+04	2.2E+07

5. The importance of reaching steady state conditions

In the early life time of any VIP, the pressure increase rate is determined by two mechanisms of supplying air molecules into the evacuated internal volume of the panels. The first mechanism is air permeation through the skin and seals of the envelope. The second mechanism is outgassing of air molecules

released from the laminate into the evacuated space. The source of this outgassing mechanism is probably air molecules trapped during the lamination processes between the films making up the laminates. After evacuating the panels, these trapped air molecules diffuse into the evacuated space until a steady state concentration gradient of air molecules is reached between the 1000 mbar pressure facing the external surface of the laminates and the very low pressure on the internal surface facing the evacuated internal space (the PE seal layer). At ambient temperature, this outgassing process may take more than 100 days before its effect on the increase rate of the internal pressure becomes negligible. At elevated temperatures, the process of air molecule outgassing is accelerated and the time required for the outgassing to stop can be reduced to about 60 days.

It is extremely important to realize that this short term outgassing phenomenon has no effect whatsoever on the long term (years) degradation rate of the panels. The steady state permeation rate of the air is the only parameter that counts. An example showing the effect of the air outgassing mechanism is shown in Fig. 6. The graph describes how $\Delta\lambda$ of the panels with the same FG core material and two different envelopes increases in the first 30 days at ambient. It can be seen that after 30 days $\Delta\lambda=0.237\text{mW}/(\text{m}\cdot\text{K})$ for laminate 1, while for laminate 2, $\Delta\lambda=0.18\text{mW}/(\text{m}\cdot\text{K})$. Relying solely on the values of $\Delta\lambda$ after 30 days would lead to the conclusion that laminate 2 seems to ensure better longevity to the panels over laminate 1. The picture looks different when examining the pressure increase rate after steady state is reached. It can be seen in Fig. 7 that the steady state pressure increase rate (dP/dt) is actually smaller for laminate 1 than for laminate 2. This means that laminate 1 will ensure slower degradation than laminate 2, even though its $\Delta\lambda$ after 30 days was larger than that of laminate 2. The calculated steady state Permeability levels also reveal the superiority of laminate 1 over laminate 2. The Permeability of laminate 1 was measured to be $1.64\text{cc}/\text{m}^2/\text{year}$ while that of laminate 2 was $3.54\text{cc}/\text{m}^2/\text{day}$.

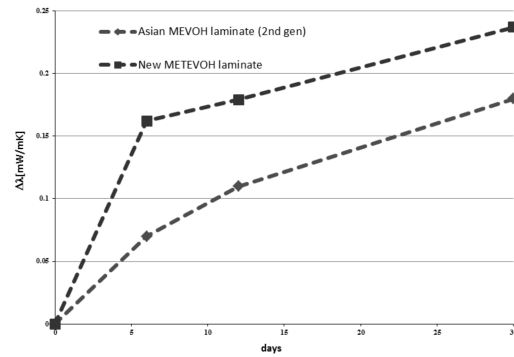


Fig. 6 The change of the thermal conductivity of two FG panels along storage time duration at ambient. $\Delta\lambda(30\text{days})=2.37\text{mW}/(\text{m}\cdot\text{K})$ for laminate 1. $\Delta\lambda(30\text{days})=1.8\text{mW}/(\text{m}\cdot\text{K})$ for laminate 2

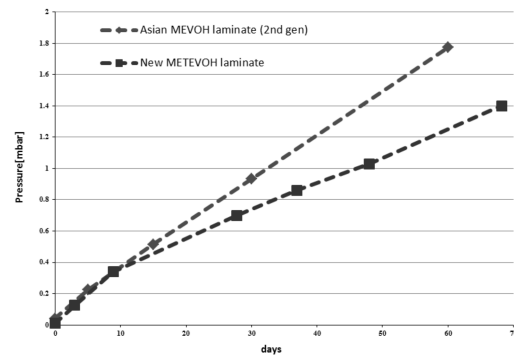


Fig. 7 The internal pressure of 2 FG panels with two different laminates as function of storage time at ambient. The steady state pressure increase rate of Laminate 1 is smaller (Permeability = $1.64\text{cc}/\text{m}^2/\text{day}$) compared to laminate 2 (Permeability = $3.54\text{cc}/\text{m}^2/\text{day}$) ensuring better longevity

6. Conclusions

(1) The new generation of METEVOH laminates reported in the article opens a new horizon to the refrigeration industry by extending the lifetime of fiberglass VIPs to more than 15 years with minimal thermal bridge effect and λ_{eff} lower than $6\text{mW}/(\text{m}\cdot\text{K})$.

(2) The air permeation rate through any type of envelope, at any atmospheric conditions, can be determined very accurately by measuring the evolution of the thermal conductivity of glass fiber VIPs with previously measured $\lambda - P$ curve. By determining the Permeability level at different temperatures, it is

possible to achieve a very accurate conversion factor between the Permeability measured at accelerating conditions to the actual conditions along the service life of the VIPs. The key factor for getting precise Permeability values is to establish very accurately the relationship between the internal pressure and the thermal conductivity of the fiberglass core used in the tests. An easy-to-operate technique for producing such $\lambda - P$ curve was also described in the article.

(3) It was shown that the short accelerating tests conducted by the VIP industry for evaluating the barrier performance of high barrier laminates can lead to very wrong conclusions. The values of $\Delta\lambda$ after just a few weeks in accelerating tests are highly affected by air

outgassing from the laminates. These out gassing processes stop after 20 to 70 days (at elevated storage temperatures steady state is reached faster than at ambient conditions) and only then the increase rate of λ reaches the real steady state value. The steady state value of the air permeation is what determines the degradation rate of fiber glass panels along their service life; therefore, the VIP industry should adopt this criterion when evaluating new laminates instead of the sometimes misleading criterion of $\Delta\lambda$ after a few weeks' storage at accelerating conditions.

References

- [1] Kaganer MG. Thermal Insulation in cryogenic engineering, Israel program for scientific translations, Jerusalem, 1969

A Study on Measuring Gas Permeability of Barriers by Using Mass Spectrometry Apparatus

Hong Zhifa^{*}, Liu Qiang

Fujian Supertech Advanced Material Co., Ltd., 13F. ChuangXin Building, No. 1300, Jimei Avenue, Xiamen, 361000, P. R. China

Abstract

In this article, the apparatus and testing methods of mass spectrometer which was applied for measuring film permeability are introduced. This method applies helium mass spectrometry to measure the helium gas permeability of barrier material, and also applies helium mass spectrometry and gravimetric analysis to calibrate the feedback from quadruple mass spectrometer. From the results, He, O₂, N₂, CO₂, and water vapor permeability for both single film and laminated film were measured. The experiments showed that this apparatus was capable to measure various gas permeability and water vapour permeability of the barrier material, and further expand the lower testing limit of the recent technique. This article also discusses the problems and corrective methods with regards to this mass spectrometry apparatus.

Keywords Barrier, gas permeability, quadruple mass spectrometer, helium mass spectrometer

^{*} Corresponding author, Tel : 86 - 15959344709, E-mail: hongzhifa0@163.com

Plastic Barrier Film Development with Ethylene Vinyl-alcohol (EVOH) Film and New Film for Warm Applications

Masakazu Nakaya *

EVAL R&D Department, EVAL Division, Vinyl Acetate Resin Company, Kuraray Co., Ltd.,
7471 Tamashimaotoshima, Kurashiki, Okayama, 713-8103, Japan

Abstract

Ethylene vinyl-alcohol copolymer (EVOH) is a thermoplastic crystalline polymer with many unique properties. It is well known as a barrier plastic, widely used in many applications such as food, medical, agricultural or automotive areas. Vacuum insulation panel (VIP) is a difficult application for us, which requires high barrier properties to maintain vacuum inside for years. In order to meet this requirement, a vapor metalized biaxially oriented EVOH film (VM-EVOH) had been developed and commercialized by Kuraray under the trade name of EVAL™ Film VM-XL. Unlike other barrier films, it has a “dual” barrier structure which consists of a VM barrier layer on an EVOH substrate with high barrier and resistance. Thanks to the excellent and reliable barrier performance, VM-EVOH has been employed as one of the major barrier materials in VIP envelopes.

Recently, KURARAY is responding to increasing inquiries for plastic barrier films which can work in a VIP exposed under severer conditions, e. g. high temperature and high humidity, in comparison with existing applications like insulation for refrigerators. This paper, presents a study on the barrier properties of different envelope structures under a variety of conditions in order to discuss diffusion characteristics. Our newly developed barrier films are included in this study.

Keywords vapor, metalized, biaxially, oriented, ethylene, vinyl-alcohol, copolymer film (VM-EVOH)

1. Introduction

EVOH is a thermoplastic crystalline polymer with many unique properties. In VIP application, as it requires high barrier properties to maintain vacuum inside for years, VM-EVOH has been employed as one of the major barrier materials in VIP envelopes mainly under cold environment. VIP for refrigerator is one of major application. Besides, kuraray is recently responding to increasing inquiries for plastic barrier films which can work in a VIP exposed higher temperature and higher humidity. As a material diffusion rate becomes generally faster in higher temperature, it is reasonable that market needs for higher barrier film is increasing. Kuraray is developing higher barrier plastic film for VIP envelope with the following two approaches.

(a) Higher barrier film for “less main surface permeation”

(b) EVOH sealant film for “less side permeation” through edge

With regards to “less main surface permeation”, because barrier properties of high barrier film had been studied mainly in ambient conditions, the barrier properties of different structures under a variety of conditions have been studied in order to characterize diffusion properties.

With regards to “less side permeation”, it has already been reported the potential benefits of EVOH in sealant layer for extending service life [1]. In order to proof this concept, evaluation as VIP for thermal conductivity has been investigated.

* Corresponding author, Tel : 81 - 8029169113, E-mail: masakazu_nakaya@kuraray.co.jp

2. Higher Barrier Film for “Less Main Surface Permeation”

For the purpose of evaluating barrier performance with several conditions, two VIP envelopes available from a commercial supplier have been evaluated with the following procedure.

2.1 Samples

Multilayer structure of each sample is shown below. In addition to measuring barrier as they are, the post-abuse treatment samples were prepared for barrier measurement in order to evaluate durability of VIP envelope. It is believed that the durability is one of important performance to predict actual performance of VIP envelope because VIP envelope is used as vacuum packaging and it has potential risk of damage, especially at the edge or corner. Gelbo-flex testing is employed as our standard test method.

#1: PET-VM (12 μ m)//VM-PET (12 μ m)//VM-EVOH (15 μ m)//PE (50 μ m)

#2: PET-VM (12 μ m)//VM-PET (12 μ m)//VM-PET (12 μ m)//PE (50 μ m)

2.2 Test item

• Gelbo-flex testing (ASTM 392F) with three cycles under 23°C 50% RH

• Oxygen Transmission Rate (OTR) is measured by OX-TRAN 2/21 or $2/21 \times 10$ (MOCON, Inc.) (ISO14663-2). In the measurement, PE layer is always faced toward 0%RH atmosphere.

• Water Vapor Transmission Rate (WVTR) by gravimetric measurement (Kuraray test method (* 1)).

(* 1) Four-side seal pouches were prepared using the VIP envelope. Calcium chloride (desiccant) was filled and sealed. The sample was stored under certain condition in environmental chamber to measure gravimetric change for WVTR.

2.3 Results and Discussions

Tab. 1 shows OTR results measured at 40°C-0/50%RH and 40°C-0/90%RH. All samples using #1 show better barrier than #2 in all conditions. Durability of each sample is compared by calculating how much oxygen permeability is increased as a result of gelbo-flex testing (Presented as OTR (Gelbo x3)/OTR (No gelbo) in Tab. 1). It is indicated #1 had better durability in this evaluation. It is understood that a “dual” barrier structure in VM-EVOH shows high barrier and resistance as expected.

Tab. 1 OTR Performance of Commercial Plastic Barrier Envelopes

Sample	OTR/(cc/m ² · day · atm)					
	40°C C - 0/50%RH			40°C C - 0/90%RH		
	No gelbo(1)	Gelbo×3(2)	(2)(1)	No gelbo(1)	Gelbo×3(2)	(2)(1)
#1	0.0010	0.0250	25.000	0.0009	0.0443	49.222
#2	n/a	n/a	n/a	0.0067	0.9350	139.55

Fig. 1 shows WVTR results with different temperature (40°C, 50°C, 60°C and 80°C) under fixed relative humidity (0/90%RH). Sample #1 and #2 show very similar characteristics and there is little difference for WVTR property, which indicates WVTR performance primarily depends on VM layers.

A temperature dependence of permeation is represented by Arrhenius equation.

$$P = P_0 e^{-E/RT} \quad (1)$$

where

P = Permeation rate,

P_0 = Permeability constant,

E = Activation energy,

R = Gas constant,

T = Temperature.

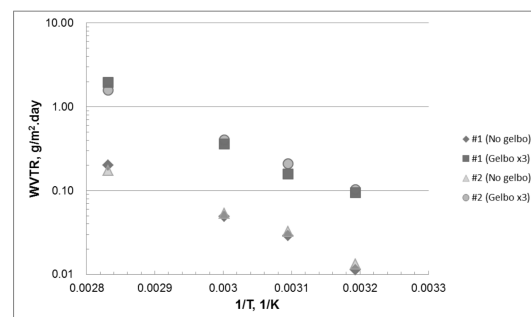


Fig. 1 Arrhenius plot of WVTR at 0/90%RH

Fitted curve of each result for equation (1) is calculated. The results are shown in Tab. 2.

Tab. 2 P_0 and E/R of Each Sample

Sample	P_0	E/R
#1	No gelbo	7.24×10^8
	Gelbo x3	5.90×10^{10}
#2	No gelbo	6.58×10^7
	Gelbo x3	3.17×10^9

Each result follows Arrhenius equation, which means barrier performance could be estimated at least, in this temperature range.

In Fig. 2, WVTR results at 50°C with different humidity are shown. Relative barrier performance of each sample is the same in all conditions evaluated.

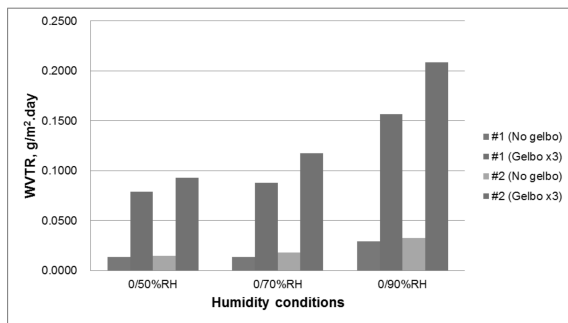


Fig. 2 WVTR at 50°C with different humidity

These results indicate a VIP envelope with favorable gas and moisture barrier property could be designed by combining VM-EVOH with other barrier films like VM-PET appropriately.

However, some potential applications require higher barrier properties which may need new barrier technologies. New barrier technologies are under study based on the material design for low permeation as well as good durability.

3. EVOH Sealant Film for “Less Side Permeation” Through Edge

As reported in [1], EVOH in sealant layer could potentially provide extending service life because of “less side permeation”. Experimental VIPs using EVOH or PE in sealant layer were prepared to observe thermal conductivity change over time.

3.1 Samples and test item

The VIP envelope structures are shown below:

#3: PET (12 μ m)//ON (15 μ m)//Foil (6.5 μ m)//

EVOH (30 μ m)

#4: PET (12 μ m)//ON (15 μ m)//Foil (6.5 μ m)//

PE (30 μ m)

EVOH: EVAL™ Film EF-E

ON: Bi-axially oriented polyamide

Specification of the VIP is as follows:

Size: 600mm×600mm×15mm

Core material: Glass fiber

Absorbent: Calcium oxide

Initial pressure: 1.2 Pa

The VIPs were exposed in a heat cycle which is room temperature for 15 hours and 100°C for nine hours. The thermal conductivity of each sample was measured periodically.

3.2 Results and discussion

Fig. 3 shows thermal conductivity change by time, up to 140 days. The VIP with EVOH sealant shows less thermal conductivity increase compared with the VIP with PE sealant. Inside pressure increase by the side permeation of oxygen and nitrogen was calculated [2]. Assuming no permeation through foil, the main surface permeation was not considered. The side permeation of water was also not considered assuming water can be completely absorbed by calcium oxide inside. The calculation resulted as Fig. 4. Fig. 3 and 4 indicate difference of side permeation could be one of major causes for less thermal conductivity change with EVOH sealant. Direct relationship between pressure and thermal conductivity of the glass fiber used will be studied to verify this hypothesis.

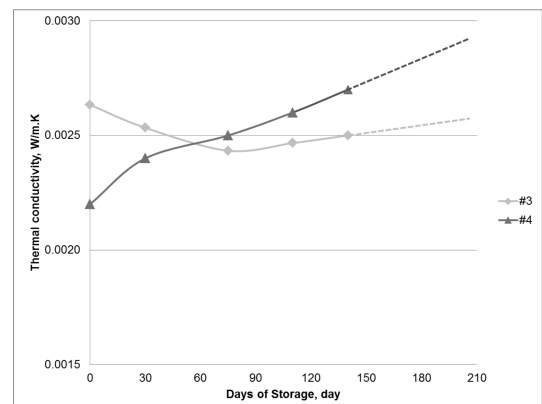


Fig. 3 Thermal conductivity change by time

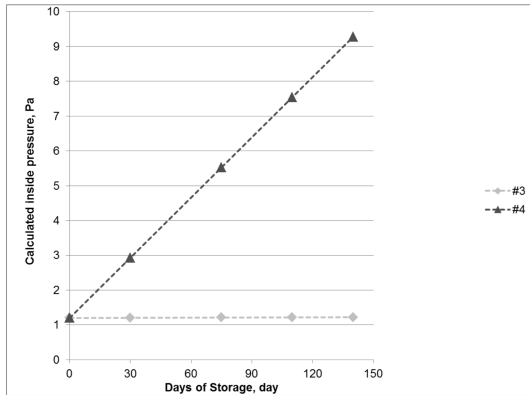


Fig. 4 Calculation of inside pressure

4. Conclusions

EVOH based film is one of high barrier plastic films which could extend service life of VIP. Two approaches have been studied to verify benefit of EVOH film.

(a) Higher barrier film for “less main surface permeation”

A VIP envelope with favorable gas and moisture barrier property were designed by combining VM-EVOH with other barrier films like VM-PET appropriately. Excellent durability and gas barrier property are major benefits of EVOH film. For higher performance, new barrier technologies are under study based on the material design for low permeation as well as good durability.

(b) EVOH sealant film for “less side permeation” through edge

The VIP with EVOH sealant shows less thermal conductivity increase compared with the VIP with PE sealant, which could be caused by less side permeation.

References

- [1] Cynthia Teniers, How laminates with Ethylene Vinyl Alcohol film (EVOH) improve the performance of VIPs, 9th International Vacuum Insulation Symposium
- [2] EVALTM Film brochure, Kuraray Co., Ltd.

Effect of Grit Spacing on Hole Diameter Accuracy and Roughness of CFRP Laminate Drilled with Brazed Diamond Core Drill

Wang Weifeng^{a*}, Zhang Yusheng^a, Chen Yan^b

a, Shanghai Aerospace Equipments Manufacturer, shanghai, 211009, P. R. China

b, College of Mechanical and Electrical Engineering, Nanjing University of Aeronautics and Astronautics, Nanjing, 210016, P. R. China

Abstract

Hole diameter accuracy and roughness are focused in the drilling of carbon fiber reinforced plastics (CFRP) laminate with brazed diamond core drill without coolant. The effect of grit spacing on hole diameter accuracy and roughness in drilling CFRP at different feed speed is studied. A simulation of heat conduction of CFRP laminate is performed to calculate thermal deformation of hole diameter. The study results indicate that hole - enlargement factor decreases with the increase of grit spacing and feed speed, and grit spacing has a relatively larger influence on enlargement factor. The surface roughness of hole wall increases with the increase of grit spacing and feed speed. When grit spacing of brazed diamond core drill is 1.6 mm and feed speed is 150 mm/min, hole quality of CFRP laminate is perfect.

Keywords brazed diamond core drill, CFRP, grit spacing, hole diameter, surface roughness

1. Introduction

CFRP laminate is one of the most advanced composite materials. With the advantages of high strength, excellent design-ability, good fatigue resistance and corrosion resistance, CFRP laminate is widely used in the field of aerospace and aviation. For CFRP laminate is anisotropic and low interlaminar shear strength, poor machining quality is the main problem, which restrict the technology development of drilling CFRP laminate. The research on hole diameter accuracy and roughness of CFRP laminate drilled with brazed diamond core drill is propitious to improve machining quality and prolong the service life of CFRP parts [1]. Many different methods are used to solve the problems of drilling CFRP. Some scholars get the conclusions that drilling a small guide hole in CFRP laminate and then using a broaching drill to expand hole diameter to the predetermined range for several times can significantly improve hole diameter accuracy and surface roughness of hole wall. But the machining efficiency of drilling CFRP

laminate is low with this method[2]. Some scholars get the conclusions that the angle between tool cutting edge and carbon fiber in CFRP laminate affects the surface roughness of hole wall and drilling-induced defects of hole exit. When the angle reaches 45°, drilling-induced defects of the hole exit are most serious. A model is established to expound the relationship between the surface roughness of hole wall and drilling-induced defects of hole exit[3].

In order to improve the machining quality and efficiency, CFRP laminate is drilled with brazed 80/100# diamond core drill under the spindle speed 15 000 rpm. The effect of grit spacing and feed speed on hole diameter accuracy and roughness is studied.

2. Drilling experiment

2.1 CFRP laminate and core drill.

The experimental 3234/G803PV CFRP laminate is a pre-impregnated material made up of medium temperature curing epoxy resin and carbon clothes what consist of T300 carbon fiber bundles. Carbon fiber

* Corresponding author, E-mail: wwf0257321@163.com

volume fraction of CFRP laminate is 60%. The woven method of fiber bundles and experimental CFRP laminate are shown in Fig. 1. Mechanical property of CFRP laminate is shown in Tab. 1, where number 1, 2, 3 represents the carbon fiber direction, vertical direction of carbon fiber within the layer and layer overlying direction [4]. Linear expansion coefficient of CFRP laminate is $6.71 \times 10^{-5}/\text{K}$ and thermal conductivity is $0.2 \text{ W}/(\text{m} \cdot \text{K})$.

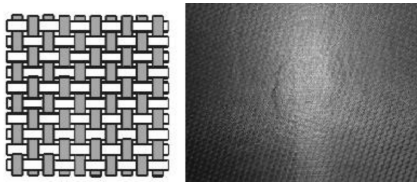


Fig. 1 Woven method of carbon fiber bundles and experimental CFRP laminate

(a) Woven method; (b) CFRP laminate

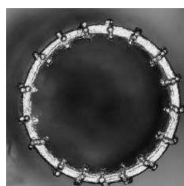
Tab. 1 Mechanical property of CFRP laminate

Young modulus			Poisson ratio		
E_1/GPa	E_2/GPa	E_3/GPa	ν_{12}	ν_{13}	ν_{23}
135	135	8.8	0.3	0.3	0.48

Tab. 2 shows the brazing parameters of core drill, which can make the exposed degree of diamond grits reach 70%~80%. As a result, the brazed diamond core drill presents good sharp degree, high efficiency and long service time[5]. Fig. 2 shows the appearance of brazed diamond core drill which is used to drill experimental CFRP laminate, when grit size is 80/100# and grit spacing is 1.6 mm.



(a)



(b)

Fig. 2 Appearance of brazed diamond core drill

(a) Brazed diamond core drill; (b) End face

Tab. 2 Brazing parameters of core drill

Process elements	Specific parameters
Brazing alloy dosage	$1(\text{mg}/\text{mm}^2)$
Brazing alloy composition	Ag - Cu - Ti
Vacuum degree	$10^{-2}(\text{Pa})$
Brazing temperature	$900\sim 920(^{\circ}\text{C})$
Holding time	$8\sim 12(\text{min})$

2.2 Experiment Design

The parameters of CNC machine tool HG410 used to drill CFRP laminate are as follows; the highest spindle speed 24000 r/min, the minimal feed speed 40 mm/min and output power 2.2 kW. The diameter of brazed diamond core drill is measured by a digital microscope HIROX KH - 7700 before the experiments. The experiments are performed at spindle speed $n = 15000 \text{ rpm}$, feed speed $v_f = 60 \text{ mm}/\text{min}$, 100 mm/min and 150 mm/min, with different grit spacing 1.0 mm, 1.6 mm and 2.2 mm. The equipments of drilling CFRP laminate with brazed diamond core drill is shown in Fig. 3. The equipments of measuring temperature of hole exit by infrared image device Fluke Ti32 is shown in Fig. 4. After drilling process, the hole diameter of CFRP laminate are measured by a digital microscope JGW-S-19JC. The surface roughness of hole wall is measured by a surface roughness measuring instrument Mahr M1. Heat image of hole exit is analyzed by SmartView software to get the temperature field around the hole exit. The effect of temperature field around the hole exit on hole diameter is calculated with a heat conduction simulation model established in ABAQUS software.



Fig. 3 Drilling CFRP laminate equipments



Fig. 4 Heat image measurement equipments

3. Experiment results

3.1 Effects of grit spacing on hole diameter

When CFRP laminate is drilled with brazed diamond core drill, hole diameter is larger than the diameter of core drill. The enlarged degree of hole diameter is evaluated by “enlargement factor D_a ”, which is expressed as follows:

$$D_a = (D - d) / d \quad (1)$$

where

D = the actual diameter of the hole,

d = the diameter of core drill.

The increase of enlargement factor D_a leads to the decrease of hole diameter accuracy. Hole diameter is measured when CFRP laminate is drilled with brazed 80/100 # diamond core drill at feed speed 60 mm/min, 100 mm/min and 150 mm/min; Tab. 3 shows “enlargement factor D_a ” of hole diameter when grit spacing are 1.0 mm, 1.6 mm and 2.2 mm at different feed speed.

Tab. 3 Enlargement factor D_a

Grit spacing mm	Diameter of core drill mm	Enlargement factor D_a		
		$v_f = 60$ mm/min	$v_f = 100$ mm/min	$v_f = 150$ mm/min
1.0	6.00	0.017	0.016	0.014
1.6		0.015	0.013	0.012
2.2		0.012	0.010	0.009

Tab. 3 indicates that the enlargement factor D_a of hole diameter decreases with the increase of grit spacing and feed speed. The enlargement factor D_a achieves 0.009 when grit spacing is 2.2 mm and feed speed is 150 mm/min, which means the stability of hole diameter is most excellent.

3.2 Effects of grit spacing on the surface roughness of hole wall

The range of the surface roughness of hole wall is symmetrical distribution around the circumference due to the experimental CFRP laminated is orthogonal woven by carbon bundles. In consideration of down cutting and up cutting in the different angle between cutting edge of core drill and carbon fiber [6], the roughness in two positions of hole wall are measured. The two positions are shows in Fig. 5, where position A represents the angle between cutting edge of core drill and carbon fiber is 0° and position B represents the angle is 45° .

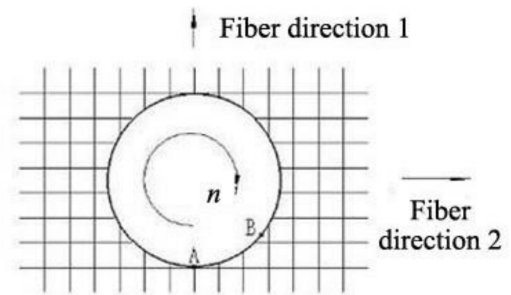


Fig. 5 Measuring positions on hole wall

The surface roughness of hole wall in position A and B are measured when CFRP laminate is drilled with brazed 80/100 # diamond core drill at feed speed 60 mm/min, 100 mm/min and 150 mm/min; Tab. 4 shows the surface roughness of hole wall with grit spacing 1.0 mm, 1.6 mm and 2.2 mm at different feed speed.

Tab. 4 The surface roughness of hole wall with different grit spacing

Grit spacing mm	The surface roughness of hole wall $R_a / \mu\text{m}$					
	$v_f = 60 \text{ mm/min}$		$v_f = 100 \text{ mm/min}$		$v_f = 150 \text{ mm/min}$	
	0°	45°	0°	45°	0°	45°
1.0	0.394	0.430	0.407	0.451	0.535	0.660
1.6	0.478	0.484	0.509	0.596	0.543	0.648
2.2	0.513	0.574	0.535	0.643	0.595	0.707

Tab. 4 indicates that the surface roughness R_a of hole wall in same angle position increases with the increase of grit spacing and feed speed. The surface roughness of hole wall in angle 45° position is larger than roughness in angle 0° position due to down cutting and up cutting of CFRP laminate drilled with brazed

diamond core drill.

4. Results and discussions

4.1 Enlargement factor D_a

From the data of Tab. 3, hole diameter is larger than the diameter of core drill when CFRP laminate is drilled with brazed diamond core drill. There are two main reasons that result in the enlargement of hole diameter. First reason is the radial run-out of brazed core drill when it is rotating at spindle speed 15000 rpm. The radial run-out is $10\sim 15\mu\text{m}$ measured by laser range finder. Second reason is thermal deformation of hole diameter what is caused by drilling heat. Drilling heat results from the power what carbon fiber fracture, matrix damage and friction between diamond grit, chips and flank face consume[7].

Drilling CFRP laminate with brazed diamond core drill, the highest temperature appears in the friction part between core drill and hole wall, which is recorded as T ($^{\circ}\text{C}$). The actual temperature field of drilling process is imported into the heat conduction simulation model established. With this conduction model, thermal deformation Δ (mm) of hole diameter can be calculated. Simulation images of thermal deformation for grit spacing 2.2 mm at different feed speed are shown in Fig. 6. Tab. 5 shows thermal deformations Δ (mm) of hole diameter for different grit spacing and feed speed. As thermal deformation of hole diameter far outweigh radial run-out of brazed core drill, reducing drilling temperature is an effective way to improve hole diameter accuracy[8]. Known from the data of Tab. 5, when grit spacing is 1.6 mm or 2.2mm, the temperature of hole exit is low, and the enlargement factor D_a is small, which lead to the improvement of hole diameter accuracy.

Tab. 5 Thermal deformations of hole diameter Δ (mm) for grit spacing 2.2 mm

Grit spacing mm	$v_f=60\text{mm/min}$		$v_f=100\text{mm/min}$		$v_f=150\text{mm/min}$	
	T	$\frac{\Delta}{\text{mm}}$	T	$\frac{\Delta}{\text{mm}}$	T	$\frac{\Delta}{\text{mm}}$
1.0	89	0.056	74	0.046	65	0.034
1.6	73	0.046	64	0.036	58	0.028
2.2	68	0.034	58	0.027	53	0.024

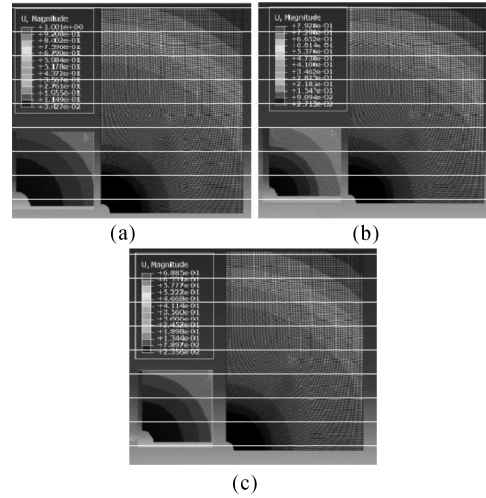


Fig. 6 Simulation images of thermal deformation

(a) $v_f=60\text{mm/min}$; (b) $v_f=100\text{mm/min}$;

(c) $v_f=150\text{mm/min}$

4.2 The surface roughness R_a of hole wall

Drilling CFRP laminate with brazed diamond core drill, the movement traces of diamond grits on core drill are helix lines, which result in residual layer is similar to internal thread on hole wall. The surface roughness R_a of hole wall increases with the increase of residual layer maximal thickness H [9].

Through the analysis of residual layer maximal thickness H , effect of grit spacing and feed speed on the surface roughness of hole wall is studied in drilling process. The geometric shape of diamond grit YK9 is rhombic dodecahedron. For diamond grits are arranged orderly, CFRP material removal form caused by diamond grits brazed on excircle face of core drill is shown in Fig. 7.

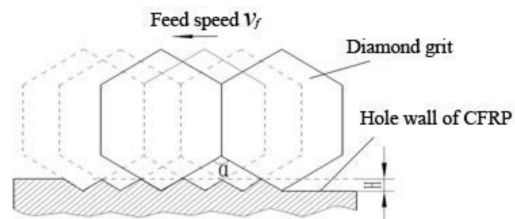


Fig. 7 CFRP material removal form

In drilling process of CFRP laminate, the feed rate v_0 of brazed diamond core drill is expressed as follows:

$$v_0 = \frac{v_f}{n} \quad (2)$$

Residual layer maximum width L_0 :

$$L_0 = \frac{v_0}{\pi D} \quad (3)$$

where

S = the distance of grit spacing.

Maximum thickness of residual layer H :

$$H = \frac{L_0}{2 \tan \frac{\alpha}{2}} = \frac{v_0 S}{2\pi D \tan \frac{\alpha}{2}} = \frac{v_f S}{2\pi n D \tan \frac{\alpha}{2}} \quad (4)$$

Maximum thickness of residual layer H increases with the increase of grit spacing S and feed speed v_f . As the increase of maximum thickness of residual layer H , the surface roughness of hole wall R_a increases and the machining quality of hole wall turns to poor.

5. Conclusions and outlook

The hole diameter accuracy and the surface roughness of hole wall are studied in drilling CFRP laminate with brazed diamond core drill. The following conclusions are drawn from the tests:

(1) Drilling CFRP laminates with brazed diamond core drill, the enlargement factor D_a of hole diameter increases with the decrease of grit spacing and feed speed. The grit spacing has larger influence on the enlargement factor D_a than feed speed.

(2) The surface roughness of hole wall in same angle position of hole wall increases with the increase of grit spacing and feed speed. In one hole, the surface roughness of hole wall increases from 0° to 45° and gets to the maximum when the angle reaches 45° .

(3) In consideration of the manufacturing requirements of hole diameter accuracy and the surface roughness of hole wall, drilling CFRP laminates with the brazed diamond core drill at the feed speed of 150 mm/min will get high efficiency and perfect manufacturing quality, when grit size is 80/100 # and grit spacing is 1.6 mm.

Acknowledgements

This work was supported by the National Nature Science Foundation of China (No. 51075210) and State Major Science and Technology Special Projects (No. 2012ZX04003-031).

References

- [1] Masahito Uedaa, Sotaro Miyake. Instantaneous mechanical fastening of quasi-isotropic CFRP laminates by a self-piercing rivet [J]. *Composite Structures*, 2012, 94: 3383-3393.
- [2] Ogawa K, Aoyama E. Investigation on cutting mechanism in small diameter drilling for GFRP (thrust force and surface roughness at drilled hole wall) [J]. *Compos. Struct.*, 1997, 38(1-4): 343-350.
- [3] Aoyama E, Nobe H, Hirogaki T. Drilled hole damage of small diameter drilling in printed wiring board [J]. *J. Mater. Process. Technol.*, 2001, 118(1-3): 436-408.
- [4] WANG Yuequan, TONG Mingbo. 3D nonlinear progressive damage analysis model for composite laminates [J]. *Acta Materiae Compositae Sinica*, 2009, 26: 159-166.
- [5] Zhao Yue. *Brazing techniques and applications* [M]. Beijing: Chemical Industry Press, 2004.
- [6] Zhang Houjiang. *Study on the Drilling Technology of CFRP* [D]. Beijing: Beijing University of Aeronautics and Astronautics, 1998.
- [7] Bao Yongjie. *The Formation Mechanism of Disfigurements during Drilling and the High-efficiency Techniques of Drilling C/E Composite* [D]. Shandong: Dalian University of Technology, 2010.
- [8] Okabe Yoji, Yashiro Shigeki. Effect of thermal residual stress on the reflection spectrum from fiber Bragg grating sensors embedded in CFRP laminates [J]. *Composites*, 2002, 33: 991-999.
- [9] Quan Yanming, Ye Bangyan. Machined Surface Texture and Roughness of Composites [J]. *Acta Materiae Compositae Sinica*, 2001, 18: 128-132.

Numerical Analysis and Optimization Methods of the Thermal Bridge Effects on Vacuum Insulation Panels

Kan Ankanga^{*}, Wang Chong^a, Zhang Tingting^b, Cao Dan^a

a. Merchant Marine College, Shanghai Maritime University, Shanghai, 201306, P. R. China

b. Chinese Association of Refrigeration, Beijing, 100142, P. R. China

Abstract

The big difference between thermal conductivity of gas barriers and that of core materials makes the thermal bridge effect on vacuum insulation panels inevitable. The thermal bridge dramatically deteriorates the overall thermal insulation performance of the vacuum insulation panels. Linear thermal transmittance was introduced to numerically model the thermal bridge. Combined with the actual installation situation, the main factors that influence the thermal bridge effect on vacuum insulation panels are thickness and thermal conductivity of the core material, thickness and thermal conductivity of the gas barrier envelopes, the size of vacuum insulation panels and the size of the gap between the panels, etc. The corresponding optimization methods and precautions to reduce the thermal bridge effect on VIP were put forward in this paper to improve the technology of manufacturing and develop the thermal system with vacuum insulation panels involved.

Keywords vacuum insulation panels, thermal bridge effect, heat transfer model, optimization methods

1. Introduction

As new and efficient thermal adiabatic materials, vacuum insulation panels (VIPs) have the history about 5 decades [1]. Due to the low air pressure inside panels, the thermal conductivity of excellent thermal performance VIP measured by the experiment can be as low as $5\text{mW}/(\text{m} \cdot \text{K})$. The thermal residence is about 6 to 10 times of the traditional insulation materials with the same thickness [2]. Typical Gas barrier envelope is made of multi-layered polyester base films which have aluminum foil or of aluminum foil [3]. However, the thermal conductivity of aluminum foil is about 20000~100000 times higher than that of the core material of vacuum insulation panels. As the result, the thermal bridge effect is formed in the course of the heat leaking. Some heat flows directly transferring from the hot plate to the cold plate across the edge of the gas barrier envelope cannot be avoided, anyway.

As the presence of thermal bridge effect, the overall thermal conductivity of VIP is much larger than the central region. The thermal bridge effect has been studied and analyzed by a number of researches domestically and abroad. Based on previous research the authors are intended to establish and analyze a model of edge linear thermal transmittance, to propose more comprehensive optimization methods of thermal bridges. Optimal innovation and great significances for the application and popularization of VIP were made.

2. Effective heat transfer coefficient of VIPs

For VIPs applications as building envelopes, edge linear heat transfer rate and angular contact heat transfer rate generated due to construction and installation, and ψ_{length} is introduced to represent it. If the value of ψ , the area A , and the circumference of the vacuum insulation pane l were known, equation (1) can be used to describe the overall heat transfer coefficient U_e of VIPs [8]:

* Corresponding author, Tel :86 - 13761032465, E-mail: ankang0537@126.com

$$U_c = U_c + \frac{\sum \phi_{i,\text{length}} - l_i}{A} \quad (1)$$

Where

U_c = heat transfer coefficient of the central region of VIPs,

l_i = side perimeter of VIP,

A = area of a side of the VIP,

$\phi_{i,\text{length}}$ = edge linear heat transfer rate of a side .

For a particular building envelope structure, U_c can be described by equation (2):

$$U_c = \left(\frac{1}{\alpha_i} + \frac{\delta_p}{\lambda_c} + \frac{1}{\alpha_e} \right)^{-1} \quad (2)$$

Where

δ_p = thickness of the VIP plate,

δ_c = thermal conductivity of the central area of VIPs,

α_i, α_e = heat transfer coefficient of hot and cold surfaces of VIP.

Equation (1) is expressed in the case of having thermal bridge effect, and equation (2) is expressed in the case of have no thermal bridge effect . So ϕ_{length} is an important parameter to characterize the thermal bridges effect of the gas barrier envelopes . This paper adopts the way of simplified numerical analysis to expound and solve the edges linear heat transfer rate.

3. Establishment and analysis of mathematical model of thermal bridges of VIPs

Suppose A as the area of VIP , the length l_p (m), the width w_p (m), the thickness δ_p (m), the thickness of gas barrier envelopes $2\delta_s$ (m) , the air temperature of cold end and hot end of VIPs T_i, T_e (°C). The thermal conductivity of the gas barrier envelopes in the joints is λ_{b1} , and the thickness is δ_{b1} . Joint is filled with insulation material, and the thermal conductivity coefficient is λ_s , the thickness $2\delta_s$. The heat flux flowing through the central area of the VIPs is $\phi_{p,\text{cop}}$, W ; the total heat flux flowing through the VIPs is $\phi_{p,\text{total}}$; the analysis model is shown in Fig. 1 .

Take some infinitesimal of gas barrier envelopes as the research object, assuming that the length direction of the X -direction, the width direction of the Y-direction, infinitesimal's heat transfer conditions in the X direction shown in Fig. 2 . By the total energy conservation, the edge linear heat transfer rate can be

expressed as:

$$2\phi_{\text{length}} = \frac{\phi_{p,\text{total}} - 2\phi_{p,\text{total}}}{l_p \Delta T} = \frac{\phi_{p,\text{total}}}{l_p \Delta T} - 2U_c w_p \quad (3)$$

Where

ϕ_1 = heat that passing through gas barrier envelopes into the micro- cell,

ϕ_2 = heat that passing through gas barrier envelopes out of the micro- cell,

ϕ_3 = heat that passing through the convective heat transfer of surface of gas barrier envelopes flowing into the infinitesimal;

ϕ_4 = heat of gas barrier envelopes coming into core material.

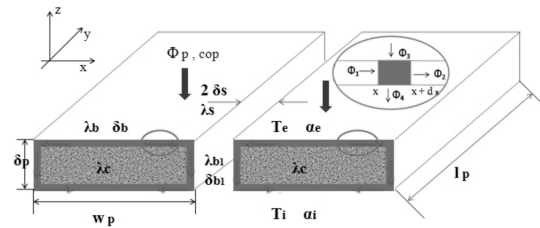


Fig. 1 The analysis model of the thermal bridge effect of VIPs

When the infinitesimal in steady state, we can get that:

$$2\phi_{\text{length}} = \frac{\phi_{p,\text{total}} - 2\phi_{p,\text{cop}}}{l_p \Delta T} = \frac{\phi_{p,\text{total}}}{l_p \Delta T} - 2U_c w_p \quad (4)$$

Taking the way of infinitesimal, equation (4) can be rewritten as:

$$\lambda_b \delta_b \left. \frac{dT_x}{dx} \right|_x = \lambda_b \delta_b \left. \frac{dT}{dt} \right|_{x+dx} + \alpha_e (T_i - T_x) - \frac{\lambda_c}{\delta_p} (T_x - T_z) dx = 0 \quad (5)$$

Where

T_x = the temperature of gas barrier envelopes of VIP in the X direction,

T_z = temperature of gas barrier envelopes of VIP in the Z direction,

λ_b = thermal conductivity of the gas barrier envelopes (i. e. , in the X- Y direction is the same),

λ_c = thermal conductivity of the core material.

3.1 Calculation of thermal bridge effect of single panel

Gas barrier envelope is assumed that its texture is regular and continuous. δ_b and λ_b are constant values. Combine ϕ_{length} with the boundary conditions and we can obtain equation (6):

$$\psi_{\text{length}} = \frac{1}{1 + \frac{\lambda_c}{\alpha_i \delta_p} + \frac{\lambda_c}{\alpha_e \delta_p}} \times \frac{\delta_b \lambda_b}{\delta_p} + \frac{\sqrt{\delta_b \lambda_b}}{\sqrt{\alpha_i} + \sqrt{\alpha_e}} \quad (6)$$

The conclusion can be made from equation (6) that, the main parameters affecting the thermal bridge effect of VIP are the external environment (α), VIP's thickness δ_p , thermal conductivity of the core material λ_c , thickness δ_b and thermal conductivity λ_b of the gas barrier envelopes. Combining equations (1), (3), (6) yields the expression of effective heat transfer coefficient U_e :

$$U_e = U_c + \frac{L}{A} \psi_{\text{length}} = \frac{\phi_{p,\text{total}}}{2l_p \tau_p \Delta T} - \frac{\psi_{\text{length}}}{\tau_p} + \frac{L}{A} \psi_{\text{length}} = \frac{\phi_{p,\text{total}}}{2l_p \tau_p \Delta T} + \left[\frac{2(L_p + \tau_p)}{l_p \tau_p} - \frac{1}{\tau_p} \right] \times \frac{1}{1 + \frac{\lambda_c}{\alpha_i \delta_p} + \frac{\lambda_c}{\alpha_e \delta_p}} \times \frac{\delta_b \lambda_b}{\delta_p + \frac{\sqrt{\delta_b \lambda_b}}{\sqrt{\alpha_i} + \sqrt{\alpha_e}}} \quad (7)$$

In addition to the influencing factors of equation (6), the effective heat transfer coefficient also has a relationship with the size of VIP, seeing from equation (7).

3.2 Calculation of thermal bridge effect of assembled VIPs.

According to the above calculation method, the edge linear heat transfer coefficient of VIP can be obtained under the assembly. It can be expressed as:

$$\psi_{\text{length}} = \frac{1}{1 + \frac{\lambda_c}{\alpha_i \delta_p} + \frac{\lambda_c}{\alpha_e \delta_p}} \times \frac{1}{\frac{\delta_p}{(\delta_{bl} + \delta_s)^2} \left(\frac{\delta_{bl}}{\lambda_{bl}} + \frac{\delta_s}{\lambda_s} \right) + \frac{1}{\sqrt{\delta_p \lambda_c \alpha_i}} + \frac{1}{\sqrt{\delta_p \lambda_c \alpha_e}}} \quad (8)$$

In addition to the influencing factors of equation (6), the edge linear heat transfer coefficient of VIP also has a relationship with the thickness δ_s and heat transfer coefficient λ_b of filling media in joints, seeing from the equation (8).

4. Modeling results and analysis

In order to make numerical analysis and simulation, we need to set certain boundary conditions for the model. According to the test standards

GB/T3399—2009[9], the boundary condition for VIPs was setting as: $t_e = 35^\circ\text{C}$, $t_i = 15^\circ\text{C}$, the corresponding heat transfer coefficient of cold and hot surfaces of gas barrier envelopes $\alpha_i = 7.8 \text{ W}/(\text{m}^2 \cdot \text{K})$, $\alpha_e = 25 \text{ W}/(\text{m}^2 \cdot \text{K})$. The thickness of VIP's core material is generally between $10 \sim 40\text{mm}$. Thermal conductivity of open polyurethane is $0.025 \text{ W}/(\text{m} \cdot \text{K})$. Thermal conductivity of fine glass fiber is $0.032 \text{ W}/(\text{m} \cdot \text{K})$. They were all introduced into equations (6), (7) and (8) to calculate and analyze.

4.1 The influence of the thermal conductivity and thickness of core material on thermal bridge effect.

According to the calculation results above, variation of ψ_{length} versus vacuum and thickness is simulated in Fig. 2. Supposed the thickness of barrier envelope is $90\mu\text{m}$ with different materials foil (Fig. 2 (a)) and MF1 (Fig. 2 (b)) gas barrier film material for the study, the variation of ψ_{length} with the same barriers, the different δ_p and the different λ_c is shown in Fig. 2.

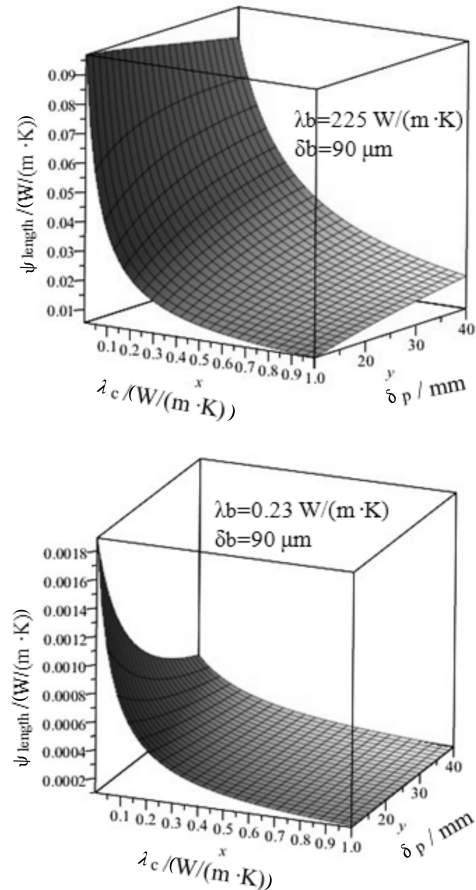


Fig. 2 Heat flux of the VIPs with same barriers, different λ_c and different δ_p

When the VIPs thickness δ_p is constant, the boundary thermal bridges show a decreasing trend as the increase the thermal conductivity λ_c of the core material, regardless of whether the gas barrier envelopes containing a metal layer. With the increase of δ_p , edge thermal bridge effect decreases under the condition of certain thermal conductivity of core material. Thermal bridges of VIPs whose gas barrier envelope is aluminum foil are far greater than whose gas barrier envelopes is MF1 (PET).

4.2 The influence of the thermal conductivity and thickness of single layer barrier on thermal bridge effect.

According to the calculation results above, plot variation under the same vacuum and the same boundary conditions. VIPs with certain kind of core material whose thickness is 30mm for the analysis were selected. The variation of ψ_{length} with the same core material, the different δ_b and the different λ_b is shown in Fig. 3.

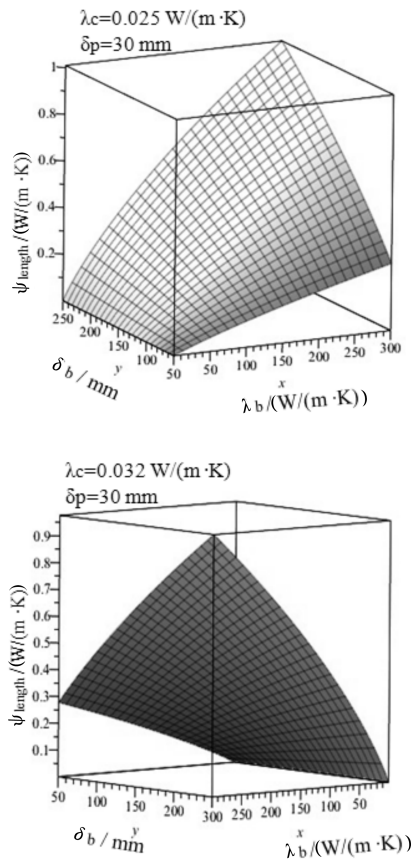


Fig. 3 Heat flux of the VIPs with the same core material, the different λ_b and the different δ_b ,

Under the condition of certain thickness δ_b of gas barrier envelopes, the boundary thermal bridges showed a decreasing trend as the decrease of the thermal conductivity λ_b . Under the condition of certain thermal conductivity λ_b of the gas barrier envelopes, edge thermal bridge effect decreases as the decrease of thickness of δ_b gas barrier envelopes.

4.3 The influence of the thermal conductivity and thickness of gas barrier envelopes in joints of VIP on thermal bridge effect.

According to the above calculation results, variation of ψ_{length} under the same vacuum and the same boundary conditions was analyzed. VIP whose core material is fine glass fiber were selected for the study. Thermal conductivity of the core material λ_c is $0.032 \text{ W} / (\text{m} \cdot \text{K})$, and the thickness δ_p is 20mm. The filling medium in gap is air (λ_s is $0.023 \text{ W} / (\text{m} \cdot \text{K})$), the spacing δ_s of it being 2mm. The variation ψ_{length} with the same core material, the different thickness δ_{b1} and the different thermal conductivity λ_{b1} is shown in Fig. 4.

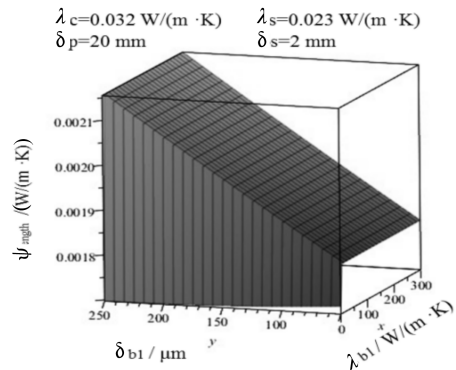


Fig. 4 Heat flux of the VIPs with same core material, different λ_{b1} and different δ_{b1}

When the value of λ_{b1} is small (less than $5 \text{ W} / (\text{m} \cdot \text{K})$), ψ_{length} increases linearly along with the increase of δ_{b1} . When the value of λ_{b1} is large (greater than $5 \text{ W} / (\text{m} \cdot \text{K})$), the growth of ψ_{length} is flat along with δ_s increasing. The thermal bridge effect caused by λ_{b1} is dominated in this condition.

4.4 The influence of the thermal conductivity of filling media in the assembled VIP and joints between two adjacent panels on thermal bridge effect.

According to the equation (6), variation of ψ_{length}

under the same vacuum and the same boundary conditions is analyzed. Select the VIP whose core material is fine glass fiber for simulation. Thermal conductivity λ_c is $0.032 \text{ W} / (\text{m} \cdot \text{K})$ and the thickness δ_p is 35 mm . Thermal conductivity λ_{b1} is $0.54 \text{ W} / (\text{m} \cdot \text{K})$ and the δ_{b1} is $90 \mu\text{m}$. The variation ψ_{length} with the same core material and the same barriers, the different spacing δ_s and the different thermal conductivity λ_s is shown in Fig. 5.

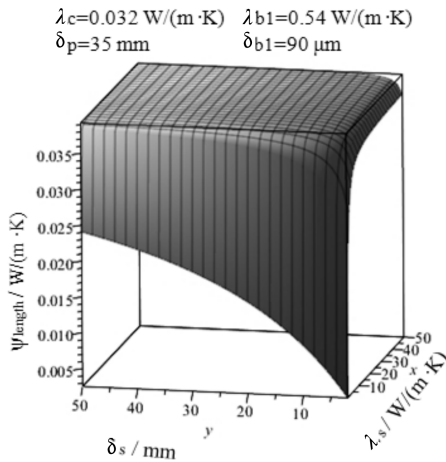


Fig. 5 Heat flux of the VIPs with same core material and same barriers, different λ_s and different δ_s

When the value of λ_s is small (less than $5 \text{ W} / (\text{m} \cdot \text{K})$), ψ_{length} roughly shows linear growth along with the increase of δ_s . The influence of δ_s on thermal bridges is dominant. When the value of λ_s is large (greater than $5 \text{ W} / (\text{m} \cdot \text{K})$), ψ_{length} growth flat along with the increase of δ_s . At this time, the impact of λ_s on thermal bridge effect is dominant. When the spacing δ_s is constant, ψ_{length} also shows a significant increase in the first as the increase in the thermal conductivity λ_s of the filling medium and then it changes gently.

4.5 The influence of VIP's size on effective heat transfer coefficient.

Take the same length and width of VIPs. Variation of U_e under the same vacuum and the same boundary conditions is analyzed. Select the VIP whose core material is fine glass fiber for the study were selected. Thermal conductivity of the core material is $0.032 \text{ W} / (\text{m} \cdot \text{K})$, and the thickness of MF2 barrier is $90 \mu\text{m}$.

The variation of U_e with the same core material and the same barrier, the different l_p / w_p and the different thickness δ_p is shown in Fig. 6.

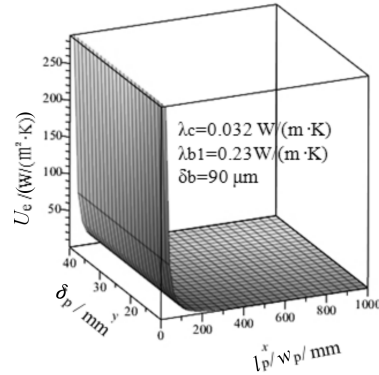


Fig. 6 Heat flux of the VIPs with same core material and same barriers, different l_p / w_p and the different δ_p

When the VIPs thickness is certain, U_e shows a significantly reduced trend first, then leveling off as l_p / w_p increasing.

When l_p / w_p VIPs is certain, U_e shows a reduced trend as an increase in thickness. When δ_p is increased to a certain value, U_e is stabilized. At this time, the corresponding l_p / w_p can be used as critical dimension to δ_p .

5. Conclusions

(1) Combine with practical application, it can be deduced that the main factors affecting edge thermal bridge effect of VIPs include the thickness and thermal conductivity of the core material, thickness and thermal conductivity of the gas barrier envelopes, VIPs' size and the gas gap between panels in the process of installation and others through mathematical modeling and calculation analysis.

(2) In practice, best raw materials should be selected and improve the level of production processes to enhance the thermal insulation properties of VIPs; Using sealing layer without metal layer based on the Serpentine edge technology to reduce thermal bridges.

(3) Larger size of VIPs are expected in the system when installing, and minimizing the gas gap.

(4) This simulation is under normal temperature conditions, so it can not truly reflect heat transfer of VIPs at different temperature and it requires further

study. In addition, the influence of the microstructure of the core material, such as porosity and fiber angle and other factors, that affect the thermal bridges need to be further studied.

Acknowledgements

The work is financially supported by the Natural Sciences Foundation of Shanghai, China (15ZR1419900). The authors would also like to render thankfulness to the Jiangsu Sunkey Package Co., Ltd. for the materials supply.

References

- [1] Y. N. Hu, K. M. Wang, Z. X. Lin. Development trends of vacuum insulation panels[C]. China energy-saving insulation material Association annual meeting, 2011
- [2] R. Baetens, B. P. Jelle, J. V. Thue, et al. Vacuum insulation panels for building applications[J]. *Energy and buildings*, 2010, 31(2):147 – 172.
- [3] M. Alam, H. Singh, M. C. Limbachiya. Vacuum Insulation Panels(VIPs) for building construction industry— A review[J]. *Applied Energy*, 2011, 88 (11):3592 – 3602.
- [4] H. Schwab, C. Stark, J. Wachtel, et al. Thermal Bridges in Vacuum-insulated Building Facades [J]. *Journal of Building Physics*, 2005, 28(4):345 – 356
- [5] C. G. Yang, X. Gao. Thermal bridge effect of vacuum insulation panels and optimization measures[J]. *Vacuum*, 2010, 47(3):78 – 82.
- [6] A. K. Kan, H. D. Han, T. T. Zhang. Numerical analysis and optimization of thermal bridges of vacuum insulation panels[J]. *Vacuum*, 2013, 50(1).
- [7] P. Lutz, R. Jeuseh, H. Klopfer, H. Freymuth, L. Krampf, K. Petzold. *Lehrbuch der Bauphysik*, 3rd edn, TeubnerVerlag Stuttgart. (1994).
- [8] S. M. Yang, W. Q. Tao. *Heat Transfer*. [M]. 4. Bei Jing: Higher Education Press, 2006:54.
- [9] Ministry of Chemical Industry. GB/T 3399—2009, Plastic thermal conductivity test methods- guarded hotplate method, [S]. Beijing:China Standard Press, 2009.
- [10] K. G. Wakili, R. Bundi, B. Binder. Effective thermal conductivity of vacuum insulation panels [J]. *Building Research & Information*, 2004, 32(4):296.

VIP System Application Practice in Shanghai Building Area

Yan Yuanyuan *

Abstract

According to the characteristics of Shanghai regional climate conditions in China, to meet the requirement of building energy efficiency of public building energy efficiency from 50% to 65%, the residential building energy efficiency by 65%. Vacuum insulation board with excellent insulation properties have more application of engineering practice, according to different structure characteristics and the characteristics of the different parts of the structure has the practice experience.

Keywords VIP, building area, decoration housing.



Shanghai first fine decoration housing project whose energy saving efficiency is 70%.



Shanghai jiading grand theatre

Building insulation used in thermal insulation, the wall heat preservation is 20 mm, roof insulation thickness is 25 mm.

* Corresponding author, Tel : 86 - 21 - 35882727, E-mail: 13816225578@163.com

A Combined Operational and Embodied CO₂ Approach: The Limits of Conventional Insulation Materials and Case for High Performance Vacuum Technology

Raymond Glenn Ogden^a, Shahaboddin Resalati^{b*}, Christopher Charles Kendrick^b

a. Associate Dean, Faculty of Technology, Design & Environment, Oxford Brookes University, Oxford, UK

b. Senior Lecturer, School of Architecture, Oxford Brookes University, Oxford, UK

Abstract

The imperative to reduce the carbon footprint of buildings will inevitably require higher levels of insulation. As building performance improves and operational energy reduces, the ratio of operational to embodied energy will continue to shift. Where very low U-values are required, the volume of material in conventional insulation is such that embodied carbon can begin to outweigh operational carbon savings during the projected lifetime of buildings, causing a net CO₂ disbenefit.

Detailed studies carried out at Oxford Brookes University based on aggregated operational and embodied CO₂ analyses suggest significant benefits for vacuum insulation in relation to a broad range of building types and design scenarios in comparison with mainstream comparator insulation materials including PUR and mineral wool, specially in relation to applications with shorter design lives where the embodied CO₂ investment has to be recovered relatively quickly.

Keywords insulation standards, vacuum insulation, retrofit, cladding systems

1. Introduction

The energy required to heat buildings accounts for 26% of total national energy consumption in the UK (DECC, 2010). It is important that this is addressed in order to reduce carbon emissions, resource depletion and climate change. The UK is committed to reducing greenhouse gas emissions by at least 80% by 2050 relative to 1990 levels (CCC, 2008). The built environment accounts for 43% of UK emissions, of which 26% is from residential and 17% from non-domestic buildings. It is estimated that around 70% of buildings existing today will be still in use by 2050 and so, whilst the performance standards of new buildings are important, it is arguably more critical that effective strategies are found for improving the thermal

performance of existing stock.

At present there are around 8000 dwelling demolitions per year accounting for only 0.03% of the total stock (Ravetz 2008). The equivalent rate for industrial and commercial premises is difficult to estimate. However based on there being 597 million m² of industrial and commercial premises in 2007 (CLG and ONS, 2008) and £6 billion of non domestic construction in the same year (ONS, 2010) coupled with little net growth in the stock, and an assumed average construction cost of £1800 per m² the equivalent demolition figure can be estimated as being around 0.5%. At these rates, and recognising the inaccuracies and uncertainties of future trends, it may reasonably be expected that replacement of 50% of the

* Corresponding author, Tel :44 - 1865 - 484286, E-mail:sresalati@brookes.ac.uk

existing building stock with new construction complying with improved current and future building standards is likely to take about 100 years.

In view of this slow rate of change, it is essential that effective thermal retrofit strategies are developed but limitations in the existing technologies pose serious issues not least in terms of the embodied energy associated with insulation materials and techniques.

Building regulations have set increasingly demanding standards for the thermal performance of envelopes with the main focus on reducing operational energy (Yan 2011, Anastaselos 2009, Ramesh 2010). Critically however, UK building regulations, and comparable international regulations pay little attention to embodied energy. Operational energy (energy consumed during the in-use phase of a building's life) has in recent decades been assumed to be around 10 times greater than the total embodied energy (the energy used to produce building materials and in construction processes from cradle to gate in this study) but as more buildings are constructed to higher levels of energy efficiency, future low and zero carbon buildings could see parity between operational and embodied energy, or even embodied energy exceeding operational energy. It is essential therefore that embodied energy is factored into refurbishment scenarios.

If so, a compelling case begins to emerge for the development of novel insulation materials with higher thermal resistance coupled with relatively low embodied energy. The case is particularly strong for retrofit applications where design lives tend to be less than those for new build, and where embodied energy can offset a greater proportion of the total operational energy savings. Of the known possible alternatives vacuum insulation is considered to be amongst the most promising (DTI project 2007, Caps 2001, Fine 1989, Materna 2001, Zwerger 2005).

2. Minimisation of Combined Operational and Embodied CO₂

Whilst there is an essentially linear relationship between building envelope U-values and heat losses, embodied energy tends to increase in an accelerating fashion as levels of insulation increase. The interaction of these factors is important. The relationship is one of

simple proportion and operational CO₂ is positively correlated only to thermal conductance (i. e. it is independent of the insulation material used).

In contrast, embodied energy profiles are neither linear, nor independent of insulation material as:

a. Required insulation thicknesses increase progressively as U-value is reduced, and

b. Embodied energy and thermal conductivity of individual insulation materials vary considerably. For example the embodied CO₂ and k value of polyurethane (PUR) are 3.48 kg CO₂/kg and 0.025 W/(m • K) respectively whilst those of mineral wool are 1.2 kg CO₂/kg and 0.037 W/(m • K).

Fig. 1 illustrates a typical curve for embodied energy (in this case associated with PUR insulation), and also the combined operational and embodied CO₂ arising for a modelled notional warehouse building. The key feature is that the aggregated total of the linear and non-linear relationship is by definition non-linear. Reductions in combined operational and embodied energy become progressively more difficult to achieve as insulation thicknesses increase.

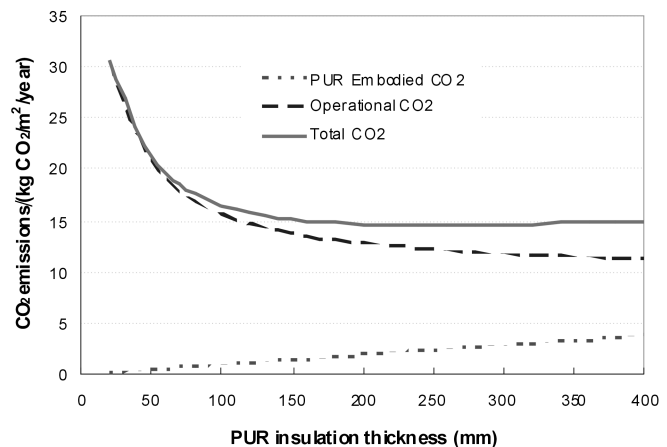


Fig. 1 Example of typical non-linear relationship between embodied CO₂ (and combined embodied and operational CO₂) based on PUR insulation

The minimum carbon point presented in Fig. 1 is the thickness of insulation beyond which the embodied carbon associated with adding to the thickness of insulation exceeds the operational carbon savings and consequently a carbon disbenefit occurs. This can vary for different building types and operational scenarios but

is within a range of thicknesses that seem entirely possible to be the requirement of regulations in future. The graph for the notional building indicates an optimum thickness for PUR insulation of approximately 260mm based on certain assumptions (including a 25 year service life and typical building operation criteria). Curves of this nature tend to flatten as service life increases or as a result of the use of lower embodied energy insulation. Both of these factors increase the optimum insulation thicknesses.

3. Quantification of the Carbon Limits of Mainstream Conventional and Novel Insulation Solutions for Industrial Claddings

Most conventional insulation materials are high in embodied energy. For any insulation material to be justified, the amount of operational carbon saved as a result of its installation must be greater than the carbon associated with its production, installation and end of life decommissioning. The optimal thicknesses of insulation for a range of industrial building types under particular operational conditions, and designed for a range of service lives, are presented in Tab. 1.

The following analyses investigate the results associated with re-sheeting of standard single span portal frame warehouses of 1000 and 3000m² and a similar 3000m² retail outlet using built up cladding systems with mineral wool and composite PUR cladding systems as conventional insulation materials and VIP as novel

insulation solution. The analyses assume the general system parameters described in Tab. 1.

A 25 year service life is often used for warehouse, industrial and retail premises. However, the appropriate service life extensions that should be delivered by retrofit measures are less clear, whether these should essentially “reset the clock”, or whether they should extend service lives by a shorter period. For the purposes of this research it is assumed that building envelope refurbishment assumes 25 year service life. This is critical to ‘net benefit’ carbon calculations as the shorter the service life the greater is the impact of embodied carbon (i. e. annualising embodied carbon = total carbon / *n* years where *n* is the design life). Refurbishment applications where service lives are of the order of 25 years can therefore be significantly more susceptible to the effects of embodied carbon than new build applications where design lives are longer.

The results Tab. 2 are simulated using IES VE software, and a London Heathrow location. Minimum CO₂ represents the point of optimum net benefit of insulation i. e. the point where the operational energy associated with heating plus the embodied energy of the materials used is at its lowest (and optimum) level. The ratio of roof to wall insulation thicknesses (and U values) reflects the higher heat losses through roofs compared to walls.

Tab. 1 Operational parameters for simulation modelling

	3000 m ² WAREHOUSE	1000 m ² WAREHOUSE	RETAIL SHED
HEATING	Natural gas — Industrial heating system — heated to 18 °C from 8am to 6pm		Natural gas — Industrial heating system — heated to 18 °C from 9am to 9pm
LIGHTING	controlled by sensors set at 300 lux		controlled by sensors set at 300 lux and displayed lighting up to 5w/m ²
AIRTIGHTNESS	air infiltration value of 0.19 ach is used with 7.5 m ³ /h/m ² air permeability rate	air infiltration value of 0.16 ach is used with 7.5 m ³ /h/m ² air permeability rate	air infiltration value of 0.19 ach is used with 7.5 m ³ /h/m ² air permeability rate

Within the context of conventional insulation, if a more highly insulated building envelope is specified then the investment in embodied energy will not be recovered through savings in operational energy. Conversely, if a less insulated building envelope is specified then more operational energy is required for heating than is saved by the reduced embodied energy of the insulation

materials.

Interpretation of Tab. 2 presents a number of key issues associated with conventional insulation technology:

(1) Greyed out cells on the table indicate where the values cannot be achieved using currently available systems, i. e. where the insulation and building envelope

technology is unable to provide the required U values due normally to the physical thickness of the required insulation (causing the practical engineering difficulties previously described). In these situations the optimal achievable values are reduced and the lowest CO₂ level is unachievable.

(2) Factoring embodied energy into an aggregated analysis serves to limit the minimum CO₂ levels that can be justified. Higher embodied energy insulation materials become more difficult to justify than lower embodied energy materials as they more rapidly lead to a CO₂ disbenefit. Lower embodied energy insulation materials allow for lower U values (up to the point where the aforementioned practical engineering difficulties prohibit effective adoption) whilst still presenting a CO₂ benefit, so more onerous insulation standards, giving improved energy thrift, can be achieved.

(3) The R value (thermal resistance) of particular

insulation materials is also a significant factor. It indicates how much insulation material is required to deliver any prescribed U value. The higher the R value, the lower the amount of insulation material needed, generating a corresponding reduction in embodied energy. Critically therefore insulation with low embodied energy coupled with high R value will achieve the lowest minimal CO₂.

The key characteristic of the equivalent minimum CO₂ for VIP is that the higher performance coupled with low embodied energy implies a net benefit up to and beyond the levels of insulation that may be reasonably anticipated (i. e. extremely low U-values). Only in one of the cases analysed, that of a retail shed does embodied energy reach a point where it offsets the beneficial effects of additional insulation. In all other cases increasing the level of insulation provided by VIP continues to reduce the combined operational and embodied energy requirements.

Tab. 2 Minimum aggregated CO₂ burden associated with embodied energy of mineral wool and PUR and operational energy required for heating (by building type)

Building type	Insulation type	Minimum CO ₂	Roof U-value	Wall U-value
		(kgCO ₂ /m ² /year)	W/(m ² · K)	W/(m ² · K)
Large warehouse	Mineral wool	13.5	0.08	0.111
Medium warehouse		10.74	0.08	0.116
Retail shed		2.19	0.13	0.18
Large warehouse	PUR	14.48	0.09	0.13
Medium warehouse		12.08	0.09	0.13
Retail shed		3.97	0.15	0.21
Large warehouse	VIP	*	*	*
Medium warehouse		*	*	*
Retail shed		0.8	0.05	0.06

* No minimum CO₂ up to 100mm VIP with 0.03W/(m² · K) U-value

According to the UK National Statistics Publication Hub, there are approximately 466 thousand warehouses and factories existing in the UK. This figure equates to 370 million square meters of warehouse buildings. The minimum achievable CO₂ associated with using VIPs in comparison to investigated conventional insulation materials saves about 0.4~1 million tonnes of CO₂ per annum (depending on building size and operational criteria) which is about 5%~12.6% of associated CO₂ with total space heating demand of industrial buildings

(about 40 TWh/year) (DECC, 2013, the future of heating). The saving associated with improving the fabric U-value down to 0.25 W/(m² · K) (assuming 0.35 as the base-case) is approximately between 2.5%~9.5% and to 0.15 W/(m² · K) is in range of 0.63%~10.7%.

These findings provide compelling evidence of the case for development of novel insulation materials as conventional solutions cannot be justified in relation to low U-values and relatively short service lives. It is

possible that other novel insulation materials may deliver similar levels of high performance however few such materials have reached the same level of technical development as vacuum insulation.

4. Conclusions

Improving the thermal efficiency of existing buildings is important to achieving national carbon reduction targets. Standards for new buildings cannot in themselves achieve the necessary reductions within a reasonable timeframe as the churn rate for new construction is simply too slow.

Current conventional insulation materials such as PUR and mineral wool cannot achieve low U-values without substantially increasing thickness, in which case the embodied CO₂ associated with these materials can potentially outweigh the savings they present in terms of reducing operational CO₂. The problem is more acute in relation to refurbishment than new build since service life tends to be significantly shorter and the number of years over which the embodied energy can be offset against is commensurately less. Future thermal refurbishment strategies must therefore focus on combined operational and embodied energy analysis. Such analysis demonstrates optimum net benefit levels for insulation solutions beyond which it is illogical to go as embodied energy burdens exceed the operational energy saved.

In the cases analysed, conventional insulation materials used in relation to 25 year service life refurbishment can only deliver net benefit levels in a limited range whereas VIPs have no technical limits and can achieve low, or extremely low, U-values (to 0.03 W/(m² · K)) and much improved levels of optimum net benefit.

High performance insulation materials such as vacuum insulation, that provide high levels of thermal insulation relative to their embodied energy, perform significantly better in reducing overall CO₂ emissions than conventional materials over a typical refurbishment service life. At present however, whilst there is good “technology push”, there is limited ‘market pull’. It is important that innovative technologies such as vacuum

insulation are commercialised in order to facilitate low energy building refurbishments. However it may only be possible to fully address this issue by collective government/industry action.

Without novel materials, the standards of thermal insulation that can be achieved using conventional insulation products will be modest and the agenda to produce low and zero carbon buildings will be compromised. On the other hand, if these new retrofit measures are introduced on an urban scale, the reduction in CO₂ emissions from existing buildings will be significant and will play an important role in achieving CO₂ reduction targets.

References

- [1] DECC, Estimates of Heat Use in the United Kingdom, 2010.
- [2] Anastaselos D et al, Energy and Buildings 41 (2008) 1165-1171.
- [3] Caps R, et al. High Temperatures - High Pressures 33(2) (2001) 151 - 156.
- [4] CLG and ONS Statistic Release: Floorspace and Rateable Value of Commercial and Industrial Properties — 1 April 2007, England and Wales, 2008.
- [5] Committee on Climate Change Building a low-carbon economy-the UK's contribution to tackling climate change, 2008.
- [6] DECC. The carbon plan: Delivering our low carbon future, 2011.
- [7] DTI project, New Cladding Solutions to Produce a Step Change in Construction. Project number: TP/2/MS/6/1/10377, 2007.
- [8] Fine A, Journal of Thermal Insulation 12 (3), 1989, 183-208.
- [9] Materna R. International Conference and Workshop on High Performance Thermal Insulation Systems - Vacuum Insulated Products (VIP), 2001, 55-62.
- [10] ONS 2010. New orders in the construction industry, 2010.
- [11] Ramesh T et al, Energy and Buildings 42, 2010, 1592-1600.
- [12] Ravetz J, 36, 2008, 4462-4470.
- [13] Yan Q and Zheng C, Energy Procedia 11, 2011, 2489-2496.
- [14] Zwerger M and Klein H, 7th International Vacuum Insulation Symposium, 2005.

Long-term Performance of Vacuum Insulations Panels in Buildings and Building Systems

Pär Johansson*, Bijan Adl-Zarrabi, Axel Berge

Department of Civil and Environmental Engineering, Chalmers University of Technology SE-412 96 Gothenburg, Sweden

Abstract

The extremely low thermal conductivity of vacuum insulation panels (VIP) leads to less required insulation thickness in different applications. This paper aims to present our research findings related to the long-term performance of VIPs based on measurements during the last five years. The measurements were performed both in laboratory and in field where the real condition are present. The performance of an exterior wall retrofitted with VIPs and a hybrid insulated district heating pipe were observed. The expected service life of both application are more than 50 years. Thus, the long-term performance of the VIPs is of interest. The results of the evaluation indicate that there is no considerable performance degradation after five years in the wall application and after three years in the hybrid insulated pipes. The results are promising. However, it is still too soon to make final conclusions of the entire service life performance of the applications.

Keywords field study, laboratory study, numerical model, retrofitting, district heating

1. Introduction

The extremely low thermal conductivity of vacuum insulation panels (VIP) leads to less required insulation thickness in different applications. This is especially beneficial in metropolitan areas with high rental costs and in cultural heritage buildings where the space for insulation is limited. Since the beginning of the 1990s several buildings have been insulated with VIPs. A survey of 19 buildings in Germany showed that there is a low degree of damages after the VIPs have been installed in the building [1].

VIPs are also used in pipe insulation. The district heating system was introduced in Sweden in the 1940s and today over 20000 km of pipes are placed in the ground. In the future buildings are expected to demand less energy for heating. Therefore, the heat transfer per meter pipe is expected to decrease. Many energy companies are also facing large renovation needs in their pipe systems. By using VIPs for hybrid insulation of district heating pipes the heat losses in the system can be

reduced.

Discussions are ongoing among researchers in the field on how to evaluate the long-term performance of VIPs. One suggestion is to measure the increase of the internal pressure and weight of VIPs stored in 23°C and 50% relative humidity (RH) initially, after 3 months and after 6 months. An accelerated ageing measurement procedure is also proposed where the thermal conductivity is assumed to be only dependent on the increased gas pressure inside the VIPs. The final thermal conductivity after storage in a cycling climate for 8 days and then in 80°C for 180 days is regarded as the 25 year value. However, the real condition of a specific application could be far from these conditions. In buildings VIPs seldom are directly exposed to moisture and temperature because they are embedded in materials in the wall, floor or ceiling. In district heating, VIPs are exposed to temperatures above 100°C and they are in a dry environment with high concentrations of the gas cyclopentane.

* Corresponding author, Tel: 46 -(0)31 - 772 1966, Fax: 46 -(0)31 - 772 1993, E-mail: par.johansson@chalmers.se

The service time of both application mentioned above are more than 50 years. Thus, the long-term performance of the VIPs is of interest. This interest is also expressed by IEA/EBC Annex 65 Long-Term Performance of Super-Insulating Materials in Building Components & Systems. This paper aims to discuss and identify the boundary conditions present in buildings and district heating pipes and their effect on the service life of VIPs. The evaluations were performed in laboratory and in field where the real condition are present. The results related to the long-term performance evaluation of VIPs during the last five years are presented and discussed.

2. VIPs in an exterior wall

A building from 1930 was insulated with VIPs in the exterior wall. Fig. 1 presents the elevation and section of the facade with the 20 mm thick VIPs which are protected by 30 mm mineral wool.

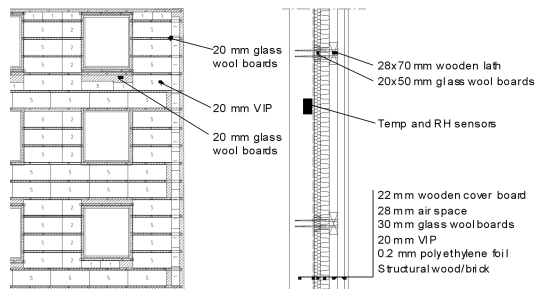


Fig. 1 Case study building wall with VIPs

To enable installation of the wooden cover board on the exterior of the insulation, mineral wool boards were cut in 20 mm thick strips and placed in the junction between two VIPs. During the construction 3 VIPs out of 180 (1.7%) were damaged and changed to new panels[2].

Temperature and RH sensors were installed in the wall on the interior of the VIPs, and sensors also monitor the interior and exterior climate. The wall was finished in August 2010 and there are now more than 4 years of complete data available. To evaluate the performance change with time the temperature measurements have to be corrected for the different indoor and outdoor conditions. A dimensionless temperature factor for the temperature in the wall can be calculated by using Eq. 1:

$$f = \frac{T_{\text{indoor}} - T_{\text{sensor}}}{T_{\text{indoor}} - T_{\text{outdoor}}} \quad (1)$$

where

T_{indoor} = indoor temperature,

T_{sensor} = sensor position temperature,

T_{outdoor} = outdoor temperature.

The lower the temperature factor is, the higher the thermal insulation on the exterior of the sensor. On the interior side of the wall the temperature factor is 0 and on the exterior side it is 1. The temperature factor in the wall is compared to a non-insulated reference wall during January 2011 to 2015 in Fig. 2.

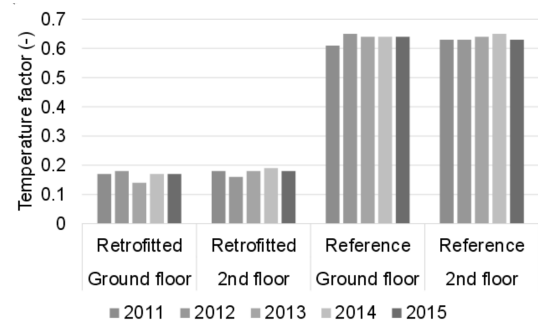


Fig. 2 Temperature factor for the wall with VIPs compared to a non-insulated reference wall for January, 2011 to 2015, calculated using Eq. (1)

The wall with VIPs has an average temperature factor of 0.17 while it is 0.64 for the non-insulated reference wall. The temperature factor is stable during the five years which means there is no significant change of the heat flow or temperature profile in the wall. During these four years the temperature and RH at the center of the VIPs was on average 22°C and 37% RH while it varied between 14~30°C and 20%~51% RH. Inside the building the temperature was between 20~33°C and 18%~79% RH while it was -13~36°C and 10~100% RH outdoor.

3. VIPs in hybrid insulated district heating pipe

VIPs have a large impact on the thermal performance of hybrid insulated district heating pipes [3, 4]. The VIPs are combined with polyurethane foam insulation as presented in Fig. 3.

One main concern is the long-term durability of the VIPs. In district heating pipes the temperature can reach 120°C. This is higher than the temperature limit for conventional VIP envelopes. Berge and Adl-Zarrabi [4]

stored VIPs at different temperatures in an oven. Some VIPs lost their vacuum already at temperatures around 70°C.

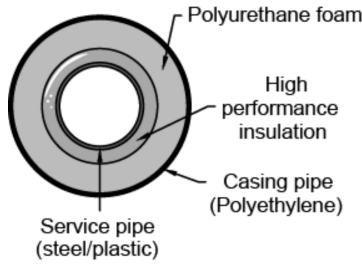


Fig. 3 Concept for hybrid insulated district heating pipes with VIPs and polyurethane foam insulation

In a pipe the temperature will not be evenly distributed throughout the cross section of the insulation, but will rather form a gradient. A hypothesis is that the sealing of the VIP envelope is the weak point of the diffusion barrier. Strategic location of the sealing could significantly improve the high temperature durability of the VIPs. For example the sealing could be located towards the colder side of the pipe.

The effect of the sealing location was tested in laboratory by measuring the temperature at different positions in a district heating pipe insulated with an 8 mm thick VIP surrounded by polyurethane foam. The relative thermal conductivity, p_λ , of the VIP and the polyurethane was calculated by Eq. (2) based on [5], assuming a constant heat flow.

$$p_\lambda = \frac{\lambda_2}{\lambda_1} = \frac{(T_1 - T_2) \cdot \ln(r_3/r_2)}{(T_2 - T_3) \cdot \ln(r_2/r_1)} \quad (-) \quad (2)$$

where

λ =thermal conductivity of layer n ,

r =radius to the boundaries,

T =temperature at certain distance.

The inner pipe of the district heating pipe had a radius of 45 mm (r_1) giving an outer radius of the VIP layer at 53 mm (r_2) and the outer radius of the polyurethane foam was 90 mm (r_3). The resulting temperatures are shown in Fig. 4.

The temperature in the service pipe is 115°C, while the temperature in the VIP envelope is less than 90°C and the temperature on the exterior of the vacuum insulation panels are around 60°C. After more than two years, no temperature increase can be detected.

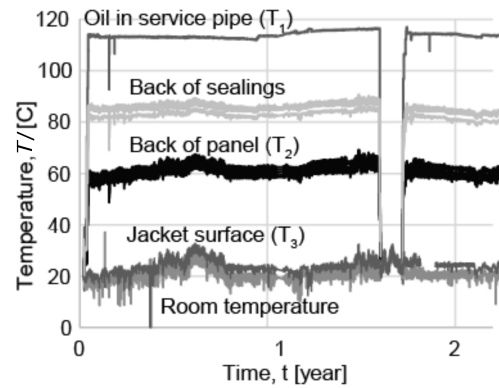


Fig. 4 Temperatures at a number of positions in hybrid insulation district heating pipes tested in laboratory

To estimate the thermal performance of the VIPs, making sure that they were not installed filled with air, the relation between the thermal conductivity of the polyurethane foam and the VIP was calculated according to Eq. (2). The calculation gave a relation between the materials of 4.4. This shows that the VIP has a consistent superior thermal performance compared to the polyurethane foam. Similar results have also been seen in field measurements [6].

4. Results and discussions

The results of the evaluations indicate that there is no considerable performance degradation after five years in the wall application and after three years in the hybrid insulated pipes. The results are promising. However, it is still too soon to make final conclusions of the entire service life performance of the applications.

During the construction of the wall several practical issues were highlighted. It is important to provide standardized fastening methods to minimize thermal bridges. Also damages of VIPs during construction and condensation risks in the wall have to be paid close attention, especially at the thermal bridges. The quality assurance of VIPs if embedded in another material such as polystyrene has to be investigated since they cannot be easily controlled on the construction site in this case.

For the hybrid insulated pipes, the VIP performed much better in the complete hybrid insulation set-up than expected from laboratory evaluation of the panels by themselves. This can be explained by a number of factors where the nature of the film and its properties

need better specification. There could also be problems with the humidity and delamination of the film inside the pipe. Also the melting temperature of the polymer film might be different between VIPs used in the laboratory and field evaluations. More investigations are also needed of the dominant permeation which could be through the sealing and not through the envelope itself. In that case, the location of the sealings, in relation to the temperature gradients, could be of large importance.

5. Conclusions and outlook

VIPs are already used in many buildings and building systems. However, the long-term performance of the product is not entirely investigated. The ongoing monitoring of the applications presented in this paper will reveal the long-term performance of VIPs in real conditions. The work in IEA/EBC Annex 65 will reveal answers to several of the other important issues raised in this paper.

Acknowledgements

The work is supported by the Swedish Research Council for Environment, Agricultural Sciences and Spatial Planning (FORMAS), the public housing corporation Familjebostäder i Göteborg AB, the energy distributor Varberg Energi, the pipe producer Powerpipe Systems AB and the Swedish District Heating Association.

References

- [1] Heinemann U, Kastner R. VIP-PROVE: Vakuumisolationspaneele - Bewährung in der Baupraxis. Wissenschaftliche Begleitforschung. Schlussbericht Energieoptimiertes Bauen, ViBau Report ZAE 2-1210-11 (2010) (VIP-PROVE: Vacuum insulation panels - Testing in construction practice. Scientific evaluation. Final report energy optimized construction). [In German]. Bayerisches Zentrum für Angewandte Energieforschung e. V. ZAE Bayern, Würzburg, Germany, 2010.
- [2] Johansson P, Sasic Kalagasidis A, Hagentoft C-E. Retrofitting of a listed brick and wood building using vacuum insulation panels on the exterior of the facade; Measurements and simulations. *Energy and Buildings* 2014; 73(April 2014):92-104.
- [3] Berge A, Adl-Zarrabi B. Using high performance insulation in district heating pipes. 13th international symposium on district heating and cooling, Copenhagen, Denmark; District energy development center; 2012, p. 156 - 62.
- [4] Berge A, Adl-Zarrabi B. Evaluation of vacuum insulation panels used in hybrid insulation district heating pipes. 14th international symposium on district heating and cooling, Stockholm, Sweden; Swedish district heating association; 2014, p. 454 - 61.
- [5] Hagentoft C-E. *Introduction to Building Physics*. Lund, Sweden; Studentlitteratur; 2005.
- [6] Berge A, Adl-Zarrabi B, Hagentoft C-E. Field measurements district heating pipes with vacuum insulation panels. Submitted to *Renewable Energy*, 2015.

Optimal Connectors for Use in Precast Concrete Sandwich Panels Containing VIP

Thierry Voellinger^{*}, Flourentzos Flourentzou

Laure Laboratoire d'Architecture Urbaine, CH - 1015 Lausanne, Switzerland

Abstract

In a traditional precast concrete sandwich panel, interior connectors join the facade layer to the structural layer. To accomplish this these interior connectors pierce the insulation layer. The application of VIP insulation in precast panels used in dense urban environments makes traditional style interior connectors obsolete, because the VIP insulation cannot be cut or pierced. Thus, new types of connectors are required that respond to the module dictated by the VIP panel sizes. We experimented with 1 : 1 scale connectors within an element measuring 3m × 1.2m. These connectors are made from fiberglass and carbon, and have a lower lambda value than traditional stainless steel connectors. The connectors used were able to be placed in a manner where they passed alongside the VIP insulation panels without piercing their protective foil covering. In addition, laying the connectors in the mold was simple and efficient. To continue to strive for precast concrete panels with optimized thermal performance, connectors must be used that are tailored to this task.

Keywords facade wall, precast concrete sandwich panel, high performance thermal insulation, vacuum insulation panel, VIP, module, connectors

^{*} Corresponding author; Tel : 4121 - 6930871 E-mail: thierry.voellinger@epfl.ch

Full-sized Vacuum-sealed Insulating Glazing (VIG) Windows for Residential Applications

Anil Parekh*

Senior Research Manager, Canmet Energy, Natural Resources Canada, Ottawa, ON, Canada

Abstract

The current state-of-the-art of the vacuum insulation glazing (VIG) technology and assessed the technical feasibility, thermal and heat transfer assessments of various components for assembly and manufacturing of VIG windows have been reviewed. The focus of this paper is to present how best VIG can be assembled in the whole window configuration that can provide minimum possible U-value without drastically affecting the vision area. Using detailed thermal and 2-dimensional heat transfer models, evaluated the relative impacts of various framing materials, size and dimensions for VIG and other assembly components to design VIG windows. The review of the current state of VIG technologies identified a number of potential options for window manufacturers and clearly identified minimum specifications that can achieve lower than $0.7 \text{ W}/(\text{m}^2 \cdot \text{K})$ windows. For example, thermal and 2D heat transfer analyses provided the required overlap of at least 55 mm, about 40 mm more than conventional, for framing components with the VIG to improve edge U-value. The industry partner working with the project team developed three test sample VIG windows incorporating the above study parameters. The measured thermal performance results confirmed that it is feasible to integrate VIG in the residential size windows that show excellent thermal performance. This study confirms the commercial viability of VIG window manufacturing for the cost-sensitive housing and building markets in North America.

Keywords vacuum-insulation glazing (VIG), housing, heat transfer, windows, thermal analysis

1. Introduction

Windows and fenestration systems are integral and common elements to all residential and commercial buildings. Energy use associated with windows account for 15% to 27% of space heating and cooling needs in residential buildings and about 8% to 13% in commercial buildings in North American cold climate zones [NRCan 2011].

The current state-of-the-art for improving thermal and solar-optical performance of glazing units include (1) low-emissivity coatings, (2) the inclusion of inert gases between glazing, and (3) low-conductance spacers and framing materials. These advances have improved the conventional thermal performance of a double-glazed window from a heat loss coefficient or U-value of $2.6 \text{ W}/(\text{m}^2 \cdot \text{K})$ ($R \sim 2$) to a very efficient commercially available window with $0.9 \text{ W}/(\text{m}^2 \cdot \text{K})$

($R \sim 6$) affording significant energy efficiency benefits for housing and buildings.

The current technology options for advancing the thermal performance of windows; however, have reached a point where any further improvement is on a path of steeply diminishing returns. For the next generation of highly efficient housing and buildings, targeted to the level of close to zero energy use, the thermal and optical performance of windows need to be much higher. One theoretically feasible option which would provide a breakthrough to improved performance would be to vacuum the space between the glazing. A high degree of vacuum (less than 0.1 Pa of absolute pressure) can effectively reduce the convective and conductive heat losses. Laboratory tests of small-scale vacuum insulated window samples have shown U-values

* Corresponding author, Tel :1-613-9471-959, E-mail: anil.parekh@nrcan.gc.ca

in the range of 0.30 to 0.45 W/(m² · K) (close to R-12 to R-16).

The Sustainable Housing Technology Roadmap for Canada has identified the vacuum insulation glazing windows as one of the mid- to long-term technology focus for very efficient housing [13]. Recently published IEA Technology Roadmap for Energy Efficient Building Envelopes identified vacuum insulation glazing (VIG) windows as one of the key emerging technologies for the residential and commercial building sectors particularly heating dominated climates [15]. The roadmap specifically narrates the thermal and solar optical advantages of vacuum insulation glazing systems.

Therefore, an important question is how much these very efficient high performance windows would affect the overall energy consumption of a home in the northern climates of Canada. For this analysis, as per the current 2012 NBC code baseline, the minimum conventional window is a double-glazed, low-E, argon-filled with a U-value of 1.8 W/(m² · K) and SHGC of 0.40 [10]. The VIG window has an overall U-value of 0.57 W/(m² · K) and SHGC of 0.48. Using several archetype house files and in different climate zones and energy analysis using HOT2000 energy analysis software [5], on an average VIG windows would save as low as 0.7 to 1.2 GJ per square meter of a window as shown in Fig. 1, enabling overall improvement in energy efficiency of a home by 7% to 22% in Canadian climates. For near and net-zero energy homes, where every bit of energy consumption counts, the net-energy positive aspects of windows is very important.

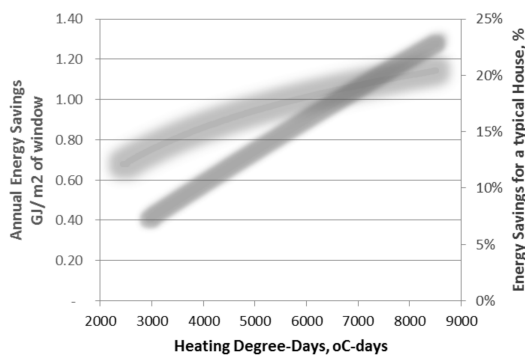


Fig. 1 Potential annual energy savings with vacuum windows

This paper focusses on integration of vacuum

insulation glazing (VIG) into the windows. The detailed thermal and heat transfer analyses are presented to depict the importance of window framing components and VIG to achieve very efficient windows with an overall heat loss coefficient, U-value, of 0.6 W/(m² · K) or lower.

2. VIG Technology Overview

The thermal resistance power of vacuum was first demonstrated in the makings of insulated glazing proposed in the patent application by a German physicist Zoller in 1913 [19]. Since this first invention, a number of variations and designs of vacuum insulated glazing have been developed and patented; however, none of these led to a successful and reliable product.

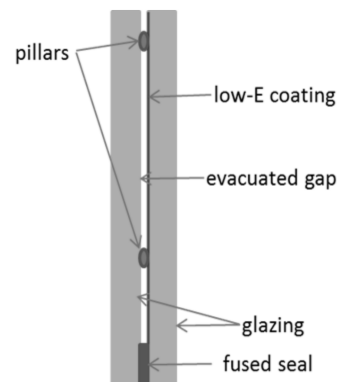


Fig. 2 Components of VIG

Vacuum insulated-glazing unit consists of two sheets of glass separated by an evacuated space. This is made possible by an array of support pillars and seal of fused solder glass around the edges of sheets as shown in Fig. 2. Due to vacuum between the sheets, there is negligible interpane heat transfer by conduction and convection. In comparison to argon, which is common inert gas filled in the conventional insulated glazing units, an evacuated gap at less than 0.01 Pa (one millionth of atmospheric pressure), can reduce the interpane heat transfer by more than 35 times, as shown in Fig. 3. The main heat flow across the glazing are therefore: the radiative heat transfer between the internal glass surfaces, the conduction through the support pillars, and the conduction along the glass sheets and through the edge seal.

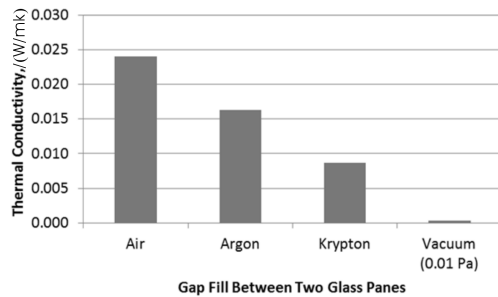


Fig. 3 Effective conductivity of interpane gaps in insulated-glazing units

During 1986—1989, Drs. Robinson and Collins from the University of Sydney demonstrated the successful production of a 60 cm by 60 cm vacuum glazing unit with a high degree of thermal insulation. The calorimetric measurements showed the center glazing heat loss coefficient of less than $0.35 \text{ W}/(\text{m}^2 \cdot \text{K})$. Subsequently, Collins and his team, working with an industry partner, produced over 600 samples of vacuum glazing of up to 1 m by 1 m. Dr. Collins and his team's modern pioneering work, between 1987 to 1995, at the University of Sydney brought forward new approaches in manufacturing of vacuum insulated glazing units. Their focus included;

- glazing pane separation pillars to resist very high compression stresses;
- reliable and consistent methods for evacuating glazing cavity to ultra-low pressures (below 0.1 Pa);
- fused-glass edge sealing methods; and
- glazing properties with low iron, higher thickness ($> 4 \text{ mm}$), tempering process.

Subsequent work with the industry partners, the following technical challenges were faced for manufacturing of vacuum glazing units;

- Structural strength of glass (glass breakage)
- Structural integrity of large size of separating pillars (effective thermal bridges which reduce the overall thermal resistance of glazing unit)
- Iterative and several step processes for fused glass edge seal
- The tempered glass provides higher structural strength to withstand the atmospheric air pressures; however, it is unsuitable for fused edge seals that required high temperature solder glass melt. Also, tempered glass is not very flat and the surface variation

can change the width of evacuated space.

As part of Prof. Collins team at University of Sydney, Dr. T. M. Simko rigorously defined and developed the calculation procedures for heat transfer processes and structural stresses of vacuum insulated glazing units. The measured data showed center glazing U-value of $0.71 \text{ W}/(\text{m}^2 \cdot \text{K})$ for an average of three same size samples. Considering the edge effects, the U-value of VIG was $1.11 \text{ W}/(\text{m}^2 \cdot \text{K})$. The edge effects, although accounted for only 14.4% of a sample, reduced the thermal performance by 36% of overall VIG [15]. Covering the VIG edges with higher thermal resistance materials is one of the ways to improve the overall thermal resistance of a VIG window.

In 2002, Bundesministerium für Wirtschaft und Technologie (BMWi), the German Federal Ministry of Economics and Technology funded a multi-year multi partner collaborative research project to investigate the technical feasibility of permanently vacuum-tight glazing systems that would be cost competitive in the European market. The BMWi VIG initiative involved a collaboration of three research institutes and five medium-sized glazing manufacturers with the following objectives [18]:

- development of Vacuum Insulation Glass (VIG) with $U = 0.4 \text{ W}/(\text{m}^2 \cdot \text{K})$;
- thermal optimization (spacers, edge seal, low- ϵ -coatings);
- optical optimization (glare and visibility of spacers, transmission, g-value);
- edge seal concepts (glass-glass-joints, metal foils, high-barrier adhesives);
- development of production process for VIG; and
- production costs similar to triple glazing.

This multi-million euro dollars collaboration resulted in significant progress in the automated manufacturing of VIG units [18]. The BMWi demonstrated the feasibilities of mass production of VIGs and summarized that the Vacuum Insulation Glass (VIG) with U-value of $0.4 \text{ W}/(\text{m}^2 \cdot \text{K})$ is possible if:

- gas pressure in cavity between two glazing is less than $\leq 0.01 \text{ Pa}$ (or 10^{-4} mbar)
- pillars are separated by at least 40 mm or more and thermal conductivity is less than $1.0 \text{ W}/(\text{m} \cdot \text{K})$

- emissivity of low- ϵ -coating on either surface 2 or 3 is less than 0.1; and, particularly important to window manufacturers,

- highly insulating frame with an overlap of VG edge by at least 40 mm or more.

In 2006, US DOE awarded an industry research contract to EverShield Windows Inc., based in Evergreen, Colorado, to develop and test a flexible edge-seal for VIG units. The project resulted in the development of innovative flexible edge seal that performed well in accelerated laboratory testing. In collaborations with various large insulated-glazing manufacturers in the US, EverShield also demonstrated a number of sample sizes achieving a whole window U-value lower than $0.57 \text{ W}/(\text{m}^2 \cdot \text{K})$. This research project produced a number of US patents and proprietary commercial value intellectual property for the participants [3]. Except for general descriptions most of these material specifications and manufacturing process information is not available.

The current state of the VIG technology is as follows:

(1) There are reliable, consistent and durable methods for generating low vacuum pressures within the gap between glazings.

(2) The edge-sealing methods have improved significantly. The German sponsored VIG project, University of Sydney's pioneering work with Japanese Nippon Steel and the US DOE's industry research project with EverShield Windows significantly contributed in the development of durable and reliable edge-sealing materials and methods.

(3) A number of North American, European, Japanese and Chinese insulated glazing manufacturers are now manufacturing larger size VIG that are in the range of 1 m by 1 m (3' by 3') to 1.3 m by 1.7 m (4' by 5').

(4) The increment cost of VIG is still high. As per one North American VIG manufacturer, a residential size triple-glazed window with one low-E, argon filled and with insulated spacer would cost about \$375 per square meter (\sim \$35/sq ft). The equivalent VIG may cost about \$500 to \$560 per sqm or 40% to 50% higher. Although, the overall U-value of VIG is two-

and-half times better than the said triple-glazed window.

(5) One of the glaring missing links is the window manufacturing industry. Window manufacturers generally assemble the insulated-glazing unit within the frame components and attach the operating hardware for the closing and opening mechanisms. Very few window manufacturers have explored the ways in which they can "integrate" the assembly of VIG in the conventional window production process.

3. Design considerations of VIG windows

The research project explored the feasibility of vacuum insulated glazing in residential-size windows for Canadian housing market. The main goals were:

- to assess design and processes of fabricating large size vacuum-sealed glazing units

- a proto-type development and fabrication potential of full-sized vacuum-sealed insulating glazing units for residential and commercial buildings; and

- the laboratory testing of prototype vacuum-sealed glazing units.

The leading driver for this research project was a mid-size Canadian window manufacturing company. This Canadian window company in partnership with off-shore proponents who are expert in vacuum technologies and impermeable fused-glass sealing are taking technical and financial risks to test and verify these applications for large size windows.

The window production process consists of:

(1) assembling an insulated glazing unit—the insulation glazing unit is generally done by insulated glazing or a window manufacturer. This includes glass cutting, assembling with a spacer bar and gas filling. Specialized insulation glazing units (IGU) are manufactured by glazing manufacturers.

(2) assembling a window — this is exclusive to window manufacturers who assemble a complete window with a frame, sash, mullions, operating and lock mechanisms along with a glazing unit with necessary sealants. Majority of small- and mid-size companies assemble windows by procuring all these components including IGUs. Most window manufacturers will opt for procuring a full vacuum insulation glazing unit.

3.1 Technical Challenges

There are a number of technical challenges and unknowns that include:

- vacuum insulated glazing unit (VIG)
 - Uncertainty around the structural strength of the glazing system to withstand stresses.
 - Durability and effectiveness of the sealing system.
 - Fabrication methods and process for large size prototypes with high degree of vacuum.
 - Development of highly-impermeable and extremely low emission glass coatings for long-term sustenance of vacuum will needed.
- window components with VIG
 - placement and assembly of VIG mainly due to steep temperature gradient-VIG and one more glazing forming a triple-glazed window is one solution preferred by window manufacturers
 - frame components to support and protect the edge of VIG
 - methods for increasing the thermal insulation surrounding the edge of VIG
- measured data on the thermal and optical performance of VIG windows
 - one of the key requirements of window manufacturers is the proven thermal and optical performance data
 - energy performance assessment of VIG windows in comparisons to conventional triple-glazed windows
 - cost benefit assessments

The research focused on how best VIG can be assembled in the whole window configuration that can provide minimum possible U-value without drastically affecting the vision area. The research efforts are not on how the VIG is designed and manufactured.

3.2 Thermal Analysis

The thermal analysis involves modeling the full-sized window with 2-dimensional heat transfer analysis. The analysis model includes: (1) analysis using published correlations for modeling vacuum and pillar array conduction heat transfer; (2) radiation heat transfer is solved explicitly using parallel plate theory; and 3) pillar array conduction heat transfer and radiation heat transfer between surfaces in vacuum space are modeled to account for point thermal bridges such as

pillars. This algorithm is now incorporated in the WINDOWS 7. 2. 8 (beta version) software [8]. The thermal analysis involved the following steps:

- Identifying, selecting and defining components of VIG window;
- Thermal and solar-optical analysis of VIG using the WINDOWS 7. 2. 8 -beta version;
- 2D thermal analysis of edge and frame components using the THERM heat transfer analysis program [9];
- Parametric analysis for determining the size of various frame components to minimize the overall U-value of a whole window without undue impact on the visible area.

Tab. 1 Description of window components

Window Components			
1	Vacuum Insulation Glazing		Parametric Variables
	Size	0.66 m × 1.57 m	
	glass thickness	4 mm	
	pillar radius	1 mm	
	pillar spacing	35 mm	(varied 20 mm to 50 mm)
	Vacuum gap	0.2 mm	
	Vacuum pressure	0.01 Pa	
	low-E on surface #3	0.068	(varied 0.022 to 0.84)
	edge seal thickness	10.5 mm	
	edge seal	fused glass	
2	Outside glass	3 mm	
	gap	6.8 mm	
	gap filling	Argon	
3	Frame	reinforced fiberglass	
	thickness	158 mm	
	height	85 mm	(varied 85 to 160 mm)

3.3 Components

Tab. 1 lists the components of windows and other dimension ranges used for this study. Thermal performance sensitivities are determined by varying material properties and model dimensions. Tab. 2 displays the material properties for each component used in the numerical simulations. Base material data is obtained from NFRC 100-2010 [11]. Tab. 3 displays the boundary conditions employed in calculating the U-value of various components of windows.

4. Analysis Results

4.1 Glazing Details

For a VIG window, it is important to consider a

“triple-glazed” configuration. VIG is made of two glazing each 4 mm thick and one with low-E coating, separated by a vacuum gap of 0.15 to 0.2 mm by pillars equally spaced around. The VIG is configured with a 3 mm conventional glazing separated by 6 to 12 mm gap and filled with argon. As shown in Fig. 4, the triple-glazed configuration improves the U-value of the whole glazing assembly.

4.2 Low-E glazing

For the VIG, the selection of a low-E glass is very important. The 2D heat transfer analysis showed that the surface #3 emissivity value significantly affect the center glazing U-value of the VIG. As shown in Fig. 5, lower the emissivity value of the surface #3 of the glazing, the better is the U-value of the overall VIG. Analysis results showed that surface #3 emissivity value must be lower than 0.10 to be able to obtain better overall U-value of the VIG. Figure 6 shows the temperature infrared plot of the edge and center of VIG cross section at a pillar away from the edge. The plot analysis showed that at each pillar (radius of 0.5 mm) the thermal bridging effect is in the radius of approximately 3.8 mm for the configurations used in this analysis.

4.3 Framing and edge insulation

One of the key considerations for achieving the lower overall U-value of VIG window is to insulate the edge of the glazing unit so that the edge losses are minimized. The project team evaluated a number of options with different framing configurations, materials and the overlap of the edge with framing components. Figure 7 shows the typical cross section of window frame.

Tab. 2 Thermal properties of materials.

Thermal properties		
	Conductivity/(W/(m · K))	Emissivity
Outside glass	1.00	0.84
VIG surface #3	1.00	0.068
Pillar	4.20	0.9
Edge seal	1.00	0.9
Fiberglass	0.0310	0.9
air cavity	0.0241	
argon	0.0164	
vaccum	0.00036	

Tab. 3 Boundary conditions used in the analysis using Windows 7.2 and THERM

Boundary Condition	Value	Unites
Indoor temperature	293.15	K
Outdoor temperature	255.15	K
Incident solar radiation on surface	0	W/m ²
Combined convection and radiation surface coefficient of heat transfer for the indoor section	7.6	W/(m ² · K)
CCombined convection and radiation surface coefficient of heat transfer for the indoor section	30	W/(m ² · K)
Density of heat flow rate at lines of symmetry Potential for condensation evaluated at indoor humicity level	0 50%	W/m ²

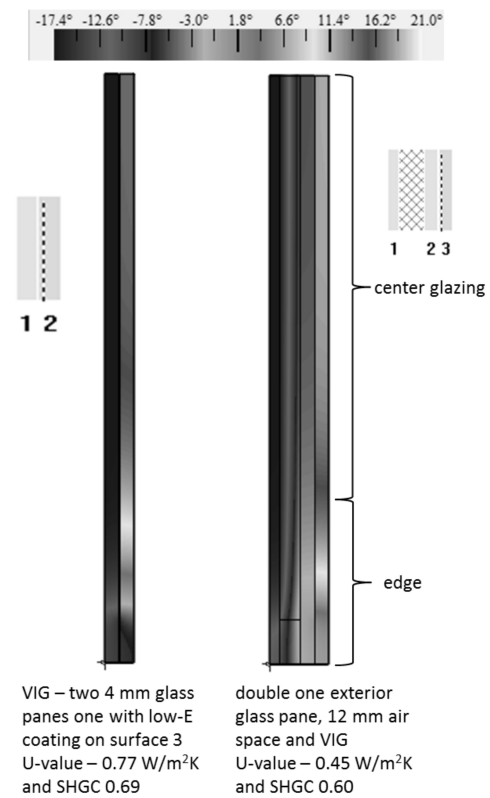


Fig. 4 Glazing configuration

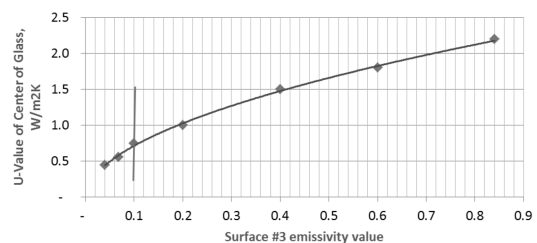


Fig. 5 Center of glazing (cg) sensitivity to surface #3 emissivity

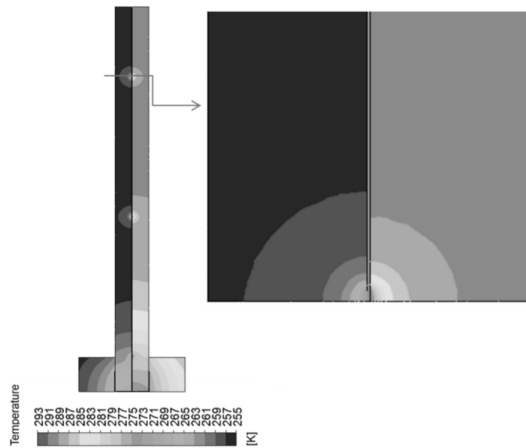


Fig. 6 Center of glazing (cg) temperature profile at the pillar

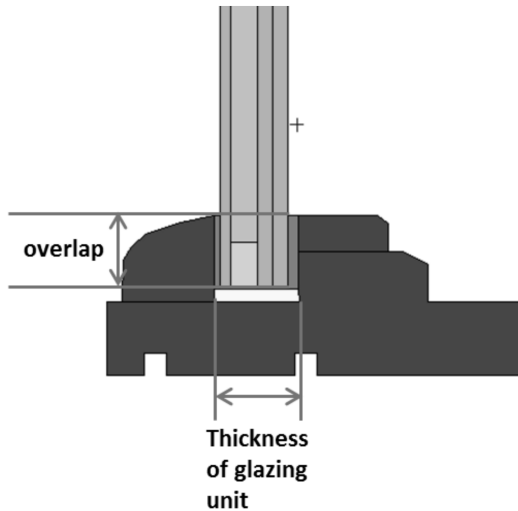


Fig. 7 Window cross section showing the framing and VIG configuration

The 2D heat transfer analyses were performed for the depth of overlap of VIG glazing edge in the frame of 0mm, 10mm, 15mm, 20mm, 35mm, 55mm, 70mm and 88mm. The conventional commercially available windows have generally edge overlap of 15 mm. The isotherm plots of overlaps of 20 mm and 55 mm are shown in Fig. 8. The 20 mm depth covers the spacer within the frame cavity; however, the 2D heat transfer analysis showed potential for condensation for maintaining indoor humidity level of 50% during the winter months when the outdoor temperature is below -18°C . Raising the overlap to 55 mm mitigated the risk of potential condensation.

These analyses results are plotted in Fig. 9. The improvement in the edge U-value is significant as the

overlap increases up to about 55 mm. Just after 55 mm the relative improvement in the edge value is small as the edge is significantly insulated to near the frame U-value.

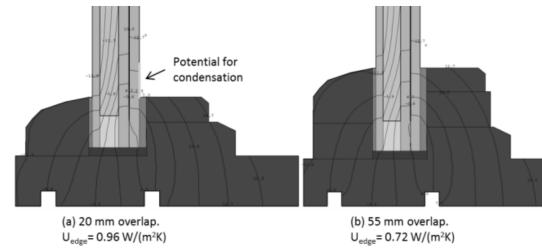


Fig. 8 2-dimensional heat transfer analysis with different overlaps of edge insulation

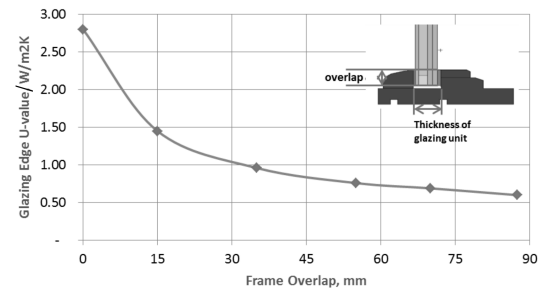


Fig. 9 Edge U-value as a function of the frame overlap

The in-depth glazing system analysis using WINDOWS 7.2.8 (beta) and 2D heat transfer analysis using THERM provided a number of design parameters for the window manufacturer to consider. These are as follows:

- Procure vacuum insulation glazing (VIG) units that have (1) vacuum pressure less than 0.01 Pa (10^{-4} milibar), (2) each glass pane is at least 4.0 mm thick, (3) spacing between two glass separated by transparent or semi-transparent pillars of about 1 square millimeter; (4) edge seal of VIG is fused-glass or metal fused with glass or very reliable seal; and (5) the surface #3 of the glazing should have a low-E coating which is highly-impermeable and extremely low emission glass coatings for long-term sustenance of vacuum.

- VIG should have center glazing U-value of 0.5 $\text{W}/(\text{m}^2 \cdot \text{K})$ or better.

- VIG should be configured with a triple-glazed form to alleviate thermal stresses on the edge.

- The framing component should be of high insulation value. Reinforced vinyl or fiberglass frames

can enhance the overall U-value of VIG windows.

- The edge of the VIG should have an overlap of 55 mm or more to improve the overall U-value of a window.
- The above specifications can achieve a VIG window with an overall U-value of $0.48 \text{ W}/(\text{m}^2 \cdot \text{K})$.

5. Prototypes and thermal performance

The Canadian industry partner* for the project procured ten VIG samples from an offshore company.

The VIG supplier provided the thermal performance data as per the NFRC 100-2010 procedures (equivalent to CSA Standard A440.2) claiming the VIG unit U-value of $0.62 \text{ W}/(\text{m}^2 \cdot \text{K})$ with solar heat gain coefficient (SHGC) of 0.42.

Tab. 4 Specifications of three VIG samples procured from an offshore Glass company.

Size	0.66 m × 1.57 m
Glass thickness	5 mm
Pillar (square)	1 by 1 mm
Pillar spacing	35 mm
Vacuum gap	0.15 mm
Vacuum pressure	<0.015 Pa
Low-E on surface # 3	0.052
Edge seal thickness	18 mm
Edge seal	fused glass

These three windows were assembled in the factory using the conventional window manufacturing practices and with conventional sealants.

Window 1: Triple glazing with a 3mm glass, 12.7mm space and VIG. The framing components consist of reinforced foam-filled vinyl frame with an overlap of depth of 15 mm (conventional practice). This has two VIG units sealed together (silicone superspacer method) into a single 35 mm (1 3/8") sealed unit.

Window 2: Triple glazing with a 3mm glass, 8 mm space and VIG. The framing components consist of reinforced foam-filled vinyl frame with an overlap of depth of 55 mm. This has one VIG unit sealed together into a 22 mm (7/8") overall sealed unit.

Window 3: This is a 10-mm thick VIG unit glazed on its own. Used rubber setting blocks to shim the VIG in place with the 22 mm (7/8") window glass stop.

Tab. 5 Overall U-value of test samples with VIG

Test Samples	U-value/ $(\text{W}/(\text{m}^2 \cdot \text{K}))$	
	Center of Glazing U_{cg}	Total U_w
WG	0.61	0.73
Window 1	0.61	0.80
Window 2	0.49	1.01
Window 3	0.62	1.11

6. Conclusions

The vacuum insulation glazing is now more than feasibility for commercial production of large size windows. A number of North American, European, Japanese and Chinese companies are now promoting the VIGs; however, the market is still marginal and small. One of the barriers is the lack of window manufacturers, who generally assemble the glazing units in the full window product, offering the VIG windows. The review of the current state of VIG technologies identified a number of potential options for window manufacturers and clearly identified minimum specifications that can achieve a leap through thermal performance.

This technical paper enumerated detailed thermal and heat transfer analyses of window components for integrating VIGs. These findings can assist window manufacturers to specify VIG that can significantly improve the overall thermal performance of windows.

Whatever the future directions for the vacuum glazing windows, the results of this paper confirm that it is possible to make very efficient full size windows in North America that exhibit excellent thermal performance. Analytic methods and procedures are well-developed to accurately determine component by component thermal and energy performance. Further work is envisaged to continue VIG window's commercial viability in cost competitive housing and building markets.

* Due to business confidentiality, names of the company as well as VIG supplier are not presented. VIG specifications are provided by the VIG manufacturer. No test or measurement details provided.

Acknowledgements

The VIG research and feasibility demonstration germinated from a window industry partner's business plan to take pro-active leadership in assembling and selling vacuum insulated glazing windows for Canadian markets. The project team gratefully acknowledges financial support of the Program of Energy Research and Development (PERD) of Office of Energy R&D (OERD) of Natural Resources Canada. This project was part of PERD Subprogram on Building Envelopes (PII 2004). We appreciate and acknowledge unflinching support of a number of individuals in the insulated glazing (IG) and window industry who provided valuable information. Insulated Glazing Manufacturers Association (IGMA) helped in connecting with right contacts in the industry.

References

- [1] Collins, R. E. and T. M. Simko. 1998. Current status of the science and technology of vacuum glazing. *Solar Energy*.
- [2] CSA A440.2 2010. Energy performance of windows and other fenestration systems. Published by Canadian Standards Association, Rexdale, Ontario.
- [3] EverShield 2009. DE-EE0004024; High Reliability R-10 Windows Using Vacuum Insulating Glass Units (VIGUs). Prepared for Department of Energy. Washington, D.C.
- [4] Green Building Advisor 2013. Cost of Windows-blog entry (<http://www.greenbuildingadvisor.com/blogs/dept/musings/choosing-triple-glazed-windows-cost-of-windows>)
- [5] HOT 2000. Energy Analysis Program for Housing and Small Buildings. Published by Natural Resources Canada, Ottawa, Ontario. (Free download at <http://www.nrcan.gc.ca/energy/software-tools/7421>)
- [6] IEA 2013. Technology Roadmap for Energy Efficient Building Envelopes. Published by International Energy Agency. ([http://www.iea.org/publications/freepublications/publication/Technology Roadmap Energy Efficient Building Envelopes.pdf](http://www.iea.org/publications/freepublications/publication/Technology%20Roadmap%20Energy%20Efficient%20Building%20Envelopes.pdf))
- [7] IGMA 2014. White Paper - Vacuum Insulation Glazing. Published by Insulated Glazing Manufacturers Association, Ottawa, Ontario.
- [8] LBNL 2013-1. WINDOWS 7.2.8 (Beta) version. Lawrence Berkeley National Laboratory, Berkeley, CA. (free download at <http://windows.lbl.gov/software/window/7/>).
- [9] LBNL 2013-2. THERM version 6.3. Lawrence Berkeley National Laboratory, Berkeley, CA. (free download at <http://windows.lbl.gov/software/therm/therm.html>).
- [10] NBC 2012. National Building Code for Canada. Published by National Research Council Canada, Ottawa, Ontario. (<http://www.nationalcodes.nrc.gc.ca/eng/nbc/>).
- [11] NFRC 2010. NFRC 100-2010-Procedure for Determining Fenestration Product U-factors. Published by National Fenestration Rating Council, Greenbelt, MO. (<http://www.nfrccommunity.org/store/ViewProduct.aspx?id=1380591>)
- [12] NRCan 2011. Comprehensive Energy Use Database. Published by Natural Resources Canada, Ottawa, Ontario. (<http://oee.nrcan.gc.ca/corporate/statistics/neud/dpa/home.cfm>).
- [13] SHTR 2012. Housing for a Changing World-Sustainable Housing Technology Roadmap for Canada, Published by Industry Canada. <http://shtrm.ca>.
- [14] Simko, T. M. 1996. Heat transfer processes and stresses in vacuum glazing. Ph. D. Thesis, the University of Sydney.
- [15] Simko T. and Collins R. 1999. Determination of the overall heat transmission coefficient (u-value) of vacuum glazing. *ASHRAE Transactions*, v. 105, pt. 2, 1999, pp. 1-9.
- [16] Simko, T. M., R. E. Collins, Beck and D. Arasteh. 1995. Edge conduction in vacuum glazing. In *Proceedings of Thermal Performance of the Exterior Envelope of Buildings IV, Heat Transfer in Fenestration II*, Geshwiler M., Alger J., Moran M. (Eds), pp. 601-611, Florida, USA.
- [17] Simko et al. 1998. Temperature-induced stresses in vacuum glazing: Modeling and experimental validation. *Solar Energy*, 63[1], 1-21, 1998.
- [18] Weinlader 2005. Vacuum Insulation Glazing Project. BMWi. <http://www.vig-info.de/>
- [19] Zoller, F. 1924. Hollow pane of glass. German Patent No. 387 655.

Study on Adhesive Performance of Vacuum Insulation Panels and Its System in Building Application

Wu Wangping^{a*}, Chen Qing^b, Chen Zhaofeng^c, Zhao Feng^d

a. School of Mechanical Engineering, Changzhou University, Changzhou, 213164, P. R. China

b. Zhejiang Institute of Quality Inspection Science, Hangzhou, 310013, P. R. China

c. Super Insulation Composite Laboratory (SICL), College of Material Science and Technology, Nanjing University of Aeronautics and Astronautics, Nanjing, 210016, P. R. China

d. Changzhou Management Office of Wall Materials and Bulk Cement, Changzhou, 213001, P. R. China

Abstract

A vacuum insulation panel includes the core material, barrier envelope and getter, which is a high performance insulation component applied in the building field. The adhesive strength of vacuum insulation panel with the concrete wall is one of the key issues for building application, considering the safety and a service life under the extremely harsh natural environment. In this paper, the adhesive performance of vacuum insulation panel and its system was studied. The core material produced by the wet method was composed of the centrifugal wool and inorganic nonmetallic powders. The barrier envelope was composed of 50 μm PE, 15 μm PET, 10 μm Al, 15 μm PET and 60 μm glass fiber textile. The vacuum insulation panel system coated with cement mortar was maintained in the thermostatic-humidistat box for 14 days. The adhesive strength of the vacuum insulation panel and its system with cement mortar was measured by a pc-controlled electronic universal testing machine. The failure mode and mechanisms of vacuum insulation panel and its system after pullout testing were suggested.

Keywords VIP, building application, pullout testing, adhesive strength

1. Introduction

Vacuum insulation panels (VIPs) are regarded as one of the most promising high performance thermal insulation materials[1]. A VIP is composed of a core material with a micro-porous structure, a vacuum-tight envelope to maintain the inside vacuum and a getter or desiccant to adsorb various gases flowing into the vacuum [2,3]. Since 2005 year, the VIPs have been applied in building field as the insulation material in Europe[4 – 6]. However, the use of VIPs have been recently increasing to in China. There are different installed approaches for VIPs applied in building sector. In Europe, the VIPs are often fixed in one skeleton frame, and then fixed along the wall, floorboard or terrace. In China, the VIPs are adhered to

the wall through thermal insulation mortar. Therefore, there are some key factors in the tall buildings, such as the adhesion performance and repair working. The adhesive strength of VIP with concrete wall is one of the key issues for building application, considering the safety and service life under the extremely harsh environment. In this work, the adhesive strength, failure mode and mechanism of the VIP and its system after pullout testing were investigated and suggested.

2. Experimental procedure

The vacuum insulation panel (size: 10 × 10 × 1 cm³) was made in Suzhou V. I. P. New Material Co., Ltd. The core material was produced by wet method with mixture of the centrifugal wool and inorganic nonmetallic powders. The barrier envelope was

* Corresponding author, Tel: 86 – 18360430572, E-mail: wwp3.14@163.com

composed of 50 μm PE, 15 μm PET, 10 μm Al, 15 μm PET and 60 μm glass fiber textile. The inner pressure of the VIP was about 0.1 Pa. The heat-seal width of the envelope was ~ 10 mm. The three sides for the envelope was heat-sealed at $\sim 150^\circ\text{C}$ holding 0.24 MPa pressure for 1.5 s, but the last side was sealed at $\sim 168^\circ\text{C}$ keeping 0.34 MPa for 1.8 s, at the same time vacuum-pumping. The envelope is not flammable making it acceptable for building applications. To measure adhesive strength of the VIP, the positive and negative surfaces of VIP were coated with epoxy resin adhesive, and then adhered to the standard stainless steel samples. At the same time these samples were dried for one day in the air. The VIP coated with cement mortar was maintained in the thermostatic-humidistat box for 14 days (Fig. 1). The temperature and humidity were $20 \pm 2^\circ\text{C}$ and 95% RH, respectively. To check bond strength of VIP system, the preparation method was similar to the VIP. The adhesive strength of the VIP and its system were performed on a PC-controlled electronic universal testing machine (Model CMT5105, SANS Corp.), see Fig. 2. The load rate of the testing was about 5 mm/min.



Fig. 1 VIP system in the thermostatic-humidistat box



Fig. 2 Pullout testing for VIP

3. Results and discussion

3.1 Adhesive strength of VIP

Fig. 3 shows the normal VIP and the failure VIP after pullout testing. The surface of standard VIP sample was smooth and the bending strength was relatively strong due to the low inner pressure (Fig. 3 (a)). Here, four samples were carried out. In Fig. 3b, one side of sample #1 VIP became deformed; the other side was still bonded to the standard stainless steel. The failure of sample #1 was due to uneven sticker on the surface. The adhesive force was not up to the standard

value (0.1 MPa) of the pullout. However, the sample was not broken. In Fig. 3c, the barrier film of sample #2 was broken. Because the sample and barrier film could be deformed, it was broken until the limited deformed strength. It can be found from the right picture that the glassfiber film was torn. However, the Al film kept it's integrity. The adhesive form was just up the standard value. In Fig. 3(d), the glassfiber film in one side was debonded to the Al film, but the sample was not deformed. The adhesive strength of the glassfiber film with Al film was very important. In Fig. 3e, the sample #4 VIP was deformed along the interface between upper and down barrier films. Some portion for glassfiber film was torn. According to the above data, the bond strength of the envelope was satisfied to the bond strength of the VIP. Fig. 4 shows the adhesive force-displacement curve for VIP. The adhesive force was in the range from 0.1 to 0.2 MPa.

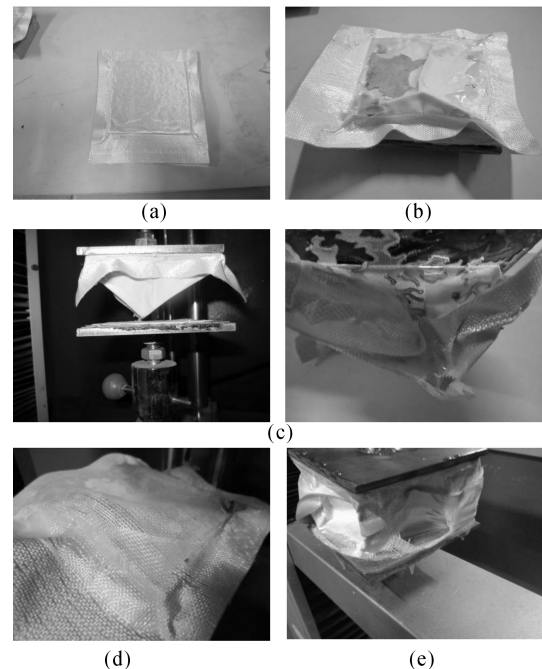


Fig. 3 Photos of VIP and the failure VIP after pullout testing

(a) Standard sample; (b) Sample #1
 (c) Sample #2; (d) Sample #3; (e) Sample #4

3.2 Adhesive strength of VIP system

Fig. 5 shows the photos of VIP sample coated with cement mortar before and after pullout testing. The result shows that the adhesive strength of VIP system was very low, about $0.06 \pm 0.01\text{MPa}$. The data was lower than the standard value in building applications.

After pullout testing, the VIP was not deformed, but it was debonded to the cement mortar. Therefore, some new installed methods would be used in practice, for example, interface treating agent for cement mortar, high strength alkaline-resistant fiberglass roving cloth inserted between VIP and cement mortar, or developing the cavity-core matrix VIP. Boafo et al. [2,3] pointed out that the bond strength of the cavity-core matrix VIP increased by $\sim 50\%$ magnitude owing to the interlocking surface topology.

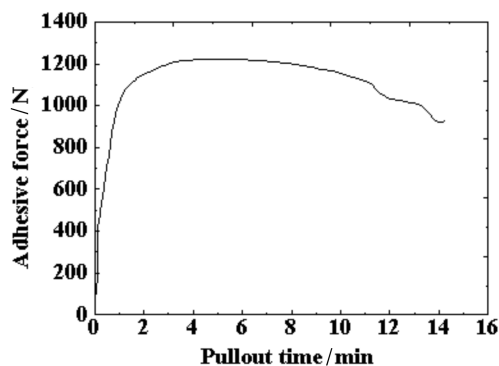


Fig. 4 Strength-time curve for VIP sample #4

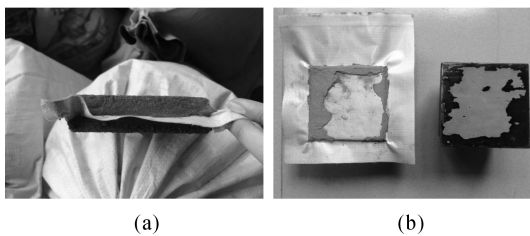


Fig. 5 Photos of VIP coated with cement mortar

- (a) VIP coated with cement mortar;
 (b) VIP system after pullout testing

The failure mechanisms of the envelopes included interface failure, cohesive failure, peeling off. According to the above results, the failure mechanisms for the VIP were interface and cohesive failures, such as deformation of the VIP with one side and along the interface between upper and down envelopes, interface between the glassfiber film and the PE film.

However, the failure mechanism of VIP system was just interface failure. The interface between the VIP and cement mortar occurred.

4. Conclusions

(1) The adhesive strength of VIP was $0.1 \sim 0.2$ MPa. The failure modes of VIP after pullout testing were deformed along one side of the VIP, outer glassfiber barrier film torn, glassfiber textile debonded to the inner PE film and deformed along the interface between upper and down barrier films.

(2) The adhesive strength of VIP system was not enough in building application, 0.06 ± 0.01 MPa. However, some new installed approaches could be used to improve its adhesive strength, including interface treating agent for cement mortar, high strength alkaline-resistant fiberglass roving cloth inserted between VIP and cement mortar, or developing the cavity-core matrix VIP.

(3) The failure mechanisms for VIP were both interface and cohesive failures. The failure mechanism of VIP system was just interface failure.

References

- [1] W. P. Wu, Y. Q. Zhou, X. Y. Hu, Z. F. Chen. Proceedings of the 11th International Vacuum Insulation Symposium, Duebendorf, Switzerland, 2013
- [2] F. E. Boafo, J-T Kim, Z. F. Chen. Energy and Buildings, 97 (2015) 98 – 106.
- [3] F. E. Boafo, Z. F. Chen, C. D. Li, B. B. Li, T. Z. Xu. Energy and Buildings, 85 (2014) 644 – 653.
- [4] S. Brunner, K. G. Wakili, T. Stahl, B. Binder. Energy and Buildings, 85 (2014) 592 – 596.
- [5] H. Simmler, S. Brunner. Energy and Buildings, 37 (2005) 1122 – 1131.
- [6] IEA/ECBCS Annex 39, VIP – Study on VIP-components and Panels for Service Life Prediction of VIP in Building Applications, and Vacuum Insulation in the Building Sector-Systems and Applications, Subtask A/B reports, 2005 (c. f. www.vipbau.ch).

Addressing Challenges and Creating Opportunities

— Application of VIPs in Canada's North

Doug MacLean^a, Phalguni Mukhopadhyaya^{b*}, Stephen Mooney^c, Juergen Korn^d

a. Technical Consultant, Energy Solutions Centre, Whitehorse, Yukon, Canada

b. Associate Professor, University of Victoria, Department of Mechanical Engineering, Victoria, BC, Canada

c. Director, Cold Climate Innovation, Yukon Research Centre, Whitehorse, Yukon, Canada

d. Research and Development Project Manager, Yukon Housing Corporation, Whitehorse, Yukon, Canada

Abstract

In Canada, with its cold climate, there is great potential to apply Vacuum Insulation Panels (VIPs) for building insulation. Recent code changes, and the cold climate of Yukon, have increased interest in better building insulation. VIPs have thermal resistance values much greater than those of conventional thermal insulation materials. In Yukon, VIPs have been used as thermal insulation in a retrofit of a commercial building, in a new home, in a greenhouse, and in new housing trailers. This paper summarizes observations, lessons learned, and performance monitoring results to help the construction community, researchers, designers, and end-users make best use of the unique properties and performance of VIPs.

Keywords vacuum insulation panels (VIPs), Northern Canada, energy efficiency, field performance

1. Introduction

In Canada, known for its predominantly extreme cold climate, the potential to apply VIPs in the building construction industry is estimated to be enormous because of the potential to reduce thermal bridging, keep wall thickness lower, particularly for mobile homes, and increase internal wall surface temperature. This is particularly so in Yukon, one of Canada's most northern territories with a minimum recorded winter temperature of $-52.2\text{ }^{\circ}\text{C}$ (lower in more isolated northern areas).

Recent code changes and the extreme cold climate of Yukon have increased interest in better building insulation in general, and in vacuum insulation panels (VIPs) in particular. Vacuum insulation panels (VIPs) have thermal resistance values up to 10 times or more than conventional thermal insulation materials. In recent years a number of interesting projects have used VIPs as

thermal insulation for exterior building enclosures in Yukon. For example, VIPs have been tested in a retrofit of a commercial building, in a new home, in a greenhouse, and in new housing trailers. All the VIPs used in these examples were $45\text{ cm} \times 13 \times 1.2\text{ cm}$ ($18'' \times 22'' \times 0.5''$) in size and had a centre of panel RSI value of 3.8 (R-value of 22).

Interest in VIPs has grown, and the number of applications is beginning to increase. The experiences with VIPs in Yukon to date are encouraging and are described for each project below.

2. Field installations

2.1 410 Jarvis Street in Whitehorse Yukon

The first pilot was done on one exterior wall of an existing building to test the design, and to build contractor confidence in the product and construction methods. Before and after infrared testing showed a reduction in thermal bridging and reduced heat loss.

* Corresponding author, Tel :1-250-472-4546, E-mail:phalguni@uvic.ca

Temperatures were monitored throughout the layers of insulation to compare the relative heat loss in each layer of insulation. Results were positives [1, 2].



Fig. 1 Installation of vacuum insulation panels (VIPs) at 410 Jarvis in Whitehorse, Yukon, Canada

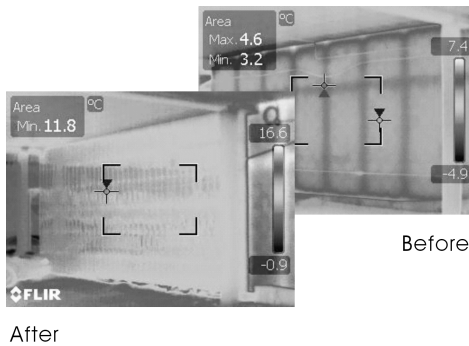


Fig. 2 Infrared images taken before and after VIPs were installed on one wall at 410 Jarvis Street in Whitehorse, Yukon Canada

Contractor reaction was also positive. Although initially apprehensive, workers at the site indicated that construction proceeded smoothly and that construction time might actually be shorter when using VIPs.

2.2 81 Kane Street, Haines Junction, Yukon

A second pilot was completed at 81 Kane Street in Haines Junction, Yukon Canada. For this pilot, the wall construction was a modification of existing construction practices.



Fig. 3 VIP insulated house at 81 Kane Street in Haines Junction, Yukon, Canada

For example, for the main floor, the outside wall, going from the outside to inside, consisted of:

- Exterior sheathing,
- 2×4s insulated with 8.9 cm (3-1/2") of mineral wool to give an RSI-value of 2.5 (R14),
- 2.5 cm (1") of foil-faced Polyisocyanurate insulation (PolyIso) installed on the interior of the 2×4s,
- 12 mm (1/2") "peeland stick" VIPs installed on the inside surface of the PolyIso insulation,
- 6 mm (1/4") of light foam to cover the VIPs, held in place with foil tape,
- 2.5 cm (1") of foil-faced PolyIso insulation installed on the interior of the 6 mm (1/4") light foam, with all joints were taped to provide an air and vapour barrier, and
- 2×4s to hold the PolyIso in place. The space between the 2 × 4s was left open to accommodate electrical lines and plumbing, and then filled with mineral wool batts.

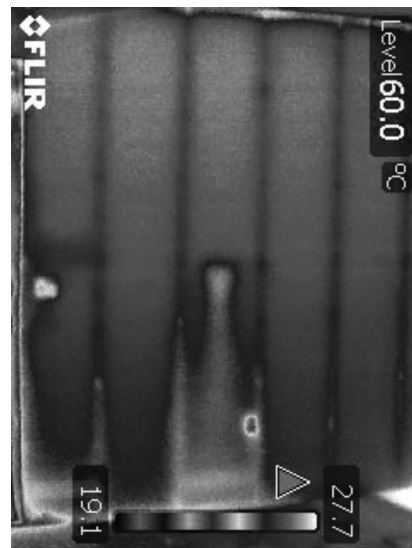


Fig. 4 Infrared image of main floor wall taken at 81 Kane Street in Haines Junction, Yukon, Canada

Again, infrared testing and subsequent monitoring with thermal sensors confirmed the effectiveness of the insulation strategy. User comments also indicated that the house is very comfortable in terms of room temperature and the heating cost is low.

The monitoring was done with standard thermistors connected to a TSCO monitoring system.

TSCO is a Yukon software and instrumentation company.

2.3 Greenhouse

In this application on a small greenhouse, at Cold Climate Innovation, Yukon College in Whitehorse, Yukon, vacuum insulation panels were installed on a mechanized sliding door. This highly-insulated sliding door significantly reduced heat loss, helping to keep the greenhouse at the required growing temperatures, even when the outside temperature dropped to -40 degrees centigrade.



Fig. 5 Greenhouse with VIP Sliding Door

2.4 House Trailers

Photo credit: Laird Herbert The house trailer shown in Fig. 6 uses 2 layers of VIPs and 4" of foam for insulation on the walls, floors and ceiling.



Fig. 6 House trailer made by Laird Herbert, a Yukon contractor.

There is growing interest in “mini-houses” or “tiny houses” or “houses on wheels”. These tiny houses insulated with VIPs are in the order of 20 square metres (200 square feet) in size. They are a response to a market need for small, economic and easily movable

housing.

Vacuum insulation panels make it possible to increase the thermal comfort of such small house trailers without sacrificing space. This is because the insulation level in the floor, walls and ceiling can be greatly increased using VIPs without increasing the wall, ceiling or floor thickness.



Fig. 7 A house trailer in its current location in Yukon. This house trailer was made by the Yukon contractor Philippe Mouchet and used VIPs in the floor

Of course, design refinements are possible in these tiny houses. For example, although insulation levels are good, noise transmission through walls is a concern with some designs. Any house that uses a combination of VIPs and batt insulation and is well air-sealed has reduced sound transmission.

Further, when the door is opened in winter, the air temperature in the unit can drop quickly. A similar problem can occur if the door does not seal tightly when closed, or if the door is not well insulated. Small air leaks can reduce the effective RSI value (R-value). These problems have been addressed by using a polyurethane foam-filled door with double seals.

Perhaps most important is proper sealing of the air barrier. Frost can develop on interior surfaces where there is air leakage in the wall, leading to moisture accumulation, mold problems and structural damage.

Moisture control with good ventilation is also important in cold climates to prevent condensation on cold surfaces, such as windows.

Finally, a convection heater alone may not be suitable in colder weather. A radiant electric heater may

be preferable and result in increased comfort.

These are all known issues that have occurred in the other types of houses but are more noticeable in tiny houses because of the specific challenges in cold weather. Even in conventional housing, however, the importance of dealing with such issues is known. For example, sealing air barrier leaks can improve the effective insulation level significantly. This has been noted in recent building science literature [3, 4].

3. Monitoring results

Monitoring was done at 410 Jarvis in Whitehorse, Yukon, and at 81 Kane Street in Haines Junction, Yukon. Although the monitoring work is not complete at the second location, results to date indicate that there has been no damage or failure of VIPs at either location. Further, there has been little indication of any significant aging of the insulation.

For the housing trailers, depending on the design, there may be more potential for damage of VIPs due to the rubbing that may occur between VIPs and adjacent materials when the unit is moved from one location to another. However, no such damage has yet been noted in the housing trailers described in this paper.

4. Conclusions

Initial results using VIPs in a commercial building insulation retrofit, in a new home, in a greenhouse and in house trailers have been largely positive. Provision for sound attenuation was a problem with one trailer design, but not with another design which included batt insulation. More attention to the design of the heating and ventilation system appears to be needed to ensure good moisture control and proper distribution of heat and fresh air in small house trailers when exposed to extremely low outdoor temperatures. Radiant heaters may be preferable to convention style heaters in this situation, but more study is needed. Finally, proper sealing of the air barrier is key in order to achieve the full insulating value of VIPs.

Acknowledgements

The authors of this paper would like to thank the National Research Council of Canada (NRC) for introducing vacuum insulation technology in Northern Canada. The authors are very appreciative of the

support of Panasonic Canada Inc., and Panasonic Corporation for supplying the vacuum insulation panels used in these pilot projects, and for their technical expertise and support. The authors will also like to thank Yukon Housing Corporation for allowing us to use a wall of one of their buildings for one pilot project, and for providing monitoring equipment. The authors would like to thank the Champagne-Aishihik First Nation for their participation in allowing us to insulate an entire new house with VIPs. The authors would like to thank the trailer manufacturers, Laird Herbert and Philippe Mouchet, as well as Erica Heuer who graciously allowed us to monitor the construction of the trailer made for her by Philippe Mouchet. The financial help and technical contributions provided by Yukon College are also highly appreciated.

References

- [1] D. MacLean, J. Korn, and P. Mukhopadhyaya, Vacuum Insulation Panels (VIPs) Arrive in Northern Canada: Institutional Building Pilot Retrofit in Yukon, Proc. of 10th International Vacuum Insulation Symposium (IVIS-X), pp. 59-64, 2011, Ottawa, ON, Canada.
- [2] P. Mukhopadhyaya, D. MacLean, J. Korn, D. van Reenen, and S. Molleti, Building application and thermal performance of vacuum insulation panels (VIPs) in Canadian subarctic climate, *Energy and Buildings*, Volume 85, Dec 2014, 672 – 680.
- [3] Building Science Corporation, Thermal Metric Summary Report, 2013, (http://www.buildingscience.com/documents/special/content/thermal-metric/BSCThermalMetricSummaryReport_20131021.pdf), 1, 116.
- [4] Canada Mortgage and Housing Corporation, Energy Efficiency Building Envelope Retrofits for Your House, http://www.cmhc-schl.gc.ca/en/co/grho/grho_011.cfm.

Bibliography

- [1] Statistical Review of World Energy 2014, Published by BP plc, (former name British Petroleum) (<http://www.bp.com/en/global/corporate/about-bp/energy-economics/statistical-review-of-world-energy.html>)
- [2] Natural Resources Canada, Energy Use Data Handbook 1990-2009, Catalogue No. M141-11/2009E-PDF, ISSN 1910-4413, 4.
- [3] McKinsey & Company, Pathways to a Low-Carbon Economy, Version 2 of the Global Green House Gas Abatement Cost Curve, 2009, (http://www.mckinsey.com/client_service/sustainability/latest_thinking/)

- greenhouse_gas_abatement_cost_curves).
- [4] D. MacLean, J. Korn, and P. Mukhopadhyaya, Vacuum Insulation Panels (VIPs) Arrive in Northern Canada; Institutional Building Pilot Retrofit in Yukon, Proc. of 10th International Vacuum Insulation Symposium (IVIS-X), pp. 10, 2011, Ottawa, ON, Canada
- [5] P. Mukhopadhyaya, D. MacLean, and J. Korn, Performance of Vacuum Insulation Panel (VIP) - Foam Composite as Exterior Insulation: Observations from a Pilot Field Study in Yukon, pp. 1 (Extended Abstract with Presentation), 9th Canada-Japan Workshop on Composites, July 30-August 2, 2012, Kyoto, Japan.
- [6] P. Mukhopadhyaya, D. MacLean, J. Korn, van D. Reenen, and S. Molleti, Field Application and Long-term Thermal Performance of Vacuum Insulation Panels (VIPs) in Canadian Arctic Climate, submitted for Re Proc. of 11th International Vacuum Insulation Symposium (IVIS-XI), Switzerland, September 2013, 97 - 98.
- [7] P. Mukhopadhyaya, D. MacLean, J. Korn, D. van Reenen, and S. Molleti . Building application and thermal performance of vacuum insulation panels (VIPs) in Canadian subarctic climate, Energy and Buildings, Volume 85, Dec 2014, 672 - 680.
- [8] P. Mukhopadhyaya, D. MacLean, J. Korn, and D. van Reenen, Field Application and Long-Term Thermal Performance of Vacuum Insulation Panels (VIPs) in Yukon, Final Project (B-1452.1) Report, National Research Council Canada, Ottawa, Canada, 2011, 1 - 40.

Impact of VIP Envelope Reflectance on the Performance of Curtain Wall System

Fred Edmond Bofo^a, Jun-Tae Kim^{a*}, Jong-Gwon Ahn^a, Jin-Hee Kim^b

a. Zero Energy Buildings Lab., Dept. of Energy Systems Engineering, Kongju National University, Cheonan, Korea

b. Green Energy Technology Research Center, Kongju National University, Cheonan, Korea

Abstract

Curtain wall is one of the most recognizable components of today's building. Despite the benefits of increased speed and quality of construction, improved day lighting and aesthetics, among others, glass curtain walls increase the energy demand for thermal comfort. Curtain wall systems composed of various glazed and spandrel configurations offer alternative solutions. Insulating the spandrel area minimizes heat losses or gains. Vacuum insulation panel (VIP) enables slim wall constructions with high performance. Furthermore, VIP's highly polished surface offers potential to reduce heat gain by restricting radiative heat transfer. The objective of this study is to investigate the thermal reflectance characteristics of integrated VIP spandrels on the performance of curtain wall system during peak cooling season. A prototype baseline building was modelled with southern facade installed curtain wall system with VIP spandrel. Primarily, due to the surface reflectance properties of the VIP's highly polished envelope, the VIP spandrel area reduced solar heat gain by about 3~4 magnitude as compared to the solar heat transmitted through the glazing area, during summer season. Sensible cooling energy demand surged for different curtain wall configurations.

Keywords vacuum insulation panel, VIP, curtain wall system, VIP spandrel, thermal reflectance, radiative heat transfer.

1. Introduction

Commercial and residential buildings consume nearly 20 % of final energy demand in the Republic of Korea. In addition, it is predicted that energy use will grow along with increasing floor area. Many of the buildings in 2050 are the ones that exist today; thus it is logical to focus on minimizing this energy demand. Aside occupant schedule and behavior, the choice of building materials and systems determine the operational energy profile for buildings. The stock of glass curtain walls abound in today's architecture due to improved day lighting levels and aesthetics, increased speed and quality of construction, among others. However, energy demand to ensure comfortable indoor thermal environment is greater in highly glazed buildings as compared to conventional buildings, especially in

summer season; since glazing systems have lower thermal performance than opaque walls [1]. In response, an updated directive in the Republic of Korea stipulates that all new buildings satisfy minimum requirements of U-value, insulation and air tightness levels, as well as installation of solar radiation control devices for glazed facades [2, 3]. Curtain walls are prefabricated building envelopes; whereas glass curtain wall is entirely composed of translucent, tinted or coated glazing, curtain wall system is composed of a translucent, tinted or coated glazed area and an opaque spandrel area (see Fig. 1). The spandrel area helps to curtail heat losses or gains. The technology already exists for the construction of more efficient curtain wall systems that ensures occupant comfort while reducing energy consumption. For instance, Dow Corning's

* Corresponding author, Tel : 82-41-521-9333, Fax: 82-41-562-0310, E-mail: jtkim@kongju.ac.kr

Architectural Insulation Panels (see Fig. 2) combine the aesthetics and convenience of curtain wall construction with the added energy-saving benefits of high-performance vacuum insulation panel (VIP) [4]. VIP offers opportunities for slim constructions and space constrained applications, without compromising performance [5].

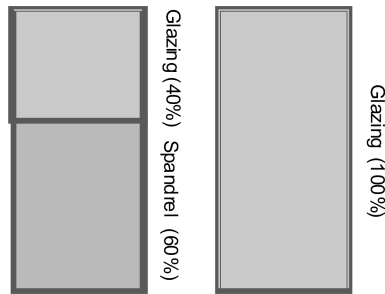


Fig. 1 View of a typical curtain wall system (left) and glass curtain wall (right)



Fig. 2 Dow Corning's curtain wall systems trade named Architectural Insulation Panel; glazed area with Building-Integrated Photovoltaic (BIPV) spandrel finish (left), and view of spandrel area showing VIP integrated between glass units (right) [4]

What's more, a recent study on the durability of VIPs in the cavity of glass units showed that, at accelerated aging cycling conditions of -20°C to 80°C temperature and 10% to 90% RH, the assembly provided ten times protection to the VIP as compared to unprotected panels [6]. The concept represents a strategy to extend the life of VIP. In order to improved curtain wall systems with VIP spandrels, other researchers have focused on durability, thermal, and structural performance issues [6 – 8].

In this study, the effect of the surface reflectance properties of VIP's highly polished envelope on the performance of curtain wall system with VIP spandrel is examined; curtain walls with different glazing and spandrel configurations are investigated using dynamic computer simulation tools.

2. Methodology

Modeling and simulations were carried out using EnergyPlus building energy simulation software by LBNL. Fig. 3 and Tab. 1 show the sectional view and macrograph of the VIP spandrel, and material parameters used for modeling, respectively.

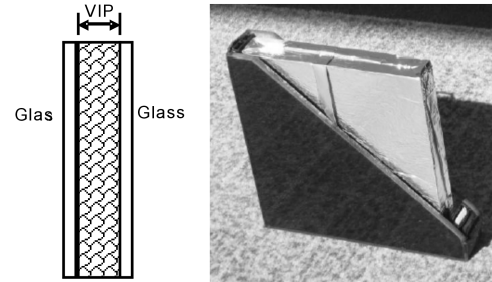


Fig. 3 Schematic diagram showing the cross-section of VIP spandrel (left) and macrograph of the VIP spandrel (right) [8]

Tab. 1 Material properties

Parameter	Clear glass	VIP
Thermal conductivity / (W/(m · K))	0.9	0.0045
Front side and back side solar reflectance	0.071	0.8
Solar transmittance	0.775	—
Front side and back side visible reflectance	0.08	—
Visible transmittance	0.881	—
Solar absorptance	—	0.02
Thermal emissivity	0.84	0.04
Density/(kg/m ³)	—	240
Thickness/(mm)	6	30

To meet the objective of this study, a baseline building model ($6\text{ m} \times 4.5\text{ m} \times 3.6\text{ m}$) which represents an office building unit was used. The building was assumed to be located in Incheon, Republic of Korea (latitude 37.28 N , longitude 136.33 E). Hourly weather data in EPW format was used. To highlight the impact of the curtain wall system on indoor thermal environment, the building was modeled with a single south facing external wall while the north, east and west walls were assumed to be interior walls. In addition, various glazing area to spandrel area scenarios were modeled and discussed. This study focuses on evaluating the VIP spandrel, thus the glazing area was double-pane glass without any shading device.

3. Results and discussions

Output can be provided by EnergyPlus on an hourly, daily or monthly basis. Hourly based results give a clearer view of the behavior of the system whereas daily and monthly results offer average representative view. Except for weather reports, results for a chosen day, 21st June, which corresponds to summer solstice day in the northern hemisphere (with the highest solar radiation due to the sun's trajectory), are presented. The average ambient temperature and relative humidity (RH) are shown in Fig. 4.

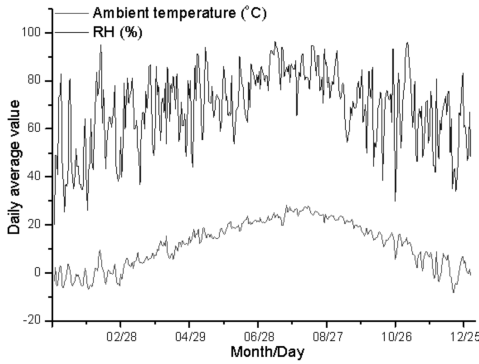


Fig. 4 Average ambient temperature and RH

The highest and lowest average daily ambient temperatures were 28 °C and -8.5 °C on 23rd July and 16th December, respectively. The average RH ranged from 20% to 96%.

3.1 Heat transfer

Taking the heat transfer of an external wall for example, various coupled heat transfer components are interrelated, namely: convection, radiation and conduction. All radiative and convective heat exchanges on both the outer and inner surfaces as well as conduction through the external wall are illustrated in detail in Fig. 5. While conduction and convection can be transferred only through a medium, radiation can be transferred across a perfect vacuum driven by difference in temperature. The sol-air effect, caused by solar radiation striking the exterior surface of the building, raises the surface temperature above. This increases heat gain into the building in summer but reduces heat loss in winter.

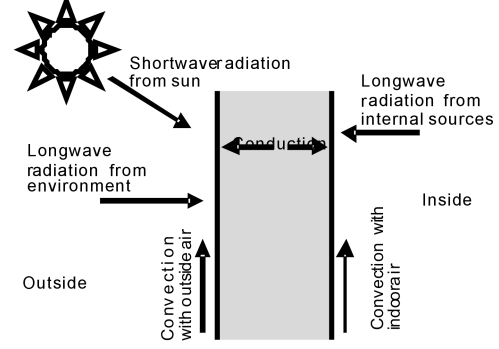


Fig. 5 Heat transfer through an external wall

For the VIP spandrel (described in Fig. 3), a number of variables affect the heat balance. Fig. 6 shows the case of a VIP in double glass units. The heat balance equation for the glass surface facing the VIP layer (i. e. face 2) can be represented by equation 1:

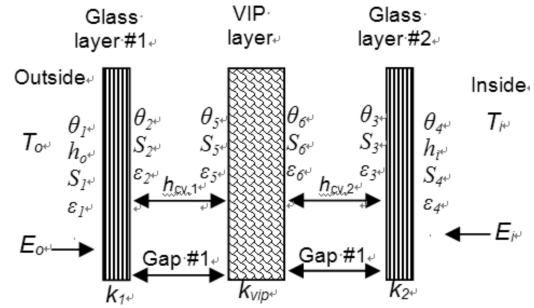


Fig. 6 Spandrel system with VIP between glass units

$$h_{cv,1}(T_{gap,1} - \theta_2) + k_1(\theta_1 - \theta_2) + \frac{\alpha_2}{1 - \rho_2 R_1} \times \left[\frac{1}{1 - \rho_6 \rho_3} (\epsilon_3 \theta_3^4 + \epsilon_6 \theta_6^4 \rho_3) + \epsilon_5 \theta_5^4 + \epsilon_2 \theta_2^4 R_1 \right] - \alpha_2 \theta_2^4 + S_2 = 0 \quad (1)$$

$$\text{and} \quad R_1 = \rho_5 + \frac{\tau_{vip}^2 \rho_3}{1 - \rho_6 \rho_3} \quad (2)$$

where 1, 2, 3 and 4 are the faces of glass surfaces, 5 and 6 are the faces of the VIP, $h_{cv,1}$ is convective heat transfer coefficient between glass and VIP layers ($W/(m^2 \cdot K)$), $T_{gap,1}$ is the effective mean air temperature in gap 1 (K), θ_i is temperature of surface layer, k_i is conductance ($W/(m^2 \cdot K)$), ρ_i is surface air density, S_i is sum of short and long wave radiation ($W/(m^2 \cdot K)$), σ is Stefan-Boltzmann constant ($W/(m^2 \cdot K^4)$), and ϵ_i is emissivity of surface. Similarly, the heat balance equation for the glass surface facing the VIP layer towards the interior (i. e. face 3), can be derived. The heat balance equation for the VIP layer towards the

exterior (i. e. face 5) can be represented by equation 3:

$$h_{cv,1}(T_{gap,1} - \theta_5)k_{vip}(\theta_6 - \theta_5) + \frac{\alpha_5}{1 - \rho_2 R_1} \times \left[\frac{\rho_2}{1 - \rho_5 \rho_3} (\epsilon_3 \theta_3^4 + \epsilon_6 \theta_6^4 \rho_3) + \epsilon_2 \theta_2^4 + \epsilon_5 \theta_5^4 R_2 \right] - \alpha_3 \theta_3^4 + S_3 = 0 \quad (3)$$

Likewise, the heat balance equation for the VIP layer towards the interior (i. e. face 6), can be derived.

3.2 VIP spandrel curtain wall system

Results showed that the reflectance of the glazing area surface is very negligible (not plotted). Fig. 7 illustrates variation of the surface reflectance of the VIP spandrel and the surface transmittance of the glazing area with time; for a curtain wall system with 50% spandrel to 50% glazing area. From Fig. 7, it can be deduced that the reflectance of the VIP spandrel area and the transmittance of the glazing area were both quite pronounced. The hourly mean reflectance coefficient for the VIP spandrel was 0.56, while the hourly mean transmittance coefficient for the glazing area was 0.48.

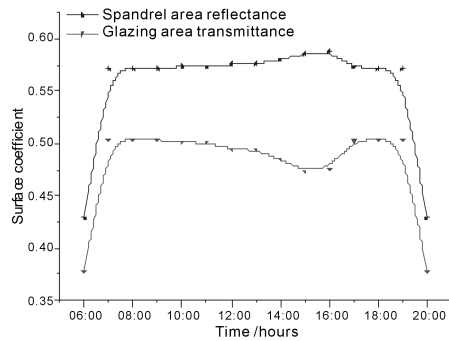


Fig. 7. Hourly reflectance coefficient of VIP spandrel area and transmittance coefficient of glazing area

It can be said that the glazing area transmits nearly as much incident solar radiation as the VIP spandrel reflects. The incident solar radiation is the total solar radiation incident on the outside of an exterior surface. It is the sum of: surface outside face incident beam solar radiation rate (W), surface outside face incident sky diffuse solar radiation rate (W), surface outside face incident ground diffuse solar radiation rate (W), surface outside face incident sky diffuse surface reflected solar radiation rate (W), surface outside face incident beam to beam surface reflected solar radiation rate (W), and surface outside face incident beam to diffuse surface reflected solar radiation rate (W). Fig. 8 is a plot of the

thermal radiation heat transfer coefficient (radiative heat gain) of the VIP spandrel and glazing areas. The radiation heat transfer coefficient describes thermal radiation heat transfer between the outside surface and air mass surrounding the surface.

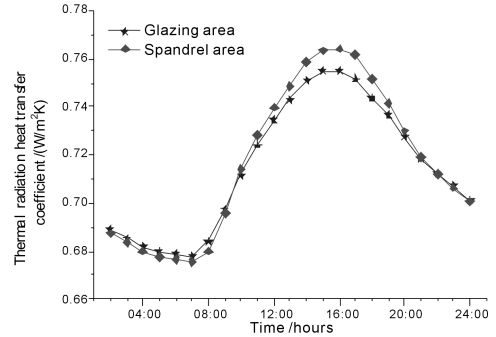


Fig. 8 Hourly thermal radiation heat transfer

VIP spandrel area and glazing area showed quite a similar trend for radiation heat transfer coefficient, especially in the early and late hours of the day but slightly different values during the late afternoon. The radiation heat transfer coefficient is the value of Hr in the thermodynamic equation:

$$Q = Hr \times A(T - T) \quad (4)$$

Where Q is heat flux, A is area and $(T - T)$ is change in temperature. Consequently, from findings in Figs 7 and 8, it can be inferred that the VIP spandrel area and glazing area admit varying amounts of incident solar radiation. Fig. 9 represents the heat gain rate of the curtain wall system's areas. The system heat gain rate is a measure of the total heat that is transmitted, dissipated or reradiated into the indoors. In the case of the glazing area, this heat gain results from the transmitted solar radiation and convection heat transfer. In the case of the VIP spandrel, this heat gain is mainly attributed to convective heat transfer at the respective faces. Also, whereas the heat gain via glazing area may be transmitted directly into the indoors, the minimal heat gained through the VIP spandrel is attributed to stored up heat transfer that is reradiated at a later time.

As depicted in Fig. 8, the glazing area gains and transmits more heat into the indoors. Thus, the simulation results are in agreement with precedent literature that concluded that glazed facades have greater energy demand to ensure comfortable indoor thermal

environment, especially in summer season; since glazing systems have lower thermal performance than opaque walls [1]. In addition, a plot of the temperature variation on both the glazing and VIP spandrel areas showed remarkable results. From Fig. 10, during peak solar radiation time, the inside surface (towards indoors) temperature of the VIP spandrel was always lower than the outside surface (towards outdoors) temperature of the VIP spandrel. The highest inside and outside surface temperatures were about 31 °C and 28°C, respectively. Conversely, the inside surface (towards indoors) temperature of the glazing area was always higher than the outside surface (towards outdoors) temperature of the glazing area. The mean difference between the inside and outside surface temperatures of the glazing area was about 1.5°C; this difference is plausibly attributed to the effect of outdoor wind current.

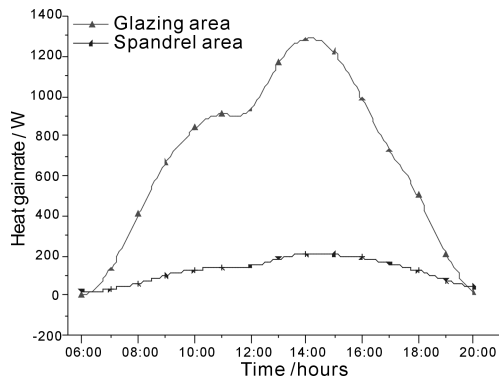


Fig. 9 Heat gain rate through the curtain wall system

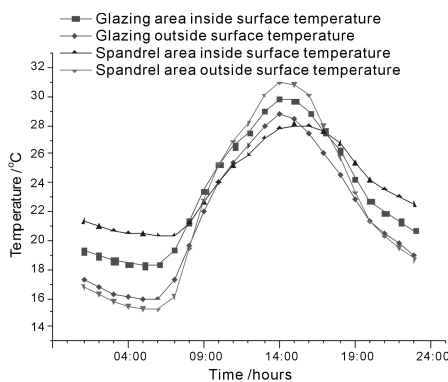


Fig. 10 Hourly surface temperatures

3.3 Building energy consumption dynamics

To quantify the effect of the glazing to VIP spandrel areas in terms of building energy consumption,

simulations were done using a baseline office building unit; the results are summarized in Fig. 11.

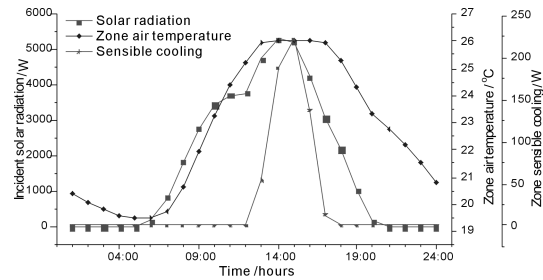


Fig. 11 Dynamics of zone air temperature and sensible cooling energy demand, with solar radiation

From Fig. 11, as the intensity of incident solar radiation increased within the day, the glazing area of the curtain wall system gained and transmitted more heat into the indoors than the VIP spandrel (as discussed in section 3. 2). Invariably, the indoor air temperature rose steadily from about 22 °C at 9:00 am to nearly 26 °C by noon. Sensible cooling energy steadily increased as well, and peaked around 2:00 pm. For the purpose of this study, cooling setpoint was set to 26 °C. Thereafter, the HVAC stayed on until 18:00 pm (in accordance with the schedule).

Also, Fig. 12 shows the relationship between various configurations by area of glazing to VIP spandrel (i. e. 100% glazed facade, 80% glazing – 20% VIP spandrel, 60% glazing – 40%, 50% glazing – 50%, and 40% glazing – 60% VIP spandrel) and the respective sensible cooling energy demand for cooling season (June to September).

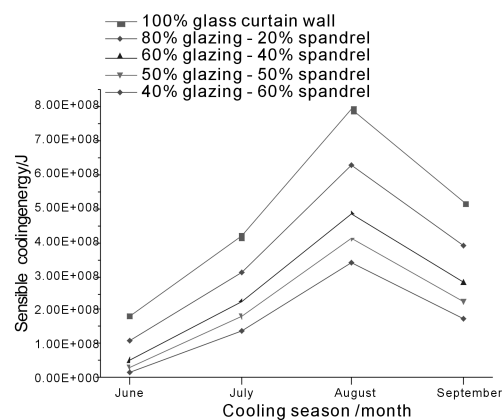


Fig. 12 Sensible cooling energy demand for various glazing area to VIP spandrel configurations

With reference to Fig. 12, the varying

configurations of the curtain wall system showed a similar trend in monthly (sum) sensible energy demand; increasing steadily from June through July, and peaking in August. The trend dipped a little in September, but it was still higher than June and July. The deduction follows that a smaller glazing area transmitted less heat to the indoors, and simultaneously a larger VIP spandrel area reduced heat gain, resulting in the lowest sensible cooling energy demand for the scenario with 40% glazing area – 60% VIP spandrel area configuration.

4. Conclusions and outlook

Commercial buildings with curtain wall systems installed are well noticeable in modern architecture. The urge for large glazing area is mainly for vision and aesthetic purposes. A curtain wall system can be designed for energy efficiency and does not need to have an overall poor thermal performance. In this study, curtain wall system with VIP spandrel has been examined. Chiefly due to the surface reflectance properties of the VIP's highly polished envelope, the VIP spandrel area reduced solar heat gain by 3 ~ 4 magnitude as compared to the solar heat transmitted through the glazing area, during summer. This is promising, especially for buildings in cooling dominated areas. Based on a baseline model, simulation results indicated that, increasing the area of the VIP spandrel while decreasing the glazing area reduced the sensible cooling load drastically. 40% glazing area – 60% VIP spandrel area obtained the lowest sensible cooling load. Given the marked sensible cooling energy demand due to the curtain wall configuration, regional or global directives are essential. It must be mentioned however, that though the technology to fabricate such a curtain wall system exist, it's not readily available; more so the method to seal the VIP in the glass units is complex. Further corporate research is needed. Also, the scope of this research was focused on the effect of VIP reflectance

during summer season or in cooling dominated areas; future endeavors will tackle winter season effects.

Acknowledgements

This research was supported by the Basic Science Research Program through the National Research Foundation of Korea (NRF) funded by the Ministry of Education (2009–0093825) and Human Resources Program in Energy Technology of the Korea Institute of Energy Technology Evaluation and Planning (KETEP) granted financial resources from the Ministry of Trade, Industry & Energy, Korea (No. 20134010200540).

References

- [1] F.P. Torgal et al., Nearly zero energy building refurbishment. 2013: Springer.
- [2] Energy saving design criteria report. Ministry of Land Infrastructure and Transport, Republic of Korea, 2014 [In Korean].
- [3] Green building construction provision law. Ministry of Land Infrastructure and Transport, Republic of Korea, 2015 [In Korean].
- [4] High performance insulation for next-generation curtainwalling - technical report. Dow Corning, 2012.
- [5] S. E. Kalnæs, and B. P. Jelle, Vacuum insulation panel products: A state-of-the-art review and future research pathways. *Applied Energy*, 116 (2014) 355 – 375.
- [6] F.D. Gubbels et al., Durability of vacuum insulation panels in the cavity of an insulating glass unit. *Journal of Building Physics*, 2014.
- [7] Carbary, L. D., et al., High Performance Curtain Wall Using Vacuum Insulated Panel (VIP) Spandrels. *Glass Performance Days*, Tampere Finland, 2013, (<http://www.glassfiles.com/articles/high-performance-curtain-wall-using-vacuum-insulated-panel-vip-spandrels>).
- [8] L. D. Carbary et al., Architectural insulation modules: thermal and structural performance for use in curtainwall construction. *Proceedings of ICBEST*, Aachen Germany, 2014.

Thermal Performance of A Steel Skeleton / Drywall Building Insulated with Vacuum Insulation Panels

Ioannis Mandilaras^{a*}, Dimos Kontogeorgos^a, Ioannis Atsonios^a, Cornelia Stark^b, S. Tephani Vidi^b,
David Marity^c, Daniel Seiler^c, Dominik Herfurth^d, Maria Founti^a

a. National Technical University of Athens, School of Mechanical Engineering, Lab. of Heterogeneous Mixtures and Combustion Systems
Heron Polytechniou 9, 15780 Zografou, Greece

b. Bayerisches Zentrum für Angewandteenergieforschung ZAE EV, Am Galgenberg 87, 97074
Wuerzburg, Germany

c. Haring Nepple AG, Hebelstrasse 75, 4056 Basel, Switzerland

d. KNAUF GIPS GK, AM Bahnhof 7, 97346 Iphofen, Germany

Abstract

Modern construction trends create the need for advanced building shells combining high thermal performance with short construction times and simplified erection approaches. Lightweight steel framed/drywall building systems coupled with Vacuum Insulation Panels (VIPs) form an attractive and versatile solution with high thermal performance and improved safety features. One of the main issues that affect the thermal performance of such wall assemblies is related to the relative positioning of the material layers to form e. g. prefabricated elements and the associated thermal bridging effect. VIPs retain their high vacuum levels with a barrier film, vulnerable to mechanical stresses and are sensitive to puncturing and/or destruction. On the other hand, a steel frame may introduce significant structural thermal bridges, and their relative importance on the overall thermal performance is likely to increase with the quality of the insulation material.

This paper addresses the thermal bridging issues and the overall thermal performance of a lightweight steel frame/drywall system in which VIPs are placed as an “internal layer” within the wall layers. This configuration provides “protection” for the VIPs, allows flexibility in installation of facade elements and at the same time permits interventions and modifications (e. g. drilling, installation of appliances) on the internal side of the wall. The proposed steel frame/dry wall system with VIPs is extensively analyzed in terms of different types of thermal bridges and their effect on the overall thermal performance. Moreover, the hygro-thermal behavior and the risk of condensation are examined.

Keywords vacuum insulation panels, VIP, thermal bridges, building envelope, lightweight building

1. Introduction

Nowadays, the building sector has a lion's share in energy consumption [1]. One of the most efficient ways to reduce the energy demands of a building is the installation of insulation at the building envelope. An innovative insulation material, which reaches thermal conductivity values less than $0.008\text{W}/(\text{m} \cdot \text{K})$, is the Vacuum Insulation Panel (VIP). So far, most of the studies concerning the VIP technology for buildings have focused on the development and optimization of

insulation systems at the material-component level. But, as the level of thermal insulation in a building enclosure becomes higher, the effect of thermal bridges is expected to become more severe [2]. Thus, scaling up from the component level to wall and envelope level in order to address the profound impact of thermal bridging on the efficiency of VIP insulation systems becomes crucial.

In the last decade, drywall lightweight construction

* Corresponding author, email: gman@central.ntua.gr

became increasingly widespread due to its advantages, such as the low construction time, structural seismic resistance, the reduction and recyclability of wastes and the decrease of loads and costs on bearing structures [3]. The concept of standardized light steel framed drywall residential buildings, aiming to build more buildings in a short period with fewer resources, is currently being investigated in the frame of the FP7 ELISSA project (www.elissaproject.eu). Walls are made of drywall materials anchored on a lightweight steel frame structure. In order to increase the energy efficiency of the building, VIPs are used for the thermal insulation of the walls.

Due to the well-known necessity of protecting the VIP's during the process of construction by bringing it in the building as late as possible [4], the ELISSA project examines the installation of the VIPs as part of an internal suspended wall system. VIPs are placed on the internal side of the envelope walls ensuring that they will be further protected during the use phase of the building. No VIPs were placed on the roof and floor in order to maintain costs at a reasonable level.

The scope of this study is to theoretically evaluate the impact of an additional layer of VIPs placed at the inner side of the external walls on the thermal bridges introduced in a light-weight building envelope. The assessment of the thermal bridges is based on the EN ISO 12011 standard [5], coupling numerical simulations of thermal bridges with the standardized methodology. The influence of the thermal bridges due to metal studs, 2D and 3D junctions on the overall thermal transmittance of the envelope is examined both without and with the addition of VIPs. Furthermore, the hygro-thermal performance and the risk of mold growth in the building envelope are investigated.

2. Description of the building

In order to assess the impact of the thermal bridges on the overall performance of the construction, a two storey building is analyzed. It is a lightweight steel framed construction based on a cavity wall system. The metal skeleton is founded on a cement base and the drywall system envelope is anchored on the steel skeleton. The overall dimensions of the building are 4.5 m × 2.5 m × 5.6 m.

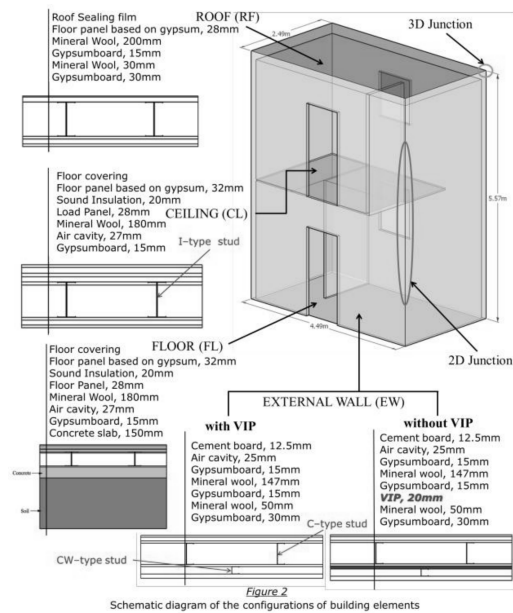


Fig. 1 Schematic diagram of the configuration of the building elements

The materials of the building elements are anchored on three different types of metal studs, C, CW and I type. An additional layer of VIPs is placed in the internal side of the External Walls (EW). The layers of the floor (FL) and the roof (RF) elements are anchored on I-type studs, 200mm in width. In the floor, a 180mm thick mineral wool layer is placed inside the cavity, while a 150mm thick foundation concrete slab and 500mm of soil were assumed for the simulations. The configuration of the ceiling (CL) (i. e. the element between the 1st and the 2nd floor) is similar to that of the floor excluding the slab and concrete layer. The Internal Wall (IW) consists of double gypsum boards on each side of the wall, with mineral wool (120mm) and an air cavity (30mm) between them, resulting in a total thickness of 207mm. The schematic diagram of the building element configurations is depicted in Fig. 1.

2. Methodology

The methodology followed in order to assess the thermal performance of the building is based on ISO 10211. Numerical simulations are performed for the calculation of the thermal transmittance of each configuration.

The main concept of the methodology is the separate analysis of the repeating and non-repeating thermal bridges. The repeating thermal bridges consist

of the metal studs at the middle part of the building elements. The non-repeating thermal bridges refer to the 2D and 3D junctions between the building elements (e. g. external wall and roof, external wall and inside wall and ceiling etc.), including the steel studs of the junction. Fig. 2 schematically presents the different types of thermal bridges.

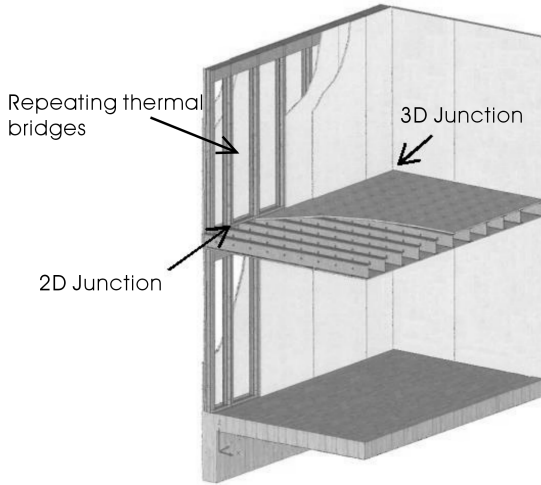


Fig. 2 Schematic diagram of the repeating and non-repeating thermal bridges

After the calculation of all the individual thermal bridges, the transmission heat transfer coefficient, H_D (W/K), is calculated by Equation 1:

$$H_D = \sum_i f_i A_i U_i + \sum_k f_k l_k \Psi_k + \sum_j f_j \chi_j \quad (1)$$

Where

f_i =factor of temperature correction of the building part i ,

A_i =the area of element i of the building envelope ,

U_i =the thermal transmittance of the clear element i of the building (center of wall) ,

f_k =factor of temperature correction of the linear thermal bridge k ,

l_k =thelength of linear thermal bridges k ,

Ψ_k = the linear thermal transmittance of linear thermal bridges ,

f_j = factor oftemperature correction of the point thermal bridge j ,

χ_j = the point thermal transmittance of the point thermal bridge j .

According to Equation 1, in order to calculate the heat transfer coefficient, the individual thermal transmittances of each configuration of thermal bridge

should be calculated. These calculations are based on CFD simulations.

The linear thermal transmittance, Ψ (W/(mK)), concerns the 2D geometries and is calculated according to Equation 2:

$$\psi = L_{2D} - \sum_{j=1}^N U_j l_j \quad (2)$$

Where

L_{2D} =the thermal coupling coefficient obtained from a 2D calculation of the component separating two environments being considered.

The point thermal transmittance, χ (W/K), of a part of the building envelope is calculated according to Equation 3:

$$\chi = L_{3D} - \sum_{i=1}^N U_i A_i - \sum_{j=1}^{N_j} \psi_j l_j \quad (3)$$

Where

L_{3D} =the thermal coupling coefficient obtained from a 3D calculation of the 3D component separating two environments being considered.

The thermal transmittance of the clear component (i. e. without the thermal bridges), U-value, of each element, is calculated according to ISO 6946 [6] taking into account the physical properties (thermal conductivity and thickness) of all the layers.

The 2D and 3D thermal coupling coefficients, L_{2D} (W/(m · K)) and L_{3D} , (W/K) were numerically calculated for every thermal bridge. A commercial CFD package (ANSYS CFX) [7] was used to simulate all the configurations and the types of thermal bridges. Regarding the boundary conditions, at the inner side of the walls the ambient temperature and the heat transfer coefficient were assumed to be $T_{in} = 20^\circ\text{C}$ and $h_{in} = 7.69\text{W}/(\text{m}^2 \cdot \text{K})$, respectively, while the respective values at the outside environment were $T_{out} = -10^\circ\text{C}$ and $h_{out} = 20\text{W}/(\text{m}^2 \cdot \text{K})$. The ground soil temperature was considered to be constant and equal to $T_{soil} = -10^\circ\text{C}$.

The thermal properties of the materials were assumed to be constant. The ventilated air cavities were assumed to be stagnant air with an “effective” thermal conductivity calculated according to ISO 6946 taking into account the convection-radiation phenomena.

The total heat flow, Φ , through each

configuration, is calculated from the simulations. Next, the thermal coupling coefficients L_{3D} of the 3D component, or L_{2D} of the 2D component is computed by Equation 4:

$$L = \frac{\Phi}{T_{in} - T_{out}} \quad (4)$$

Where

Φ =the total heat flow expressed in $[W/(m \cdot K)]$ in case of 2D thermal coupling coefficient and in $[W/K]$ in case of 3D thermal coupling coefficient.

The hygro-thermal performance of all types of thermal bridges was assessed by means of the temperature factor, $f_{Rsi}(-)$, which is calculated by the Equation 5:

$$f_{Rsi} = \frac{T_{si} - T_{out}}{T_{in} - T_{out}} \quad (5)$$

Where

T_{si} =minimal internal surface temperature.

Mold growth is expected, when the relative humidity on a surface is higher than 80% for several days. Therefore, the mold growth is avoided when the temperature factor is greater than 0.7 [8]. The commercial software HEAT3 was utilized. The outside air temperature was assumed to be equal to $T_{out} = -5^{\circ}C$ with thermal resistance $R_{out} = 0.04 (m^2 \cdot K) W$, the inside air temperature was $T_{in} = 20^{\circ}C$ with $R_{in} = 0.25 m^2 \cdot K/W$ and relative humidity $RH_{in} = 50\%$. In the cases of ground, the temperature of soil was $T_{soil} = 10^{\circ}C$ without thermal resistance and the boundary condition in 6.23m depth for the border of the foundation slab was assumed as adiabatic.

4. Results and discussions

All the thermal bridges of the building with and without the additional VIP layer were evaluated. In total, 8 cases concerning the impact of metal studs at the center part of walls, 14 bi-dimensional intersections and 12 three-dimensional junctions between the building elements were examined. The individual and the overall contribution of the thermal bridges on the total heat transmittance of the building were investigated highlighting the improvement due to the installation of VIPs.

The impact of the repeating thermal bridges on the thermal performance of the building envelope is depicted

in Fig. 3. The figure presents the effect of the metal studs on the thermal transmittance of each element for the cases with and without the VIP layer (Fig. 3(a)) and the linear thermal transmittance of the three types of metal stud at the different elements of the building envelope (Fig. 3(b)).

The U-value of the clear external wall is 0.16 $W/(m^2 \cdot K)$ in the case without the VIP layer, while the installation of the VIP layer decreases the U-value of the clear wall by 31%. However, the effect of the metal studs increases the U-value of the external wall by 50% for the case without VIP and 27% for the case with VIP. Concerning the roof and the floor, the repeating thermal bridges (repeating metal studs) increase the U-value of clear elements by 169% and 210%, respectively. It is reminded that the roof and the floor are not insulated with VIPs.

As it is shown in Fig. 3(b), with the installation of the VIP layer, the linear thermal transmittance of the three metal studs is reduced by ca. 64% to 83%. The linear thermal transmittance of I-type stud is ca. 40% higher than the respective of C-type stud, while the impact of CW-type stud is almost negligible.

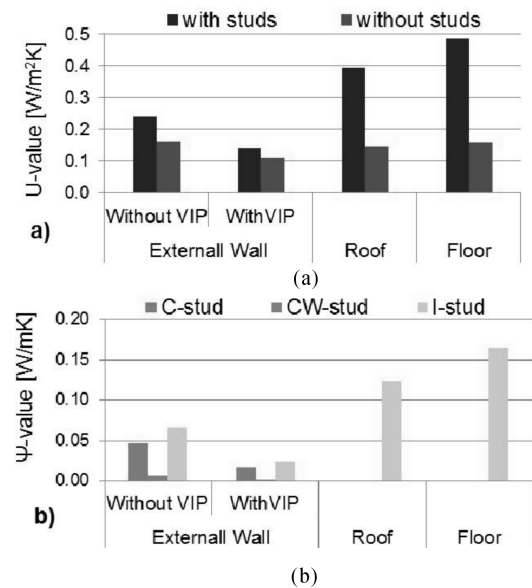


Fig. 3 The impact of repeating thermal bridges on

(a) the U-value of the building elements;

(b) the linear thermal transmittance of metal studs

The linear thermal transmittance of all the 2D junctions of the building elements examined in this work are presented in Fig. 4, indicating the effect of the

additional VIP layer. It is obvious that the VIP layer improves the impact of the 2D junctions on the thermal performance of the building, decreasing the Ψ -value by 12% to 92%, depending on the type of the intersection (Fig. 4 (a)). It is observed that the linear thermal transmittance has negative values at the junction between external walls (EW+EW), meaning that this thermal bridge has positive effect on the total thermal performance of the buildings' envelope. Fig. 4 (b) presents the 2D intersections that are not affected by the additional insulation. As it is shown, the most important thermal bridges are the junctions that include the floor, the roof and internal wall.

Fig. 5 illustrates the impact of the VIP layer on the point thermal transmittance of the 3D junctions of the examined building envelope. The VIPs improve the thermal performance of all 3D thermal bridges. The point thermal transmittances are decreased up to 138% due to the installation of VIP layer in the external walls. At the junction of two external walls with the ceiling, the effect of the junction is positive on the total thermal performance of the building envelope in the case of the additional internal insulation, while at the all other intersections the impact is negative.

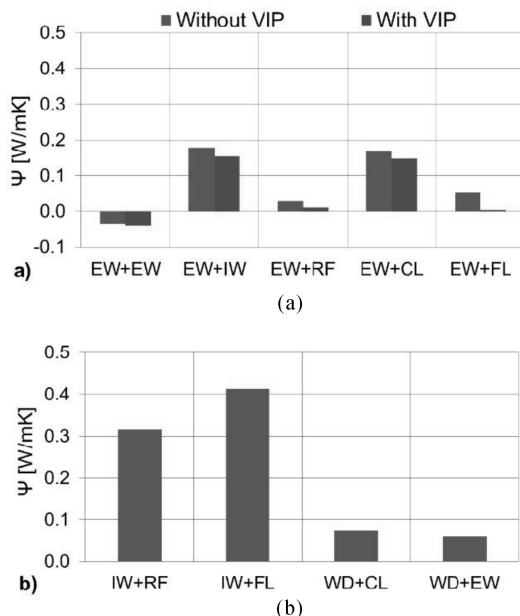


Fig. 4 The linear thermal transmittance of all 2D junctions. (a) Junctions where all elements include VIPs and (b) Junctions where only one of the elements includes VIPs.

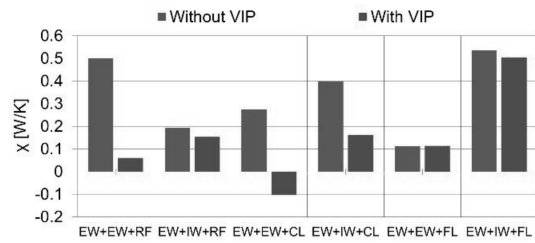


Fig. 5 The impact of VIP on the point thermal transmittance of all 3D junctions.

The contribution of the thermal bridges and the impact of the VIP layer on the overall thermal performance of the building envelope are depicted in Fig. 6. The installed VIPs decrease the total thermal transmission through the envelope, H_D , by ca. 33%. The contribution of the metal studs is 30% of the total transmittance in both cases. Although the additional insulation reduces the linear thermal transmittance of all the metal studs at the central part of the walls, the percentage impact of them remains the same because of the high Ψ -values of the studs at the roof and floor, where extra insulation is not installed. The total impact of the 2D and 3D thermal bridges is 31% at the case without the VIPs, while in the case with the VIPs is 25%. The 2D and the 3D junctions contribute the same percentage at the case without VIP, showing that 3D intersections are as important as 2D. For the case with VIP, the transmission of the point thermal bridges is 4 times lower than that of the 2D junctions.

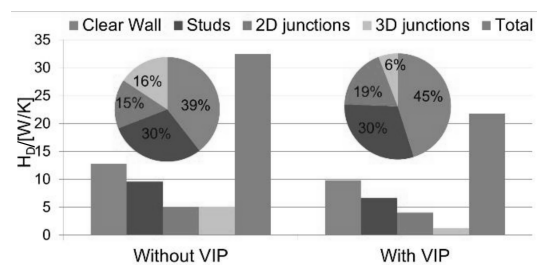


Fig. 6 The impact of thermal bridges on the overall thermal transmittance at the two cases

The results of the hygro-thermal analysis show that mold growth is not expected at the middle part of the building elements, since the temperature factor is higher than the critical value of 0.7 for both cases with and without the VIP layer. The additional VIP layer increases the temperature factor by 14%, on the middle

part of external walls with metal studs.

Fig. 7 presents the temperature factor of all non-repeating configurations for the case with VIP. It is obvious that there is no condensation risk at the 2D junctions, except from the intersection between the window frame and the external wall. On the other hand, the growth of mold is possible on all 3D junctions. The lowest temperature factor is recorded at the intersection between external wall-internal wall and floor with value equal to 0.6.

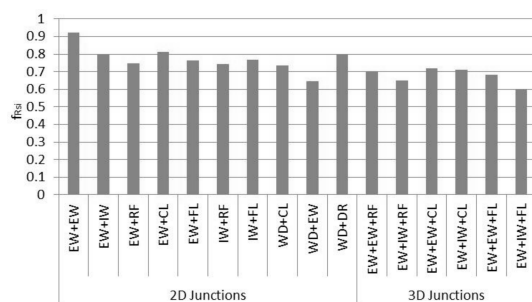


Fig. 7 The temperature factor of no repeating thermal bridges configurations at the case with VIP.

5. Conclusions and outlook

This work examined the impact of thermal bridges on the overall thermal transmittance of a metal framed lightweight drywall building envelope and the effect of an additional layer of VIP placed on the inner side of the external wall. Three types of thermal bridges were analyzed; thermal bridges resulting from metal studs (repeating thermal bridges) and 2D and 3D junctions (non-repeating thermal bridges) between the elements of the building envelope.

The impact of the thermal bridges on the thermal transmittance is strong, increasing the transmittance by ca. 61% ~ 55%. The results show that the highest contribution on the total thermal transmittance is owed to the metal frame of the building (approximately 30%). The effect of the 2D junctions is about 15% ~ 19%, while the impact of the 3D intersections can be 6% ~ 16%, in contrast to many researchers who neglect the effect of point thermal transmittance.

The internal insulation with VIPs results in a reduction of the overall thermal transmittance by 33%. Concerning the thermal bridges, the additional internal insulation with VIPs, decreases the impact of non-

repeating thermal bridges by 6%, while the impact of repeating thermal bridges is not influenced. The VIP layer decreases all linear and thermal transmittances up to 130%. Contrary to the outcome of other studies, the additional internal insulation of the external wall decreases the thermal bridges, not only relatively, but also quantitatively.

Finally, the hygro-thermal analysis shows that the improvement of thermal bridges by adding the VIP layer, results to a decreased risk of condensation at the internal surfaces of the envelope. For the case with VIPs, mold could appear on the 3D junctions of the building and especially at the floor corners.

Acknowledgements

The authors acknowledge the financial support of the European Commission in the frame of the FP7 – 2013 – NMP – ENV – EeB project ELISSA (www.elissaproject.eu).

References

- [1] U. S. Energy Information Administration (EIA), Monthly Energy Review, 2014.
- [2] I. Mandilaras, I. Atsonios, G. Zannis, M Founti, Thermal performance of a building envelope incorporating ETICS with vacuum insulation panels and EPS, *Energy and Buildings* 85 (2014), 654 – 665.
- [3] E. De Angelis, E. Serra, Light steel-frame walls: thermal insulation performances and thermal bridges, 68th Conference of the Italian Thermal Machines Engineering Association, ATI2013, *Energy Procedia* 45 (2014), 362 – 371.
- [4] S. Brunner, K. Ghazi Wakili, T. Stahl, B. Binder, Vacuum insulation panels for building applications-Continuous challenges and developments, *Energy and Buildings* 85 (2014), 592 – 596.
- [5] EN ISO 10211, Thermal bridges in building construction - Heat flows and surface temperatures - Detailed calculations, 2007.
- [6] EN ISO 6946, Building components and building elements - Thermal resistance and thermal transmittance - Calculation method, 2007.
- [7] ANSYS CFX-Solver Theory Guide, 2009.
- [8] DIN 4108-2, Thermal protection and energy economy in buildings - Part 2: Minimum requirements to thermal insulation, 2013.

A Comparative LCA Study of a Swedish Multifamily Building—the Primary Energy Use and GWP of Buildings with VIPs and Conventional Insulation Materials

Peyman Karami^{*}, Kjartan Gudmundsson

Department of Civil and Architectural Engineering, KTH - Royal Institute of technology, Stockholm, Sweden

Abstract

An improved thermal insulation of new and existing buildings is necessary to reach the “20-20-20” targets. This study puts emphasis on comparing the environmental impacts, GWP and total Primary Energy use, of retrofitting a Swedish standard building, with VIPs and conventional insulation. In this study, the spatial properties together with material specifications of the Building Information Model (BIM) are used to calculate the GWP and PE of the materials, both renewable and non-renewable, from cradle-to-gate. Analysis of the results illustrates that the VIPs are a very competitive alternative. Nevertheless, the results prove that the VIPs have a measurable environmental impact caused by product stage and further investigations of the matter must be a part of future work.

Keywords vacuum insulation panels, life cycle assessment, GWP, primary energy use, Building Information Model (BIM)

1. Introduction

The EU-commission has made a decision for reducing the Greenhouse Gases (GHG). This is known as the “20-20-20” targets [1] that set three key objectives for the year 2020 compared to the emission in the year 1990. Sustainable methods, including the application of new building technologies as well as refurbishment of external envelopes of existing buildings, are therefore needed. The use of vast thicknesses of traditional insulation will however have some partially negative environmental consequences. VIPs, with an unprecedented thermal insulation performance, are an interesting alternative, not at least since they may offer the possibility to save some living space area. Until now, the application of VIPs has been limited to a small number of buildings [2-8]. The service life time of a VIP can be defined as the time at which the required thermal conductivity has been surpassed, while a further account of service life is given in ISO 15686-2 [9]. One of the most important aging mechanism of VIPs is the permeation of gas through the envelope that may be enhanced at higher temperatures

and humidity and is further increased at the edges [10]. The edge effect will get greater with the ratio of edge length over area of the panel [11]. A number of studies put emphasis on life cycle analysis and service life predictions of the VIPs [12 – 14].

The LCA method is defined by SETAC, the Nordic guidelines for LCA and within the ISO 14000 series [15]. It can be applied on all levels of the building process from the design phase to the operation of existing buildings. Life cycle assessment is a system analysis tool for evaluating environmental impact of a product or a process over their entire life cycle, from raw material acquisition to end-of-life [16] and [17]. The general LCA methodology is described in the ISO 14040 standard and is comprised of four iterative phases, which are the goal and scope definition, inventory analysis, impact assessment and interpretation [18]. Evaluation of environmental impact consists of four steps. The first step includes definitions of the environmental impact categories, such as global warming or acidification and is followed up by the second step that associates the categories with the

^{*} Corresponding author, Tel :46 – 737801609, E-mail: peymank@kth.se

presumptive mass flow and environmental loads. The third step includes ranking and weighing of the calculated impact in order to make it possible to do the evaluation. As this makes the method somewhat subjective it is of great importance that the model used is clear and transparent as well as in line with the objectives of the study. The fourth and final step includes conclusions and recommendations. Although the application of standards gives possibility to compare life cycle analysis easier, the exact technique to calculate the environmental impact is not, in some cases, clearly defined. In the construction sector, the European committee for standardization, CEN, has developed a standard for calculating the environmental impacts of buildings and construction products with further details [19] and [20].

According to EN 15978 the life cycle of a building is divided into four stages, product, construction, use and end-of-life [20]. A number of Studies have shown that the use stage of buildings accounts for over 60%~90% of the environmental impacts compared to whole life cycle [21]. But with lower energy use, due to global and national environmental goals, the focus moves from the use stage to the product stage. Gustavsson et al. [22] showed that the PE in the production stage of low-energy buildings with a service life of 50 years could be up to 60% of the total depending on energy supply system compared to 45% for conventional buildings. Using district heating instead of electrical heating in a passive house resulted in a 40% lower primary energy use [22]. The ratio between building material production and operational energy is also highly dependent on building service life. Wallhagen et al. [23] showed that the relative CO₂ emission from building materials varied from 86% to 37% when the expected life time from 10 to 100 years for a newly built office building in Sweden. But after improvements of the materials and energy sources the variation was from 93% to 59%. Further investigations of building's environmental impacts, both production and operation, can be found [24-25]. In the case of LCA of VIPs, a number of studies [26-30] include evaluations of environmental impact of VIPs, but, none of those are concerned with VIPs with vacuumized fumed silica core.

Kunic et al. [31] concluded that VIPs have a small GWP compared to other insulation materials. Our previous study, Gudmundsson et al. [32] shows a comparatively higher impact. In a comprehensive study, Schonhardt et al. [33] performed a comparative LCA study of regular VIP with fumed silica and metalized polymer multi-layered film, comparing the results with the equivalent amount of EPS and glass wool. This study [33] shows a reduction potential of about 45% in the environmental impact of the VIPs if the panels would be manufactured with an alternative core or through the application of more energy efficient processes. Furthermore the same study shows that up to 90% of the energy use in the production of VIPs is derived from the core material, while only 4% of the energy used relates to the production of the film.

The environmental impact of a design alternative must be quantified if the potential effects of altering a design are to be evaluated. This can be done with the help of a Type III environmental product declaration, EPD, according to ISO 14025 and EN 15804, that give an account of the "Cradle-to-gate" stages in terms of environmental LCA (ISO 14040 and 14044), while a comprehensive LCA will also include the end-of-life stage "Cradle-to-grave". Aspects related to the use-stage of construction products are usually ascribed to the product itself and this stage is not a part of the EPD and the reader must therefore put the presented data into the overall performance context of a building [34]. To approve and publish an EPD, it must be critically reviewed and it must also be independently verified, either externally or internally.

By the use of EPDs from four different sources, three well-known VIP manufacturers and one input data from previous work [33] this study puts emphasis on comparing the environmental impact of retrofitting a hypothetical Swedish building with conventional insulations and with VIPs, for both material production and operation.

2. Building case study

The cradle-to-gate environmental impact of a Swedish standard building were assessed while the results were then compared with the impacts of well-insulated buildings with conventional insulations and

with VIPs. These well-insulated buildings were designed to have an equivalent U-value. The effect of the thermal bridges across the building constructions is not included in calculations of the U-value. A 2 story multifamily building of 4 apartments with a total living area of 520 m² was modelled in Autodesk Revit®. Each apartment is assumed to be inhabited by a family of 3~4 people. The load bearing construction is assumed to be a concrete frame. The Swedish “Boverket” prescribes a value of less than or equal to 80 kWh/m² per year for the energy consumption of a residential building, located in the climatic zone of Stockholm city [35]. To meet the Swedish passive house standards, a relatively low U-value of 0.10 and 0.066 W/(m² · K), must be reached in the wall and the roof, respectively. In the case of the standard building, the external walls and the roof are assumed to have a U-value of about 0.2 and 0.13 W/(m² · K). In the case of the well-insulated buildings, the U-value of the wall and roof have values of 0.09 and 0.065 W/(m² · K). The operational energy calculation is carried out with the VIP Energy software while the building reference time is set to 50 years. All the building components that used in the LCA evaluations are regular and available at the market today. The LCA of the building follows EN 15978 and the LCA for the building products was obtained from EPDs of the manufacturer in compliance with EN 15804. In this study a LCA approach using EPDs as input data is demonstrated for a simplified and yet reliable LCA analysis of buildings. The life cycle assessment includes the impact categories; PE use, both the renewable and non-renewable energy and GWP. The goal of this study is to compare environmental performance of a conventional and a low-energy building regarding insulation materials. Three different buildings are evaluated in this work. Firstly, a standard building with 180 mm traditional insulation in the wall and 270 mm in the roof. Secondly, a regular well-insulated building insulated with 400 mm and 520 mm thick mineral wool in the wall and roof. Thirdly, a well-insulated building with VIP sandwiched element consist of 25 mm EPS, 2×30 mm VIP, 25 mm EPS in the wall, and 25 mm EPS, 2×40 mm VIP, 25 mm EPS and an extra 45 mm thick mineral wool, in the roof.

The building life cycle stages that are included in this study are the production of building components as well as the operation of the buildings. Fig. 1 illustrates the life cycle stages in more details. The LCA analysis of this study does not include stages such as “transport to building site and construction (A4-A5)” as well as “end-of life (C)” due to a much lower environmental impact compared to the total life cycle of the building (A-C).

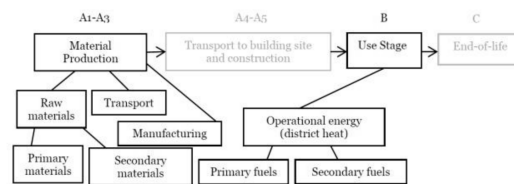


Fig. 2 LCA stages, those in grey are not included

The LCA input data for the building materials were gathered from EPDs published by the international EPD system, Norwegian EPD system (EPD Norge), German EPD system (IBU) and occasionally directly from the manufacturer. It is known that concrete has a high environmental impact in constructions and therefore it was important to use concrete data that is detailed and representative of the building type. The concrete was designed based on exposure class in accordance with SS EN 206:2013 “Concrete - Specification, performance, production and conformity” and its Swedish application SS 137003:2008. Two concrete types were chosen; one with a water-cement-ratio of 0.60 and C 25/30 in strength for internal load bearing walls and one with a ratio of 0.55 and C 30/37 for external walls, balcony slab and foundation. The concrete materials for the LCA analysis are manufactured for Norwegian market, the data was chosen with the assumption that the standards in Swedish markets are similar to those in Norway. The concrete contains 2 weight-% reinforcement from a well-known manufacturer in Sweden. The EPDs for the traditional insulations are average data representing a mean value from different manufacturers. The mineral wool is representative for the European market and the EPS for the Scandinavian market. In the case of the VIPs, the EPDs applied in sensitivity analysis received from four different sources (Tab. 1), three well-known VIP manufactures at the time of this study in 2015. The assessment is carried out based on the data from

Germany, due to a shorter transport distance from fabric to a hypothetical building site in Stockholm. The fourth source is the input data that has been used in previous work [33]. No recycled material was included in the calculation of the life cycle assessments of the EPDs for the insulation materials. Operational energy for maintaining a comfortable indoor temperature in the building comes from district heating, which is based on the LCA calculations by “Fortum Värme AB” for Stockholm year 2013 using the alternative generation method for heat allocation. The environmental impact for production and transport is 90 g CO₂ eq/kWh and a primary energy factor of 0.21. Fossil fuels represent 12% of district heating. In the raw material stage, secondary materials from another system process as waste and recycled material are considered having zero environmental impact when entering a new system. The same consideration was made for secondary fuels. Transport emissions for VIPs were calculated using a 16~32 ton freight lorry with a EURO 4 class from ecoinvent version 3.01.

This study includes evaluations of the environmental impact of VIPs for a building context using EPDs. Since the EPDs are producer/country specific, it was of special interest to perform a sensitivity analysis of how the total environmental impact of the building varies with different LCAs depending on country and producer. The sensitivity analysis was carried out with available EPDs, from four different sources (Tab. 1), in accordance to EN 15804. The EPD for VIP producer III was not third party verified but was still considered to be useful. The sensitivity analysis was performed by comparing the results from different EPDs within the same category of insulating materials and density range. In the sensitivity analysis, a comparison was made with 1 kg VIP.

Tab. 1 GWP and PE use for 1 kg of studied VIPs

1 kg VIP / Gate	GWP/ kg	Renewable PE/MJ	Non-renewable PE/MJ
Producer I Germany	9.4	64	162
Producer II Global	11.1	38	147
Producer III Belgium	6.6	29	120
Producer IV Germany [33]	6.2	30	130

3. Result and discussion

3.1 Environmental impact of buildings

The result of the buildings operational energy calculation shows that the standard building amounts to 92.96 kWh/m² per year while the regular well-insulated and the VIP well-insulated buildings have values of 61.81 and 56.74 kWh/m² per year, respectively. This value includes the energy for heating, energy for space cooling and domestic hot water. The standard building surpasses the limit of 80 kWh/m² per year [35] and has the highest energy use. The regular well-insulated building consumes about 33% less energy while the building with VIPs uses about 39% less energy. The total operational energy use of the buildings are then converted to GWP and PE and added to the impacts from material production stage (Fig. 2,3)

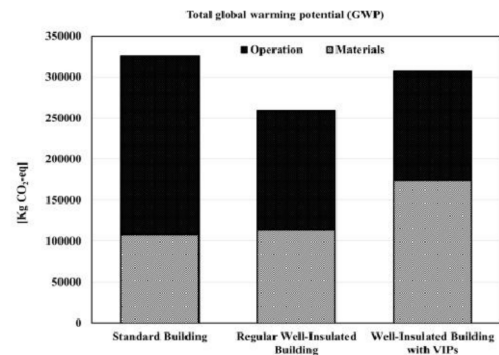


Fig. 3 Total GWP

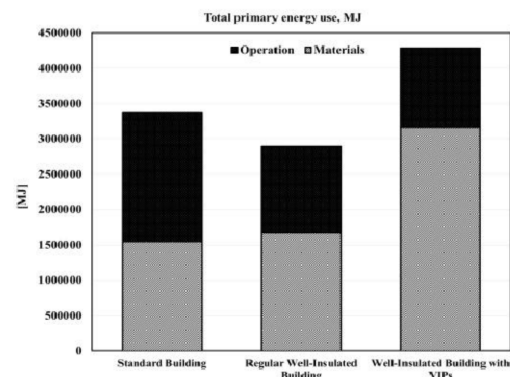


Fig. 4 Total PE

The values illustrate that the impacts for the standard and regular well-insulated buildings are relatively, similar to previous work [21-25]. This study, does however, include the LCA of a VIP insulated building. In the case of GHG emission of VIP

retrofitted building, more than half of the total emission (57%) is related to the production of building components, while in the case of regular well-insulated building, more than half of GHG emission (56%) is, in contrast, related to the operation phase. In the case of standard building, a significant share of GHG emission is related to the operation phase of building which accounts for two thirds of the total emission (67%). The emission for the operation phase of a standard building highlights the dire necessity of insulation. It can be seen that the total energy of operation was significantly reduced in the case of well-insulated buildings. Analysis of the PE use (Fig. 4) shows that more than two third (up to 74%) of the total PE of the well-insulated building with the VIPs is related to the production stage of building components. While in the case of the regular well-insulated building, about 58% of total PE is due to production of material and 46% in the case of the standard building. This is partly in line with the results of [22] that showed the PE in the production stage of low-energy buildings with a service life of 50 years could be up to 60% of the total depending on energy supply system compared to 45% for conventional buildings.

In general, the GHG emission of the VIP insulated building is approximately 6% lower than for the standard building. It must be observed that the emissions can be further reduced through the application of an alternative VIP core material or/and utilization of renewable resources. It is also of interest to notice that, compared to the standard building, the GHG emissions can be reduced by 21% adding more traditional insulation while this, in turn, would result in a significant loss of living space area

In the case of well-insulated buildings, the results of Fig. 4 illustrate that the effect of reducing the energy use of the materials from cradle-to-gate clearly outweighs the operational energy use of the building. When looking at both impact categories, VIPs seem to have a potential for further improvement, especially when it comes to the production of the core material [33, 36-38]. This may include the exploitation of alternative eco-efficient production processes and sustainable production strategies focused on reducing the

production energy and the use of renewable resources. For instance, our previous [36, 39] include assessments of new precipitated silica core materials.

3.2 Sensitivity analysis

This study includes sensitivity analysis of VIPs using EPDs from four different independent data sources. This includes the GWP and PE use for the production of 1 kg of vacuum panel. The results are shown in Fig. 5 in which the upper graph illustrates the GWP (kg CO₂ eq/kg material) and the graph below represents the PE use (MJ).

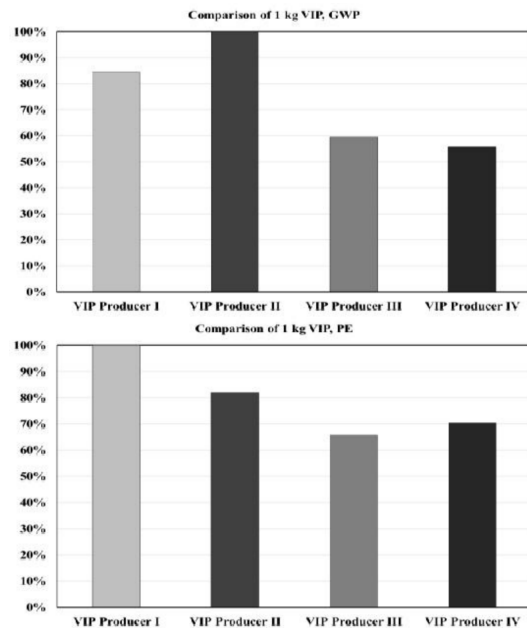


Fig. 5 Comparison of different VIPs

The analysis for the VIPs shows the smallest impacts in both categories for producer III and producer IV. The impacts are fairly close, with only a difference of 5% in the GHG emissions as well as 6.8% in the PE use. The analysis also shows that the producer I and II have in contrast the highest impacts, while these impacts are relatively close, with a comparatively greater difference of 16% in GHG emission and 18% in PE use.

This may be due to the differences in the VIP production process and/or different energy sources. The VIP manufacturing processes have thus a great potential for further investigations by aiming to reduce the environmental impacts of VIP production. The EPDs of the VIPs show different supplies of energy, producer I

uses 100% hydropower at plant and producer II uses a plant specific power mix while producer IV uses a power mix from Kempten while producer III has an unknown power mix and energy use. A more definite conclusion would require more complete and transparent EPDs from the producers since a number of key's full information were not transparent or were totally missed.

4. Conclusions and outlook

This study contains a comparison of the sum of the environmental impacts from three buildings, a standard and two well-insulated buildings with traditional insulation materials and with VIPs. The GWP and PE use (both renewable and non-renewable), for both the building's material production and building operational phase (50 years), have been assessed.

The well-insulated building with VIPs has measurable environmental impacts, mostly during the production process of the building materials. It must be noted that the VIPs have measurable environmental impacts but, in the case of primary energy use, those are outweighed by the reduction of operational energy. It must also be noted that the building with VIPs has a lower total GHG emission for both the material production and operation phase, compared to the standard building. The lack of transparent data does, however, call for further investigation.

Acknowledgements

The authors wish to thank FORMAS.

References

- [1] European Union commission, climatic actions, http://ec.europa.eu/clima/policies/package/index_en.htm
- [2] IEA Annex 39, Subtask A, H. Simmler et al. 2005.
- [3] IEA/ECBCS Annex 39 HiPTI (Subtask B) 2005
- [4] K. Ghazi Wakili et al. in 7th IVIS, Empa, 2005.
- [5] H. Schwab et al. Thermal Envelope and Building Science 28 (4) (2005) 345 – 355.
- [6] A. Binz, in: Proceedings of 7th IVIS, Empa, 2005.
- [7] R. Baetens et al. Engy and Bldg 42 (2010) 147 – 172
- [8] S. E. Kalnæs et al. App Engry 116 (2014) 355 – 375.
- [9] ISO 15686-2, 2001(E) Bldg and Const. Assets
- [10] H. Simmler et al. Engy and Bldg 37(2005) 1122 – 1131.
- [11] PH. Schwab et al. Thermal Envelope and Building Science 28 (4) (2005) 293 – 318.
- [12] S. Brunner et al. Vacuum 82 (7) (2007) 700 – 707.
- [13] S. Brunner et al. Vacuum 100 (0) (2014) 4 – 6.
- [14] E. Wegger, Building Physics 35 (2011) 128 – 167.
- [15] W. Trinius, PhD thesis, KTH, Stockholm, 1999.
- [16] D. F. Ciambrone, Environmental life cycle assessment, CRC Press inc, NY; Lewis, 1997
- [17] S. Joshi, Industrial Ecology, 3(2-3) (1999) 95 – 120.
- [18] ISO 14040, 2006. International organization for Standardisation.
- [19] CEN 2012, EN 15804. EUC for standardisation.
- [20] CEN 2012, EN 15978. EUC for standardisation.
- [21] M. Buyle et al., Renewable and sustainable energy reviews, 26, (2013) 379 – 388.
- [22] L. Gustavsson Engy and bldg 42 (2010) 210 – 220.
- [23] M. Wallhagen, et al., Building and environment, 46 (2011) 1863 – 1871.
- [24] T. Ramesh, Engy & Bldg 42 (2010) 1592 – 1600.
- [25] I. Zabalza Bribián et al., Building and Environment 46 (2011) 1133 – 1140.
- [26] F. Intini et al. Life Cycle Assess 16 (2011) 306 – 15.
- [27] T. Gao, Appl. Mat. & interf. 5 (2013) 761 – 767.
- [28] S. Proietti et al. Appl. Energy 112 (2013) 843 – 855.
- [29] A. D. La Rosa Con. & Bldg Ma55 (2014) 406 – 414.
- [30] R. G. Ogden in 11th IVIS, Switzerland, 2013.
- [31] R. Kunic et al. in 11th IVIS, Switzerland, 2013.
- [32] K. Gudmundsson in XIII-DBMC Brazil, sep. 2014.
- [33] U. Schonhardt et al. Dott, FHBB, MuttENZ ESU-services, Uster, December 2003
- [34] K. Gudmundsson in 12th BMC, Portugal, 2011.
- [35] Regulations and guidelines, Boverket, BFS 2015:3 BBR 22
- [36] E. T. Afriyie, Engy&Bldg 75 (2014) 210 – 215.
- [37] G. W. Scherer, Non-Cryst. So 215 (1997) 155 – 168.
- [38] R. A. Venkateswara et al. Materials Chemistry and Physics 77 (2002) 819 – 825.
- [39] P. Karami et al. Engy & Bldg 85 (2014) 199 – 211.

ETICS with Vacuum Insulation Panels for Retrofitting Buildings from the Great Swedish Housing Program “Miljonprogrammet”

Peyman Karami ^{a*}, Kjartan Gudmundsson ^a, Folke Björk ^a, Luc Heymans ^b

^a Department of Civil and Architectural Engineering, KTH - Royal Institute of technology, Stockholm, Sweden

^b MICROTHERM, R&D, Industrie park-Noord 1-BE-9100 Sint-Niklaas, Belgium

Abstract

The unique thermal properties of VIPs make them a compelling alternative for many building applications. This work illustrates a new VIP mounting system that can be used to improve the energy efficiency of buildings that are typical of the great Swedish housing program of the late sixties and early seventies, “Miljonprogrammet”.

The embedded VIPs are glued to the outside of the existing wall structure, while a L-profile connected directly to the aerated concrete wall carries a facade board on which rendering may be applied. A T-profile provides a ventilating air gap between the facade board and the structure. The suggested technical solutions have been evaluated through full scale measurements in a climatic chamber. The measurement results are used to derive the resulting U-value of the wall after retrofitting. The thermal properties of the materials were obtained through independent measurements by the means of TPS technique. The analysis of the result values shows a significant improvement in the resulting U-value of the retrofitted wall compared to non-retrofitted.

Keywords vacuum insulation panels (VIPs), miljonprogrammet, retrofitting, climatic chamber, resulting U-value

1. Introduction

Buildings are the largest consumers of energy worldwide [1]. Today’s buildings are responsible for 40% of the world’s energy use and GWP. A 30 % increase in the global energy demand for buildings is expected by 2035 [1] and the EU-commission has set three key objectives for the year 2020 compared to 1990 levels, known as the “20-20-20” targets [2].

In Sweden, about 21% of the energy use can be related to the heat losses through the climatic envelopes of buildings. The Swedish “Boverket” prescribes a value of less than or equal to 80 kWh/m² per year for the energy consumption of multifamily residential buildings, located in the climatic zone of Stockholm [3].

Due to the comparatively great heat transmission losses, the Swedish “Million Program” from the 60s and 70s is a challenging and attractive task for research.

According to “Boverket” the apartment blocks from the “Million Program” must be refurbished by 2025 with a U-value target of 0.18 W/(m² · K) after renovation [5]. A number of studies put emphasis on the improved thermal efficiency of these buildings and a comprehensive summary of pre and post-renovations using traditional insulations can be found in the literature [6 – 8]. The unique thermal properties of VIPs make them a compelling alternative for Swedish “MillionProgramme”.

The application of VIPs has been limited to a fairly small number of buildings [9], while a number of studies [9-18] give comprehensive account of theoretical discussions and a state-of-the-art review of VIP products, laboratory or in situ measurements of the implementation of the panels in a retrofit project as well as life cycle assessments. It is obvious that the

* Corresponding author, Tel :46 – 737801609, E-mail: peymank@kth.se

implementation of VIPs calls for a building technology that provides an adequate protection of the VIPs, while allowing for necessary maintenance and renovation. It has also been shown that the joints at which the panels meet give rise to thermal bridges that increase the heat loss through the building envelope. Our previous parametric study shows that the thermal edge loss can be compensated with an adjacent layer of thermal conductivity in the range of traditional insulations [19]. The report of the IEA [10] includes a number of studies that performed risk assessments of building physics performance (heat, air, and moisture) in VIP retrofitted buildings. Further investigations can be found in the literature [20-22].

The purpose of this study is to propose a new robust ETICS system with VIPs for the “Million Program” and to evaluate the thermal performance of the system.

2. Method

Prior to the full scale laboratory experiments, the influence of various design factors is evaluated through one-at-a-time parametric analysis and the risk of excessive moisture conditions is investigated through dynamic simulations. The suggested technical solutions are then evaluated through full scale measurements in a climatic chamber. This includes monitoring of temperature and relative humidity at various locations in the wall construction, over a period of 1 year. These steps also offer possibility to do a comparative study between the calculated and the real thermal transmittance.

2.1 Parametric analysis

Much work has been done to investigate the impact of factors such as VIP thickness and geometry, VIP laminates and the hygrothermal properties of materials at the joints, on the heat flux across a VIP retrofit project [24 – 28].

The new VIP mounting system is based on some of the findings of our previous study [19] that includes a parametric analysis of the impact of the thermal conductivity of the materials at the joints of panels and that of the adjacent insulation layer as well as at the fasteners on the thermal bridges that can be seen in Figs. 1 and 2. The results can be compared to a U-value

of about $0.09 \text{ W}/(\text{m}^2 \cdot \text{K})$ for a construction with no thermal bridges.

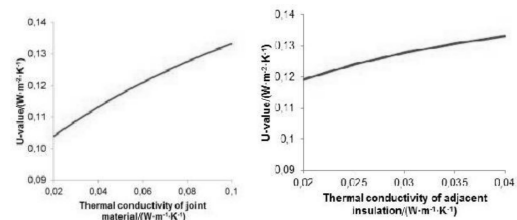


Fig. 1 The resulting U-value as a function of the thermal conductivity of the joint (left) and of the adjacent insulation (right)

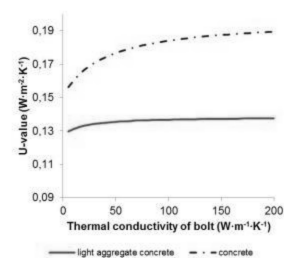


Fig. 2 The resulting U-value as a function of the thermal conductivity of the bolt

As shown in Fig. 1-left, the application of a material with a high thermal resistance at the VIP joints has a significant influence on the thermal bridge. Going from a value of 0.10 to $0.02 \text{ W}/(\text{m} \cdot \text{K})$ will give a reduction that amounts to about 30% of the total heat loss. In the case of adjacent insulation material, as is shown in Fig. 1-right the influence of improving the outer insulation layer does also have a significant effect on the heat flux, although somewhat smaller. Fig. 2 illustrates how the thermal performance of the fasteners affects the resulting U-value. The red solid line shows that the influence of the bolts is almost negligible in the case of a light aggregate concrete wall retrofitted with VIPs, in contrast to the results for a massive concrete wall as illustrated by the blue dotted line.

2.2 Dynamic simulations of moisture

An assessment of the relative humidity, RH, were carried out by simulations of heat flux and moisture transport [23]. This includes transient modeling of vapor diffusion with Comsol Multiphysics® allowing for sorption in the material as well as enhanced moisture transport at high relative humidity. This was done with

climatic conditions as described by EN15026, while the average hourly values for outdoor temperature and relative humidity are retrieved from an IWECC (international weather for energy calculation) climate file for Stockholm.

The 2D plot of Fig. 3 shows the RH through the retrofitted wall with exterior VIPs while each graph of the Fig. 4 gives the one year variations of RH ranges in the selected points, shown in the Fig. 3.

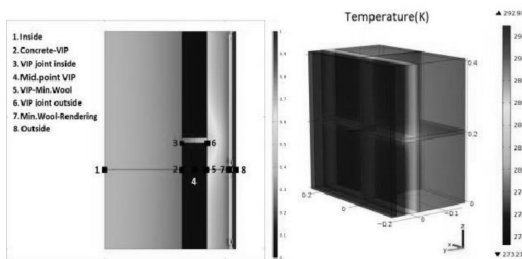


Fig. 3 2D simulations of RH distribution at long term extreme conditions and 3D module of heat flux

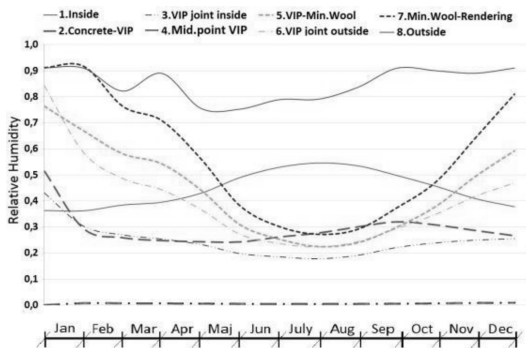


Fig. 4 RH as a function of time

A 3-dimension simulation was carried out with Comsol Multiphysics® in order to illustrate the effects of thermal bridges due to the mechanical fasteners at the joints where the panels meet.

In essence, the study shows that the layers on the outside of the VIPs have a moisture content that is very close to that of the outside environment while the layers on the inside have a temperature and moisture content that is close to that of indoors. Thus, a calculation of the RH illustrates that the placement of the VIPs on the outside of the wall does not pose a moisture problem to the construction. Furthermore, it has been shown that the model indicates no risk of high relative humidity at the joints of the panels.

The model does not, however, take into account

the penetration of rainwater and possible leakage through the joints of the panels. A ventilated air gap is commonly used to ventilate excessive moisture due to leakage at joints while reducing the pressure of driving rain and providing a barrier to capillary transport from the wet outer surface.

2.3 In-situ measurement with climatic chamber

On the basis of the parametric analysis and the simulations a new ETICS with VIPs for aerated concrete is proposed. The thermal bridges at the fasteners and the joints of the VIPs are minimized with a new mounting system while a ventilated air gap provided by the system allows for the drying out of excessive moisture. This study puts particular emphasis on proposing a VIP technical solution with certified, standard and commercially available components.

The technical solution, suggested in this study, is evaluated through full scale measurements in a climatic chamber. The chamber consists of two rooms with a length, width and height of 3, 3 and 4 m, in that order. A wall construction of aerated concrete blocks, representative of the “Million Program”, was built in the climatic chamber. The wall, measuring about 12 m², is insulated with a VIP sandwich consisting of a 20 mm thick VIP embedded between 20 and 10 mm thick Expanded Polystyrene (EPS) panels, attached by the means of industrial adhesive glues and tape. Prior to the mounting of the VIP sandwiched panels, four different adhesive glues and a number of different adhesive tapes were tested. All the tapes are commercially available and certificated for freezing temperatures. Prior to installation, the VIP sandwiches were compressed by the means of mechanical loads, up to 3.0 kN. In the case of gluing, up to 24 h were spent on compressing the VIP sandwiched panels in order to gain stability. A relatively short compressing time (minutes) was used for the adhesive tapes. The size of the VIPs used in this study were 1200 × 600 mm² (type A) and 600 × 500 mm² (type B). Prior to the experiment the wall was allowed to dry for 3 months. The VIP sandwiches were then glued to the outside of the existing wall structure, by the means of an adhesive (hydraulically setting mortar) that is specially design to be used for adhesion and levelling of porous materials, e. g. EPS panels, to a

rough surface material such as cell blocks or concrete. The adhesive is certificated for loads up to 80 kN/m^2 parallel to the wall. A 3 mm thick L-profile (stainless steel) connected directly to the aerated concrete wall carries a facade board on which rendering may be applied. A T-profile (3 mm thick stainless steel) provides a flexible ventilating air gap between the facade board and the structure (Fig. 6). Prior to fastening the L-profile to the cellblocks, special bolt screws with various geometric sizes were tested for load-bearing capacity. This study includes the first application of these specially designed facade connections with VIPs.

A number of experiments were performed in order to evaluate the thermal properties of the materials. In a recent study it has been shown that the difference between the material properties in real case and the standard data can lead to differences between the measured and calculated result values [22]. In this study, the Transient Plane Source (TPS) technique (TPS 2500S-ISO/DIS 22007-2, 2) was therefore used to evaluate the thermal properties of the materials used in the wall. Prior to laboratory experiments, a number of cubes, with flat surfaces, were built by cutting cellblocks and EPS panels. A cubed shaped steel frame was, in addition, applied to form the “hydraulically setting mortar” that used to attach the VIP sandwiches to the surface of the cell block (Fig. 5).

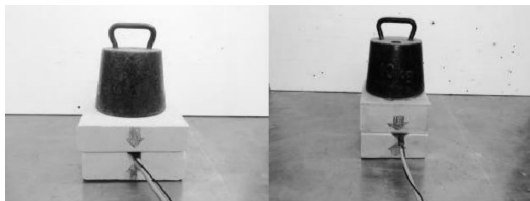


Fig. 5 The transient thermal experiments with TPS

The laboratory measurements are carried out with several temperature sensors and RH sensors while the heat flow across the wall was measured with heat flow meters of the type PU43 (produced by TNO Institute of Applied Physics, Delft; Netherlands). Prior to the in situ measurements, the heat flow meters were calibrated with a standard reference material[®] (SRM 1450d) high-density Fibre Glass Board, certificated by the National Institute of Standards and Technology.

The heat flow meters were mounted in different

positions on the interior surface as illustrated in Fig. 6. 80 temperature sensors of type T (Copper/Constantan thermocouple) as well as Type K (Chromel/Alumel thermocouple) were installed at various coordinates in the plane of the wall and at the material layer boundaries as shown in Fig. 6.

To monitor the indoor and outdoor relative humidity, a number of sensors (Mitec RH sensors) were used. However, the authors of the study were not able to manage the indoor and outdoor humidity in the climatic chambers. All the sensors are connected to a number of data loggers (Mitec AT 40 g) that were used to record and store data every 1 hour.

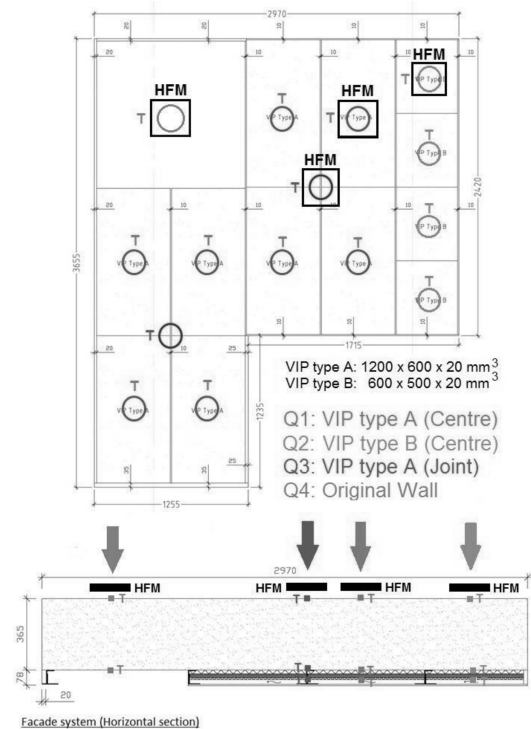


Fig. 6 Technical solution for retrofitting and placement of the sensors

A number of methods for in-situ measuring and monitoring of building envelopes can be seen in the report of [31] where the test facility designed was based on the objectives of international standards. Laboratory procedures and principles for determination of thermal transmittance of building elements can be found in [29]. The thermal measurements in this study have been carried out according to the governing standard, NS-EN ISO 8990:1997 [32]. A steady-state measurement with a climatic chamber can be carried out by measuring the

heat flow through a wall construction of given thickness and a known temperature difference across the wall. This requires that the temperatures on both sides are kept at constant values and the materials must reach equilibrium in order to eliminate the effect of the thermal inertia of the wall construction. The thermal transmittance or U-value of the wall can then be calculated using the following equation

$$\frac{\lambda_{\text{Block}}}{d_{\text{Block}}}(T_{\text{si}} - T_{\text{Block-VIP}}) = U_{\text{Wall}}(T_i - T_e)$$

Where the left side is the heat flux through the aerated concrete block a function of the thermal conductivity of the block, its thickness, d_{block} and the temperature drop, ΔT_{block} while the right side gives a corresponding expression for the heat flux from the interior surface to the outer surface of the wall as a function of the U_{value} of the wall, U_{wall} and the inside temperature, T_i and outside temperature T_e .

3. Results and discussions

The laboratory experiments started in December 2014. This is an ongoing work and the results of preliminary measurements, for a period of two months, is shown in this study. The laboratory experiments were carried out through measurements at three climatic time sequences with different outdoor temperatures, while the indoor air temperature is intended to be representative of Swedish residential buildings. The thermal conductivity of the building materials, measured with TPS, is listed in table 1 together with the calculated U-value.

Tab. 1 The thermal conductivities of the materials and the calculated U-value

Materia	$\frac{d}{\text{mm}}$	$\frac{\lambda}{\text{W}/(\text{m} \cdot \text{K})}$	Source	$\frac{R}{\text{m}^2 \cdot \text{K}/\text{W}}$
Aerated concrete blocks	365	0.118	TPS	3.09
Hydraulically setting mortar	2	0.959	TPS	0.002
EPS	20	0.0329	TPS	0.608
VIP	20	0.007	Manufacturer	2.857
EPS	10	0.0329	TPS	0.304
Rsi	-	-	Standard value	0.14
Rse	-	-	Standard value	0.04
Rwall	-	-	-	7.041
Calculated U-value/ $(\text{W}/(\text{m}^2 \cdot \text{K}))$	417		Before retrofitting	0.305
			After retrofitting	0.142

The average values of indoor/outdoor temperatures and other measured temperatures measured at different locations of the construction, as shown in Fig. 6, are listed in Tab. 2.

Tab. 2 The average temperature values represent the climatic condition at different locations of the wall

Placement	With out VIPs	VIPcentre 1200×600 mm ²	VIPjoint 1200×600 mm ²	VIPcentre 600×500 mm ²
Indoor air /°C	26.51			
Interior surface temperature/°C	23.3	25.8	25.55	26.03
Concrete blocks-VIPcentre /°C	—	7.45	0.99	7.15
Exterior surface temperature/°C	-14.5	-15.68	-14.63	-14.9
Outdoor air /°C	-17.06			
Measured U-value/ $(\text{W}/(\text{m}^2 \cdot \text{K}))$	Before retrofitting 0.28			
	After retrofitting 0.136			

These values are from selected periods of the 2 month in situ measurements. It must be noted that each temperature value represents an average of at least 3 adjacent sensors. The spread of values was small (up to 0.3°C) in comparison with the $\pm 1^\circ\text{C}$ standard deviation of the sensor values (according to the manufacturer,) and is assumed to have a negligible effect. As expected the temperatures are higher at the interior surfaces with VIPs due to the increased thermal resistance of the wall and for the same reason the outdoor surfaces of the corresponding sections are lower. Furthermore the temperatures at the joint of the panels indicate a thermal bridge effect as expected and shown in Fig. 7.



Fig. 7 IR-camera shows temperature distribution

The heat flux measurements for the bigger panels give a U-value of about 0,136 W/(m² · K) for centre of panel which correspond to a decrease of about 52% when compared to the wall without panels. This, remarkably, is very close to the calculated U-value of Tab. 1.

The temperatures on the exterior surface and between the concrete and the VIP sandwich suggest that the bigger panels have a slightly better performance, possibly because a greater area to perimeter ratio and hence a smaller thermal bridge as reported in previous research [24-28]. The measured indoor temperatures contradict this but can most likely be explained by unfavourable air distribution in the indoor chamber.

4. Conclusions and outlook

This study demonstrates a robust, effective, simple and fast system for external mounting of VIPs. It has been shown how the ETICS can be used for retrofitting of buildings from the Swedish "Miljonprogrammet". The system is based on standard and commercially available products and should allow for the re-mounting in case of damaged or deteriorated panels.

The system is based on parametric analysis and has been evaluated through full scale measurements. The result of the parametric analysis highlight the fact that the thermal properties of the material used at VIP joints has a remarkable influence on the thermal bridges. Going from a thermal conductivity value of 0.10 to 0.02 W/(m · K) will give a reduction that amounts to about 30% of the total heat loss. Improving the outer insulation layer does also have a significant effect on the heat flux, although somewhat less than the effect of lowering the thermal conductivity of the VIP joint. Results from 3D simulations with Comsol[®] show that the fasteners deserve careful consideration. The study indicates that the application of the VIPs at the outside of construction will not lead to high relative humidity in the wall or at the joint while attention must be given to leakage at joints and penetrating rain.

The results so far show that a comparatively thin external insulation can lower the U-value of the wall construction by about 52%.

This is an ongoing work and the results shown in

this paper are based on measurements from a period of two months. Current efforts include the use of infrared thermography to quantify the whole-wall U-value and thermal bridges and future work will include further dynamic simulations and full scale measurements of heat and moisture distributions across the wall construction. The future work will also include a discussion concerning the method, e. g. our investigations so far illustrate that the use of adhesive tape for embedding VPs between EPS panels deserves further investigation.

Acknowledgements

The authors wish to thank the FORMAS.

References

- [1] Policy Pathways; Modernising Building Energy Codes, OECD/IEA-UNDP, USA, edition 2013.
- [2] European Union commission, climatic actions, http://ec.europa.eu/clima/policies/package/index_en.htm.
- [3] Regulations and guidelines, Boverket, BFS 2015;3 BBR 22.
- [4] Vision for Sweden 2025, Boverket, ISBN pdf: 978-91-7563-135-6, Karlskrona, Sweden, April 2014.
- [5] Regulations and guidelines, Boverket, BFS 2012;6 BBR 19.
- [6] J. O. Dalenbäck et al. In Proceedings Ökosan, Graz 2011.
- [7] Bebo, Brogården-miljonhusen blir passiva, [In Swedish] 2011.
- [8] Swedish Environmental Research Institute Ltd. 2009, March 18.
- [9] IEA/ECBCS Annex 39HiPTI (Subtask B) 2005.
- [10] K. Gudmundsson in XIII-DBMC Brazil, sep. 2014.
- [11] IEA Annex 39, Subtask A, H. Simmler et al. 2005.
- [12] K. GhaziWakili et al. in 7th IVIS, Empa, 2005.
- [13] H. Schwab et al. Thermal Envelope and Building Science 28 (4) (2005) 345 – 355.
- [14] A. Binz, in: Proceedings of 7th IVIS, Empa, 2005.
- [15] R. Baetens et al Engy & Bldg 42 (2010) 147 – 172.
- [16] S. E. Kalnæs et al App Engry 116 (2014) 355 – 375.
- [17] T. Nussbaumer et al. Applied Energy 83 (2006) 841 – 855.
- [18] W. Platzer et al 8th VIPs Symposium (2007).
- [19] K. Gudmundsson. 9th VIPs Symposium (2009).
- [20] S. Brunner et al. Vacuum 82 (2007), 700-707.
- [21] E. Sveipe et al. Bldg Phys. 35 (2011) 168-188.
- [22] P. Johansson, Energy & Bldgs 73 (2014) 92 – 104.
- [23] K. Gudmundsson, P. Karami. Journal of Civil Engineering and Architecture, Issue 7 (2013).
- [24] IEA/ECBCS Annex 39, HiPTI Subtask B, 2005.
- [25] K. GhaziWakili, Bldg Res&Info32 (2004) 293 – 399.
- [26] K. GhaziWakili, Eng&Bldgs 43(2011) 1241 – 1246.

- [27] K. GhaziWakili, in 7th IVIS Switzerland, 2005.
- [28] A. Binz at al. In 7th IVIS Switzerland, 2005.
- [29] T. Haavi et al. Bldg Phys. 36(2012) 212 – 226.
- [30] M. Erb in IEA/ECBCS Annex 39 HiPTI 2005.
- [31] C. Peng, Enrgy and Bldigs 40 (2008) 2076 – 2082.
- [32] NS-EN ISO 8990:1997; Thermal insulation. Determination of steady-state thermal transmission properties. Calibrated and guarded hot box, 1997.

Utilization of Vacuum Insulations for Masonry Construction Elements Production

Jiří Zach^a, Jitka Hroudová^{a*}, Vítězslav Novák^a, Azra Korjenic^b

a. Brno University of Technology, Faculty of Civil Engineering, Institute of Technology of Building Materials and Components, Veverí 331/95, 602 00 Brno, Czech Republic

b. Senior researcher, Vienna University of Technology, Faculty of Civil Engineering, Institute of Building Construction and Technology, Karlsplatz 13, 1040 Vienna, Austria

Abstract

One of the major issues of using vacuum insulation in buildings is their problematic installation and the risk of their damage during and after fitting which results in the degradation of their thermal insulation properties. One of the solutions can be fitting the vacuum insulation directly into hollow masonry pieces (small-size insulators in several layers). The paper describes the possibilities of using small-sized vacuum insulation for the production of ceramic masonry elements containing integrated insulation of very high thermal resistance. The integration of a vacuum insulator into a masonry block minimises the necessity to additionally adjust the insulator at the construction site and furthermore it greatly increases the protection of the insulator against mechanical damage. The choice of placement of the vacuum insulator in a block can eliminate the risk of damage (e. g. drilling or otherwise breaking through) in the structure during its service life.

Keywords vacuum insulation, thermal conductivity, masonry constructions, thermal resistance, masonry elements

1. Introduction

One of the current global topics is economical use of non-renewable resources whether in terms of efficient use of energy obtained from them or in terms of reducing the pollution produced by their processing. In connection with this there is pressure to reduce the energy demands of buildings as it is this which constitutes one of the substantial parts of total energy consumption. This fact is confirmed by the Kyoto pyramid which identifies quality thermal insulation of building envelopes as the most effective means of reducing energy [1, 2].

In terms of masonry building envelopes, the best thermal insulation properties can be attained by the use of load – bearing elements with the best possible thermal insulation properties, division of the load-bearing part of the envelope from masonry or refitting the vertical

structures with insulation.

When using conventional ceramic masonry blocks, one of the options to improve the final thermal insulation properties of the structure is additional insulation (interior or exterior). This method brings a number of negatives. It is especially a necessity to undertake further technological steps in order to fit additional insulation systems which adds to the construction time as well as the total budget. Moreover, there is a risk of defects occurring and, by extension, problems caused by low-quality/unqualified installation of the thermal insulation system. Another negative is the increase of the building's total wall thickness due to the use of thermal insulation systems [3]. In new constructions, it is more suitable to use ceramic masonry blocks which themselves meet high requirements on thermal insulation properties. One of the options are blocks with

* Corresponding author, Tel :420 – 541 – 147 – 525, E-mail: hroudova.j@fce.vutbr.cz

integrated thermal insulation [4, 5].

2. Development of ceramic masonry blocks

There are three basic directions in the development of ceramic masonry pieces used in exterior walls. The matter at hand is the improvement of thermal-technical properties of the very cast from which the blocks are made, next the geometrical arrangement of the internal ribs of the blocks and at the same time the most rapidly evolving direction of development is fusing the ceramic masonry block and thermal insulation or integrating the thermal insulation into the cavities of the block respectively [4, 6].

Both in terms of the development direction focused on the properties of the ceramic cast of the block and of the geometrical arrangement, there are currently no possibilities of any further significant improvement. The improvement of the thermal-technical properties of the cast is achieved mainly by light weighting of the cast which brings a reduction of thermal conductivity but also a deterioration in mechanical properties which in effect limits further possibilities of improving the thermal insulation properties. The case of geometrical design of the block concerns mainly the creation of the highest possible number of overlaying cavities situated perpendicularly to the direction of heat flow and the reduction of the thickness of the ribs (especially in the direction of the heat flow). A decrease in rib thickness brings a problem in terms of manufacturing and causes deterioration of the mechanical properties of the blocks. In both cases, an optimal ratio between mechanical and thermal-technical properties has been found. For this reason, the development of ceramic masonry elements is focused on blocks with integrated thermal insulation [4, 6].

The integration of thermal insulation into the cavities in ceramic masonry blocks is performed in particle and liquid state or with a piece of insulator. Particle and liquid insulators can be applied in small as well as large cavities in the block without any need of substantial changes of its internal structure. Particle insulators (e. g. polystyrene) are applied as granules which, upon having filled the cavities, undergo additional expansion and are thus fixed in place. Liquid insulators are most often a mixture of filler and binder

where the insulator is fixed by hardening of the binder after the mixture has been compacted inside the cavities. Another type of liquid insulators are ones based on PUR/PIR foam which are sprayed into the cavity and are fixed in place by means of their own expansion. PUR/PIR foams expand and harden in the cavities relatively quickly; however, their price is typically too high to enable them to be used for this purpose. When pieces of insulation are used, the shape of the block must be changed. The insulation piece is usually inserted in cavities up to 30 to 45 mm wide. For this purpose, it is good to use easily compressible insulators (e. g. mineral wool) which are compressed prior to being inserted in the cavity and are fixed in place after release. In this case of insulation integration it is not necessary for the insulation to harden in the cavities which adds to the efficiency of the manufacturing process [4, 6].

In the past, research at Brno University of Technology was undertaken focusing on the integration of fibrous thermal insulation materials in the cavities of ceramic masonry blocks as a substitution for mineral wool most commonly used today. Current research follows this by, among others, examining the possibilities of vacuum insulation with a core insulator based on recycled textile fibres or natural fibres to be integrated in ceramic masonry blocks.

3. Use of natural fibres in cores of vacuum insulated panels (VIP)

Although VIP were developed in early 20th century, they only saw first application in 1999 [7]. VIP were first applied in home appliances and cargo containers. Recently, VIP have been more commonly associated with civil engineering. They find their use in floor and roof construction and a passive house using these panels has also been built using these panels [8].

At the beginning, VIP core insulation material was made from siliceous aerogels but the production of aerogels is expensive and consumes much energy. Aerogels also have rather low mechanical properties. For this reason, other insulators were begun to be used in early 20th century, such as mineral wool, polyurethane and polystyrene foam [7]. Apart from

these traditional insulators, some alternative ones are beginning to find their use, e. g. melamine formaldehyde fibres [9]. Research performed abroad [10] as well as at Brno University of Technology shows that insulators based on natural fibres can be successfully used in VIP given the low thickness of their primary fibres and low thermal conductivity.

An advantage of these insulators is the low energy cost of their production and the use of easily renewable sources of secondary raw materials provided the fibres used are agricultural crop leftovers, waste fabric, etc.

In terms of the use of plant fibres in VIP it is appropriate to use fibres as thin as possible in order for them to yield the best thermal insulation properties. Suitable ones are e. g. cotton fibres which reach thermal conductivity of about $0,005 \text{ W} \cdot \text{m}^{-1} \cdot \text{K}^{-1}$ after vacuum sealing. Given the fact that the core insulation in VIP is covered by a vapour-proof film, there is no risk of degradation of its thermal insulation properties due to moisture or biotic attack [11].

4. Use of VIP as insulation integrated into ceramic masonry blocks

The use of VIP in exterior masonry has been tested as an insulation system (both interior and exterior as well as contact and non-contact). However, this application brings several problems. There are complications connected especially with fitting and connecting the individual panels without compromising them or creating significant thermal bridges [12 – 14]. Nevertheless, the limitations of this VIP application are currently mainly determined by the high price of the panels together with fitting and certain operations connected with using the building during which the panels must not be compromised. VIP price reduction can be achieved mainly by using cheaper insulation materials in the panel core, such as the above-mentioned insulators based on natural fibres. Increasing the protection of VIP from mechanical damage can be done by means of integrating the panels in the cavities of ceramic masonry blocks.

Research being performed at BUT includes an examination of the possibilities of using VIP with a core material based on natural fibres and common types of VIP as integrated insulation in ceramic masonry blocks.

The goal is to design a single-layer masonry of low thickness with the best possible thermal insulation properties. There is an effort to achieve a greatest possible improvement in thermal insulation properties with minimum increase in price of the masonry elements.

The basic masonry chosen had thickness of 300 mm as common masonry pieces of this thickness do not meet the high standards of most EU countries (in terms of building envelopes). Heat transfer coefficient of conventional THERM-type masonry pieces of 300 mm thick ranges from $0,25 \sim 0,70 \text{ W} \cdot \text{m}^{-2} \cdot \text{K}^{-1}$ in dependence on the geometrical structure of the blocks, cast properties and coursing joint properties. The design involved large cavities of 40 mm in 5 rows with increased rib thickness perpendicular to heat flow direction. The geometrical design of the block is shown in Fig. 1.

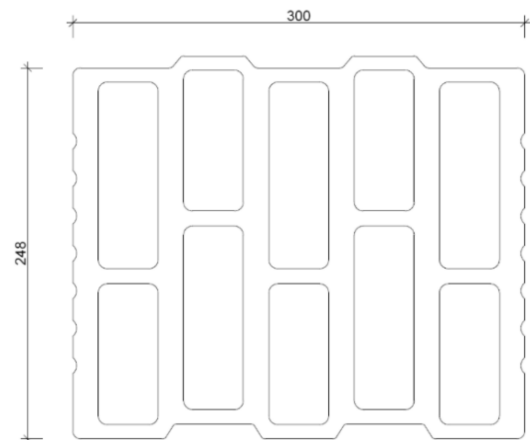


Fig. 1 Block design

The following insulators were chosen;

- (1) basic mineral fibre insulation (MW) with thermal conductivity of $0,035 \text{ W} \cdot \text{m}^{-1} \cdot \text{K}^{-1}$.
- (2) commercial VIP based on pyrogenous silica with thermal conductivity of $0,007 \text{ W} \cdot \text{m}^{-1} \cdot \text{K}^{-1}$.
- (3) experimental VIP based on defibred cotton core insulation with thermal conductivity of $0,006 \text{ W} \cdot \text{m}^{-1} \cdot \text{K}^{-1}$ (the value was rounded up to thousands).

The thickness of the VIP was set to be 20 mm i. e. 50 % of the thickness of each cavity while the VIP are protected by geotextile from each side in order not to

damage them during insertion in the block; subsequent fixation is performed by means of inserting 2 mats of mineral wool (with thermal conductivity value of $0.035 \text{ W} \cdot \text{m}^{-1} \cdot \text{K}^{-1}$) each 12 mm thick where their compression down to 10 mm fixates the insulator in the cavity.

Fig. 2 shows a diagram of the cavity filling. The calculations were performed with the value of thermal conductivity of the ceramic cast of $0.275 \text{ W} \cdot \text{m}^{-1} \cdot \text{K}^{-1}$ (based on the knowledge of average calculation values of thermal insulation of ceramic block casts from the largest produces in Czech Rep.) while different ways of filling the cavities were modelled.

5. Calculation of thermal insulation properties of the blocks containing VIP insulation

Based on the block geometry, computational models were designed where VIP were placed in the 1st, 2nd and 3rd row starting from the exterior and then in combinations: 1st + 2nd row; 2nd + 3rd row; 1st + 3rd row and 1st + 2nd + 3rd row. There were a total of 7 computational models. The calculations always included simulations with one of the three above-described insulators. Given the fact that the block cavities were filled with mineral wool of uniform properties in places with no VIP (insulator No. 1), the results for the application of insulator No. 1 in all cavities were identical. It was a block filled only with mineral wool which functioned as reference - REF.

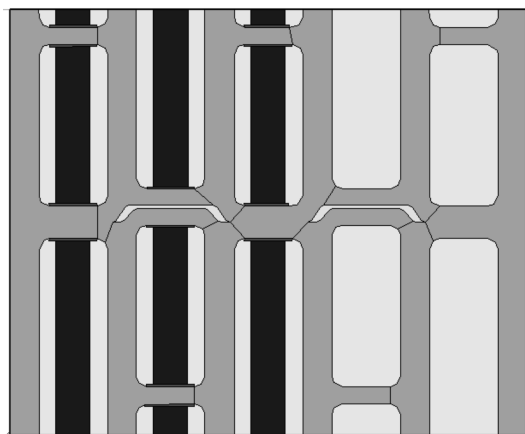


Fig. 2 Diagram of the block design (red-ceramic cast; yellow-mineral wool; blue - VIP; green-air)

The calculations were performed on a typical masonry cut-out in accordance with EN 1745 which was

exposed to the action of a thermal field $\theta_1 = \theta_i = +21 \text{ }^\circ\text{C}$, $\theta_2 = \theta_e = -15 \text{ }^\circ\text{C}$. The calculation was performed using the finite element method according to EN ISO 6946. Thermal-technical properties of the masonry building materials were chosen in accordance with the values listed above. The equivalent value of thermal conductivity of air in the butt joint cavities in the direction of heat flow was determined according to EN ISO 6946. The calculation results are in the following Fig. 3:

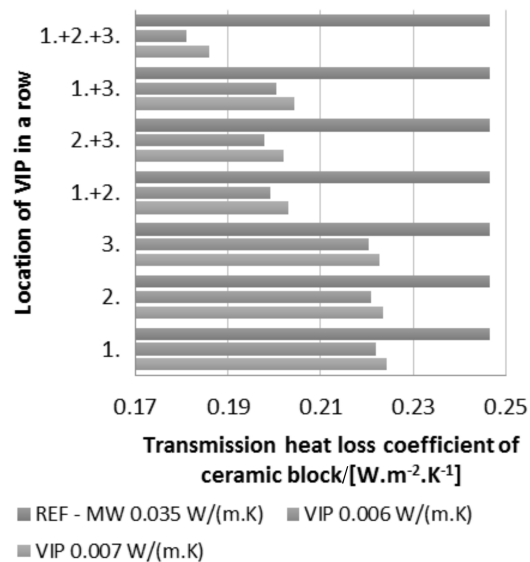


Fig. 3 Chart of heat transfer coefficient of the block using VIP

6. Evaluation of results

The results indicate that the use of VIP as thermal insulation integrated in the block cavities achieves an improvement of final thermal-technical properties. The comparison of the improvement brought by the use of VIP in one, two and three cavity rows in a block is shown in Fig. 4.

The use of VIP in one row of cavities brought an improvement in thermal-technical properties by 11 to 12%; in two rows, the improvement in thermal insulation properties ranges between 22% ~ 26 % and when three rows of cavities were fitted with VIP, the improvement is between 34% ~ 38 %. It is therefore apparent that in order to achieve a more significant improvement in the properties of the masonry pieces VIP must be placed in at least two rows. Where VIP was fitted in two rows, it was found that placing the insulation closer to the centre of the block is more

effective (in terms of thermal insulation).

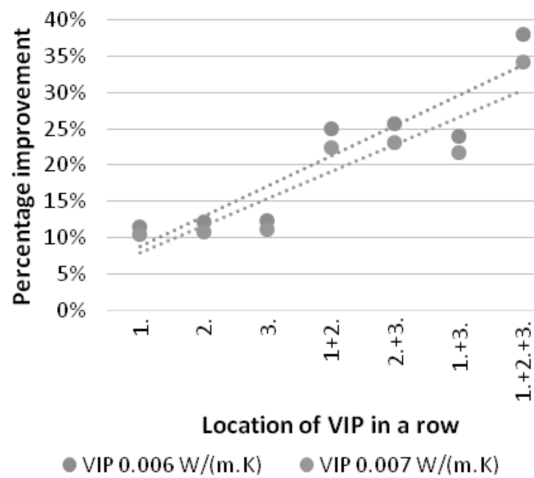


Fig. 4 Chart of gradual improvement of thermal insulation properties with the use of VIP

Where VIP was fitted in one row of cavities, it follows that the most suitable placing is in the middle, i.e. 3rd row. This design also brings a number of benefits. VIP placed in the 3rd row is sufficiently protected against mechanical damage from the interior as well the exterior. Placing the VIP in the middle of the block is more compatible with implementing other details of the construction, such as window and door fitting. The number of rows filled with VIP is also important in terms of costs, as fitting more rows increases the price per one block. Due to these facts, the subsequent model examination of hygrothermal behaviour was performed with the arrangement where one row of VIP was placed in the 3rd cavity.

The calculation of hygrothermal behaviour in a block with VIP in the third row of cavities was calculated over the period of one year. For comparison, the same calculation was performed with a block where all cavities were filled only with MW (insulator No. 1). Evaluation of the hygrothermal behaviour of the block was performed using the WUFI® 2D computational software (non-stationary heat transfer-finite element method).

First the block geometry was modelled in a simplified form. Next the density of a point grid for the observation of the individual properties was set. In the following step, appropriate materials were selected from the material database (see above).

Next, the initial and climatic conditions were entered. Hygrothermal behaviour was observed for Holzkirchen area (Germany). The block face exposed the exterior was determined to be the most loaded side - west. On the interior, the method was according to EN 13788 where Humidity Class 2 was chosen.

- Assumed characteristics for the exterior:
Heat transfer Coefficient; $25 \text{ W} \cdot \text{m}^{-2} \cdot \text{K}^{-1}$
- Assumed characteristics for the interior:
Heat transfer Coefficient; $8 \text{ W} \cdot \text{m}^{-2} \cdot \text{K}^{-1}$

The results of calculation of the hygrothermal behaviour of the whole block (version A-using VIP in the third row; version B-a block with only mineral wool insulation) for reference period 1st Oct 2010 - 1st Oct 2011 are in Fig. 5 and Fig. 6.

The comparison of the hygrothermal behaviour of the block containing VIP in the third row and with only MW reveals that the application of VIP in the cavities reduces the overall water content in the block during the year. However, in this case the fact that VIP is non-absorbent, and thus exhibits essentially 0 % water content, must be taken into account. The use of VIP reduces the water content in the block below 1 % continually over a half-year period. Where only MW is used, this value is attained for only about half that time.

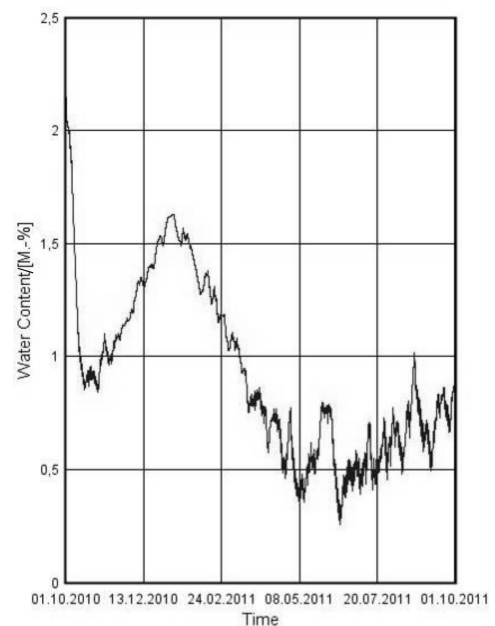


Fig. 5 Water content in time in ceramic block with VIP

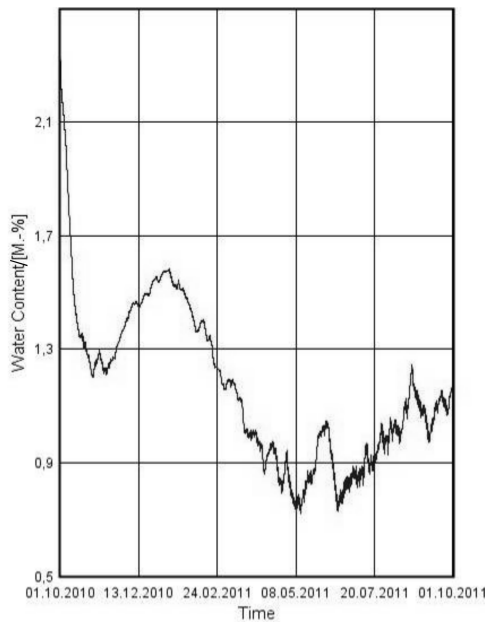


Fig. 6 Water content in time in ceramic block with MW

7. Conclusions

Based on the research performed, it was found that VIP can be successfully integrated into large-sized cavities in ceramic blocks. A design of application and fixation of VIP in the cavities of blocks was performed. VIP based on recycled cotton was determined to be potentially suitable, as a lower price can be assumed as opposed to VIP based on SiO_2 [11]. Next, it was found that, in order to bring a significant improvement in thermal insulation properties, VIP must be fitted in at least two rows of cavities. It is more beneficial to place the VIP closer to the centre of the block. In this position, a VIP is better protected from mechanical damage.

The determination of hygrothermal behaviour of ceramic block masonry containing one row of VIP has revealed that a block thus modified exhibits good overall thermal insulation properties, no condensation accumulates in any part of it over the year and in overall comparison exhibits an average water content lower than that of a block fitted with mineral wool only.

It can be concluded that the application of VIP in ceramic masonry pieces can significantly improve the thermal insulation properties of a single-layer structure. In terms of the VIP itself, there is no need to address the complicated issue of anchoring (which is a usual

problem of vertical structures) and, enclosed in the ceramic block, the VIP is protected from mechanical damage which ought to ensure its long service life in the structure.

Acknowledgements

This paper has been worked out under the project No. LO1408 “AdMaS UP - Advanced Materials, Structures and Technologies”, supported by Ministry of Education, Youth and Sports under the “National Sustainability Programme I” and under the project of TACR ref. n. TA04020920.

References

- [1] S. E. Kalnæs, B. P. Jelle, Vacuum insulation panel products: A state-of-the-art review and future research pathways, *Applied Energy* 116 (2014) 355 – 375.
- [2] Kyoto Protocol to the United Nations Framework Convention on Climate Change, Kyoto (1997).
- [3] J. Zach, N. Žižková, V. Novák, J. Hroudová, L. Sokola, Use of ETICS for the restoration of building envelopes, (2014).
- [4] J. Zach, J. Brožovsky, J. Hroudová, M. Sedlmajer, Development of ceramic blocks for masonry constructions with thermal insulation filling on the basis of easily renewable raw materials and by-products, 15th International Brick and Block Masonry Conference (2012) 52 – 54.
- [5] P. HEINRICH, Development of thermal properties of brick masonry, *Construction magazine: Magazine of civil engineers, technicians and entrepreneurs* (2011) 6 – 7.
- [6] J. Zach, J. Hroudová, M. Sedlmajer, A. Korjenic, Study of hygrothermal behavior of advanced masonry components made with utilization of secondary raw materials, 2nd Central European Symposium on Building Physics (2013) 169 – 174.
- [7] S. Brunner, K. G. Wakili, T. Stahl, B. Binder, Vacuum insulation panels for building applications—Continuous challenges and developments, *Energy and Buildings* 85 (2014) 592 – 596.
- [8] H. P. Ebent, J. Fricke, U. Heinemann, Vacuum insulation panels—From research to market, *Vacuum* 82 (2007) 680 – 690.
- [9] V. Nemanic, M. Žumer, New organic fiber-based core material for vacuum thermal insulation, *Energy and Buildings* 90 (2015) 137 – 141.
- [10] J. Vėjelienė, Impact of technological factors on the structure and properties of thermal insulation materials from renewable resources, Doctor dissertation 2012.

- [11] A. Korjenic, V. Petránek, J. Zach, J. Hroudová, Development and performance evaluation of natural thermal-insulation materials composed of renewable resources *Energy and Buildings* 43 (2011) 2518 – 2523.
- [12] F. E. Bofo, J. T. Kim, Z. Chen, Configured cavity-core matrix for vacuum insulation panel: Concept, preparation and thermophysical properties, *Energy and Buildings* 97 (2015) 98 – 106.
- [13] A. Lorenzati, S. Fantucci, A. Capozzoli, M. Perino, The Effect of Different Materials Joint in Vacuum Insulation Panels, *Energy Procedia* 62 (2014) 374 – 381.
- [14] P. Johansson, C. E. Hagentoft, A. S. Kalagasidis, Retrofitting of a listed brick and wood building using vacuum insulation panels on the exterior of the facade: Measurements and simulations, *Energy and Buildings* 73 (2014) 92 – 104.

VIPs Thermal Performance in Buildings: Research Experience and Roadmap

Stefano Fantucci, Alice Lorenzati^{*}, Alfonso Capozzoli, Francesco Isaia, Marco Perino

Politecnico di Torino, Corso Duca degli Abruzzi 24, Turin 10129, Italy

Abstract

Vacuum Insulation Panels have seen a fast development in the building sector due to their high insulating performance. For this reason several researches were and are performed on this topic. The present work summarizes the research activities carried on Vacuum Insulation Panels by Politecnico di Torino during these last years. In particular, a critical discussion of the most relevant results obtained by the research group are presented. The aim of the paper is to show how the conducted investigations have provided reliable data on VIPs actual performances and general guidelines to assess the VIP thermal properties under actual working conditions.

Keywords vacuum insulation panels, thermal bridge, building application, linear thermal transmittance.

1. Introduction

In the present paper, research results obtained in the last few years by Politecnico di Torino on VIPs thermal performance analysis are presented. In particular, the most relevant investigations were carried out at different scales:

- at panel scale, a series of measurements were performed to analyze repeatability and uncertainty related to the measurement of the thermal conductivity;
- at component scale, the thermal bridging effects and the influence of different joint materials were investigated through both numerical and experimental analyses;
- at system scale, the thermal behavior of a VIP insulated building facade was assessed;
- at building scale, the influence of thermal bridging effects on the energy performance was finally evaluated.

Moreover, the future research steps are provided in the conclusions section.

2. VIP experimental characterization

The current measurement procedures for assessing the thermal conductivity of super insulating materials can be affected by a significant uncertainty given their

very low thermal conductivity. For this reason, the measurement procedure needs to be properly investigated. In fact the nominal lower limit of the measurable thermal conductivity of a test apparatus (Guarded Heat Flux Meter-GHFM) is usually around $0.0015 \div 0.0020 \text{ W}/(\text{m} \cdot \text{K})$. Moreover, the very low value of heat flux that is generated during the tests requires an appropriate measurement accuracy.

The experimental results were obtained using a GHFM apparatus whose technical specifications are reported in [1].

The research was aimed at verifying the reliability of existing testing methods (EN 12667:2001), through:

- the determination of the correct test boundary conditions in terms of minimum temperature difference between the two plates of GHFM and average temperature of the specimen;
- the analysis related to repeatability and accuracy of the measurement procedure.

2.1 The effect of test condition

Several tests were performed on a 30mm thick VIP varying the average temperature of the specimen θ_{avg} , and the VIP surfaces temperature difference $\Delta\theta$

^{*} Corresponding author, Tel :39 - 011 - 090 - 4550, E-mail:alice.lorenzati@polito.it

respectively.

2.1.1 Influence of temperature difference

The results reported in Fig. 1 show the influence of both the test temperature difference $\Delta\theta$ and the heat flux ϕ_{avg} on the relative uncertainty $\Delta\lambda$ related to λ_{cop} (center of panel thermal conductivity) measurements, determined according to UNI CEI ENV 13005:2000, for a VIP panel.

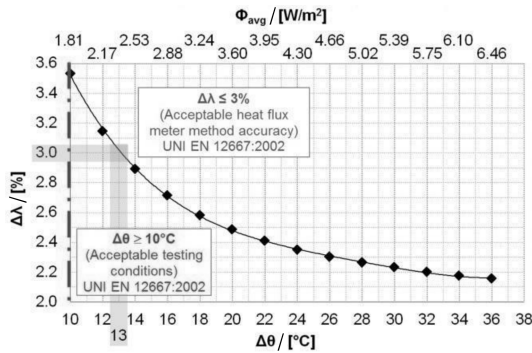


Fig. 1 Percentage uncertainty $\Delta\lambda$ in function of $\Delta\theta$, and relative heat flux Φ_{avg} [2]

Analyzing the figure, it can be inferred how the relative uncertainty $\Delta\lambda$ assumes acceptable value (lower than 3%) according to EN 12667:2001 for Φ_{avg} and $\Delta\theta$ higher than 2.35 W/m² and 13°C respectively. The results demonstrated that in order to obtain a low relative uncertainty a temperature difference of at least 20°C between the lower and upper plate of GHFM is recommended.

2.1.2 Influence of temperature on center of panel thermal conductivity λ_{cop}

The average working temperature of an insulating material influences its thermal conductivity. Traditional insulating materials presents an almost linear relationship between thermal conductivity and average temperature (at least in the typical building temperature range).

Fig. 2 shows how the variation of VIP thermal conductivity as a function of the average temperature follows instead a non-linear trend. This trend was deeply investigated in [2] and it was found that it depends significantly on the internal gas pressure in the core material.

In particular, the λ_{cop} of VIP was found to span from 0.0043 W/(m · K) ($\theta_{avg} = 2.5^\circ\text{C}$, building envelope external insulation in winter conditions) to

0.0061 W/(m · K) ($\theta_{avg} = 52.5^\circ\text{C}$, domestic hot water tank insulation), changing therefore its thermal conductivity in relation to the specific use.

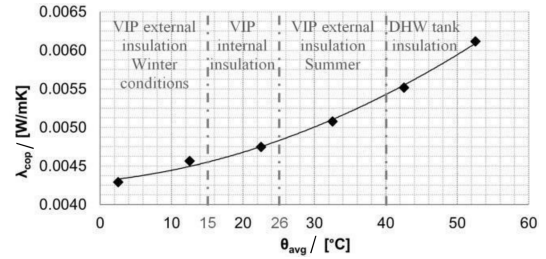


Fig. 2 Relation between λ_{cop} and θ_{avg} [2]

2.2 Reliability and repeatability

The analysis, aimed at investigating the measurement repeatability, was carried out on 5 different VIP panels (characterized by different core materials and manufacturers). The measurement was carried out according to EN 12667:2001, considering a nominal temperature difference between the GHFM plates of 20°C and taking into account the analysis reported in section 2.1.1.

The repeatability is in the range of the measurement accuracy $\Delta\lambda$ as shown in Fig. 3. As expected, the variation of $\Delta\lambda$ for VIPs having the same thickness depends on the thermal conductivity and also on the heat fluxes generated between the plates. In particular it was found that when the thermal conductivity decreases the measurement uncertainty increases; these results are coherent with those reported in section 2.1.1.

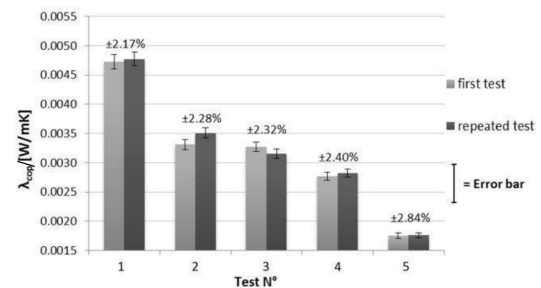


Fig. 3 Repeatability of measurements - Results from repeated test on different samples λ_{cop} [W/(m · K)], [1]

3. Thermal bridging effects on system performances

In order to use VIPs in building envelopes, the panels need to be jointed to each other and to be fixed onto additional supporting materials. Given the very low

VIP thermal conductivity, these additional materials cause thermal bridging effects. For this reason, specific studies on supporting structures or systems are required. The overall energy performance of the insulating assembly (coupling of VIPs with a joint, Fig. 4) can be significantly lower due to the thermal bridging effects. In order to verify the influence of the thermal bridges on the overall energy performance of the VIPs assemblies, an experimental campaign using a GHFM apparatus was carried out, analyzing different joint materials and configurations [3]. Firstly, a measurement method was proposed, tested and verified on the basis of the available literature data, and on the criteria described in section 2 [2]. Afterwards, a series of measurements on different samples were performed. The experimental results were then compared with a 2D numerical model based on the FDM. Moreover, the same numerical model was adopted to simulate the effects of thermal bridges when VIPs are inserted in typical walls [4]. Finally the results obtained were used to assess the overall thermal performances of a typical facade with different assembly configurations [5].



Fig. 4 VIPs assembly with structural joint

3.1 Experimental and numerical VIPs assemblies investigation

Experimental analyses were carried out in accordance with the results obtained in section 2, in order to reduce the measurement uncertainty. A set of point temperatures were therefore kept equal to 35°C for the hot (lower) plate of the GHFM and to 15°C for the cold (upper) plate, with an average testing temperature of 25°C.

Two kinds of assemblies were tested. The first assembly was realized by coupling directly two VIPs, generating a thermal bridging effect due to the air joint between the panels. The second assembly type was

obtained by coupling VIPs with different structural joints. Four different widths of the air joint (measured through a photographic survey), and three different materials for structural joints (XPS, MDF and Para natural rubber) were analyzed. The analyzed structural joints were 36mm wide. Thermal conductivities of air joints were obtained in accordance with the EN ISO 6946: 2008, whereas thermal conductivities of the structural joint materials were experimentally evaluated through GHFM.

In a second stage of the activity, the experimental results were used to verify the reliability of a numerical model. The model was built using the software Physibel BISCO, as described in [4].

The linear thermal transmittance of the thermal bridge, were assessed both experimentally and numerically (Air Joint: $\Psi_{EXP,AJ}$ and $\Psi_{NUM,AJ}$; Structural Joint: $\Psi_{EXP,SJ}$ and $\Psi_{NUM,SJ}$). Investigations were performed on 20mm VIPs thickness. Further details are provided in [3 – 5].

STRUCTURAL JOINTS “SJ”

The properties which mainly influence the performance of assemblies with structural joints are the thermal conductivity of the joint material, λ_{SJ} , and their thicknesses .

In Fig. 5 the linear thermal transmittance of the bridge as a function of the joint thermal resistance is shown. Experimental and numerical results are in good agreement, with a Ψ_{SJ} maximum percentage difference of 11% (for the rubber joint).

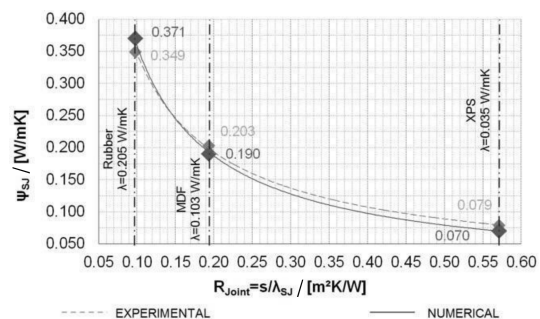


Fig. 5 Ψ_{SJ} related to R_{Joint}

AIR JOINTS “AJ”

In this case the thermal performance of the assembly are strictly dependent on the width of the air gap. To evaluate this effect, four different widths were

analyzed. Fig. 6 shows the experimental and numerical results, related to Ψ_{AJ} evaluation.

The experimental analysis results were follows a curve that can be linearized with a good approximation. The maximum Ψ_{AJ} deviation between experimental and numerical results was found to be 8%, demonstrating a good reliability of the numerical model. For this reason, further analyses were carried out only through the calibrated numerical model.

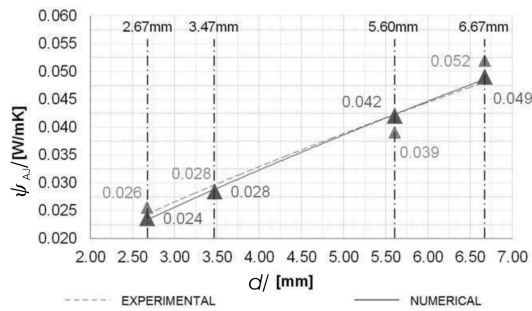


Fig. 6 Ψ_{AJ} related to air joint width d

3.2 Actual behavior of typological walls and facade configuration: numerical simulations

The analysis was aimed at investigating the behavior of different wall configurations refurbished making use of VIP. Additional internal and external thermal resistances ($R_i + R_e$) (with respect to the VIP position) were considered in the numerical simulations as a function of the wall typology. The boundary conditions were kept equal to that of the previous simulations; additionally, Aerogel Based Product blanket (ABP) was considered as structural joint ($\lambda_{ABP} = 0.015 \text{ W}/(\text{m} \cdot \text{K})$). For these analyses a 30 mm thick VIP panel was studied. Results are shown in Fig. 7.

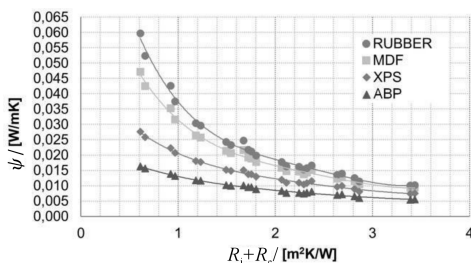


Fig. 7 Ψ as a function of $R_i + R_e$ [4]

The linear thermal transmittance (Fig. 7) of the different wall configurations tends to converge to a narrow range for high thermal resistance $R_i + R_e$. A decrease in linear thermal transmittance ψ was observed

when the total thermal resistance of the bounding layers increases. This behavior underlines that the higher the thermal resistance of the bounding layers, the lower the weight of the thermal bridging effect (as expected). An important outcome from these results shows that ABP is a particularly suitable material to be used as VIP joint, because of its very low thermal conductivity. The percentage differences between the equivalent thermal conductivity λ_{eq} (e. g. the thermal conductivity which takes into account the thermal bridging effect) and λ_{cop} were calculated to make further consideration on the influence of the thermal bridging effects (Fig. 8). Three different thicknesses were considered: 10, 20 and 30 mm.

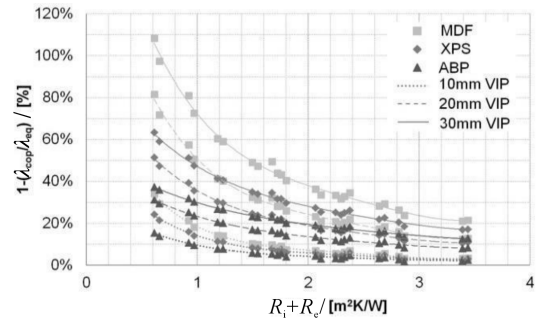


Fig 8 Percentage difference between different thermal conductivities, as a function of $R_i + R_e$ [4]

Increasing the VIP thickness, the range between the minimum and the maximum value of the percentage difference also increases. Moreover, the higher the thermal resistance of structural joint, the lower is the influence of panel thickness on the overall thermal behavior. This result shows the advantages in coupling VIPs and ABP.

Finally, a typical facade was modelled (Fig 9), to compare the influence of different joint materials on the average wall thermal transmittance U_{avg} [5].



Fig. 9 Facade geometry [5]

Tab. 3 Average thermal transmittance $-U_{avg}$ - of the typological facade model [5]

Structural Joint material	U_{VIPcop}	U_{avg}	$\frac{\Delta U_{avg-VIP}}{\%}$	$\frac{\Delta U_{avg}}{\%}$
	W/(m ² · K)	W/(m · K)		
ABP	0.367	0.491	+34%	—
EPS		0.571	+55%	+16%
MDF		0.627	+71%	+28%

In Tab. 3 the values of thermal transmittance are reported for different structural joint materials. Moreover, the ΔU_{avg} percentage differences between the VIP + ABP configuration (reference value) and the other configurations using different materials as VIP joints are presented. The $\Delta U_{avg-VIPcop}$ represent the difference between the assembly average thermal transmittance U_{avg} and the thermal transmittance at VIP center of panel U_{VIPcop} .

On the basis of these results an economic analysis was performed (only considering the insulating material cost). The use of EPS or MDF as structural joint causes a reduction in costs of 12% and 11% respectively if compared to ABP; however, the average thermal transmittance U_{avg} increases of 16% (EPS) and 28% (MDF). As expected, the increasing of costs due to coupling VIPs and ABP assemblies is almost negligible if compared to the increase of assembly insulating performances (more details about this study are available in [5]).

3.3 Building scale assessment

With the aim of evaluating the influence of VIP thermal bridging effects at the building scale, the energy performance of an archetype residential building was evaluated taking into account a number of VIP-refurbished wall configurations [4].

The building used as case study is located in Torino ($DD = 2617$), the window has U-value equal to 2 W/(m² · K), floor and ceiling are adiabatic and natural ventilation was considered equal to 0.3 h⁻¹ (Fig. 10). To take into account different aspect ratios, four cases were simulated (Fig. 10): the walls between two building units are adiabatic.

To evaluate the influence of thermal bridging effects, the simulations were carried out considering:

the equivalent thermal conductivity (λ_{eq}), an equivalent thermal conductivity provided by the producer and the center of panel thermal conductivity. For sake of brevity, only the results using λ_{eq} are shown in Fig. 11. The parameters chosen to evaluate the building energy performance are the heat transfer coefficient by transmission H_{tr} , the total energy losses by transmission Q_{Htr} and the building energy need Q_H .

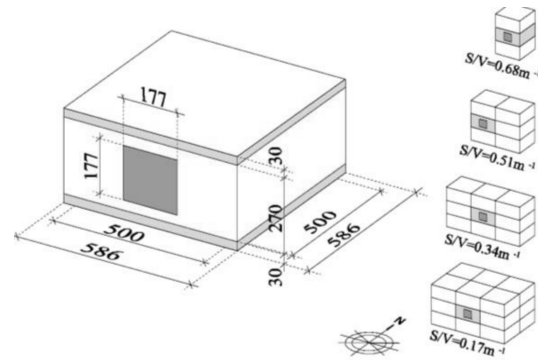
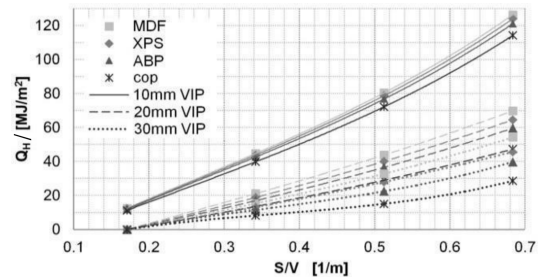

Fig. 10 3D model of building cases (quotes in cm) [4]

Fig. 11 QH variation for different VIP thickness and different S/V ratio [4]

Fig. 11 shows the building energy need Q_H as a function of the aspect ratio for a solid wall refurbished with VIPs applied on the wall internal surface ($R_i + R_e = 1.232$ m² · K/W). It is clear that by increasing the VIP thickness the influence of thermal bridging increases. For the highest S/V ratio and VIP thickness, an increase of about 36% of the building energy need can be observed if a poor performing material (MDF) is used as VIP joint instead of ABP. With the same aspect ratio considering XPS, as coupling material, an increase of about 60% of the building energy need was observed, respect to the case in which the thermal bridging effect is neglected (cop in Fig. 11)

4. Conclusions and future prospective

On the basis of these research experiences it can be

highlighted that;

- VIP experimental characterization needs to be performed considering proper boundary conditions. In particular, temperature difference greater than 20°C are recommended to avoid unacceptable uncertainties for the evaluation of λ_{cop} .

- The thermal bridging effects are poorly affected by the joint material for high values of the total thermal resistance of the bounding layers ($R_i + R_e > 2 \text{ m}^2 \cdot \text{K/W}$).

- In order to minimize the effect of thermal bridges coupling VIPs with SIMs (e. g. ABP) as joint appear to be a valuable solution.

- The thermal bridging effects are important and need to be properly considered. The heat transfer coefficient by transmission (H_{tr}), for example, can increase up to 50% when thermal bridges are taken into account. To effectively decrease their influence, the total thermal resistance of the bounding layers should be increased or, alternatively, low-conductive materials should be used to couple VIPs.

On the basis of the gained experience of the last years on VIP thermal performance, the ongoing and next research studies will be focused on:

- Analysis the actual thermal performance of VIPs at building level through long term monitoring;

- Investigations on technological solutions aimed at improving the coupling among VIPs and the way to insert VIPs in the building structure, considering the

minimization of thermal bridging effects;

- Analyses aimed at investigating the economical profitability of the application of VIPs for building refurbishment.

Acknowledgements

This research has been carried out as part of the research activity supported by ENEA - “Sviluppo di metodologie strumenti di misura ed analisi dei consumi energetici degli edifici pubblici”, and in the frame of the IEA - Annex 65.

References

- [1] A. Capozzoli, S. Fantucci, F. Favoino, M. Perino, Vacuum Insulation Panels: Analysis of the Thermal Performance of Both Single Panel and Multilayer Board, *Energies* 8 (2015) 2528 – 2547. DOI:10.3390/en8042528.
- [2] A. Lorenzati, S. Fantucci, A. Capozzoli, M. Perino, VIPs thermal conductivity measurement: test methods, limits and uncertainty, *Energy Procedia* (2015) (Accepted).
- [3] A. Lorenzati, S. Fantucci, A. Capozzoli, M. Perino, The effect of different material joint in Vacuum Insulation Panels, *Energy Procedia* 62 (2014) 374-381. DOI:10.1016/j.egypro.2014.12.399.
- [4] F. Isaia, S. Fantucci, A. Capozzoli, M. Perino, Vacuum Insulation Panels: thermal bridging effects and energy performance in real building applications, *Energy Procedia* (2015) (Accepted).
- [5] A. Lorenzati, S. Fantucci, A. Capozzoli, M. Perino, Coupling VIPs and ABPs: assessment of the overall thermal performance in building wall insulation, *Energy Procedia* (2015) (Accepted).

Enhancement of Effective Thermal Conductivity

SeongMoon Jung^{*}, Myung Lee, SonCheal Bang, SungSeock Hwang, JungPil Han, SeungMin Jeon

CRD Lab, LG Hausys R&D, 77 Heungan-daero 81 beon-gil, Dongan-gu, Anyang-si Gyunggi-do, Korea

Abstract

Due to the heterogeneous structure of vacuum insulation panel consisting of core material and envelope, effective thermal conductivity (ETC) is generally used to differentiate the performance of VIP. ETC is calculated by the sum of thermal conductivity value of center of panel and edge of envelope (linear thermal transmittance); $\lambda_{\text{eff}} = \lambda_{\text{cop}} + \psi(d) dp/A$, where cop is center-of-panel, d is the thickness of the VIP (in the heat flux direction) (m), A is the surface area of the VIP (perpendicular to the heat flux direction) m^2 and p is the perimeter of the surface A (m). Actually, ETC value is matched well with the energy efficiency measured after installing in refrigerator. VIP manufactures have been keen competitions to get the lower ETC value through the modification of core material and envelope. Recently, it is noticed that the simple replacements of materials cannot lead to further reduction of ETC value. The detailed approaches based on scientific mechanism are needed to win in VIP market. In this paper, An approach to overcome technical limitations, and the kinds of efforts needed to make a breakthrough in the performance of the VIP, are discussed.

Keywords vacuum insulation panels, effective thermal conductivity, linear thermal transmittance

1. Introduction

Recently the energy regulation of refrigerator has become tightened. From September 2014 in USA, the 10% increase in the energy efficiency was necessary to qualify for the energy star [1]. In Europe, Energy Efficiency Index (EEI) has been gradually strengthened [2]. These changes in the energy regulation are encouraging the manufactures of refrigerator to find new and efficient solutions further to reduce the energy consumption. There are two approaches; (1) the efficiency of compressor, (2) the performance of insulator. In the view of the insulator, it is no doubt that vacuum insulation panel is the simple and easy solution [3][4]. In real market, there have been strong efforts to upgrade the qualities among the VIP suppliers, because the manufactures of refrigerator are consistently demanding the improvement of the performance of a VIP.

2. VIP Performance

Generally, Most of VIP suppliers announced the

center-of-panel thermal conductivity of their product measured by Heat flow meter as a performance standard. Heat flow meter checks total heat flow occurred between two different temperatures. The detector of heat flow meter locates on the center. If the structure is homogeneous, there is no issue. But, in the case of the heterogeneous structure like a vacuum insulation panel consisting of core material and envelope, the center-of-panel thermal conductivity may not fully represent the performance of the insulator, due to the heat transfer through the envelope (linear thermal transmittance). Actually, there are two routes of heat flux that can be divided into in the conventional structure of VIP: (1) Center of panel, (2) Edge of envelope (linear thermal transmittance) and the effective thermal conductivity of VIP considering these is expressed below as sum of these two terms [5].

$$\lambda_{\text{eff}} = \lambda_{\text{cop}} + \psi(d)dp/A \quad (1)$$

where cop is center-of-panel, d is the thickness of the VIP (in the heat flux direction) (m), A is the surface

* Corresponding author, Tel :82 - 31 - 4504414, E-mail:jungsm@lghausys.com

area of the VIP (perpendicular to the heat flux direction) m^2 and p is the perimeter of the surface A (m). There are several methods to evaluate effective thermal conductivity of vacuum insulation panel.

2.1 Modified guarded hot plate (M-GHP) test

This test was proposed by EMPA (Swiss Federal Laboratories for Materials Testing and Research) [5].

All thermal resistance measurement are carried out in a guarded hot plate two-specimen apparatus. The guarded hot plate is an absolute test method requiring no calibration with reference samples. The apparatus have an overall size of $500mm \times 500mm$ with a metering area of $250mm \times 250mm$.

2.2 Reverse Heat Leakage (RHL) test

This is a procedure normally used by the appliance manufacturers to evaluate the thermal insulation properties of a VIP. In the beginning of VIP application to refrigerator, the maker required simple specification to the VIP supplier. But, in real test with the refrigerator installing VIP, energy efficiency was not matched with the center-of-panel thermal conductivity of VIP (Tab. 1). Thus the maker set up new guideline and test method, called RHL (Reverse Heat Leakage).

$$Q = UA (T_{in} - T_{out}) \quad (2)$$

Where Q is power input (W), U is thermal transmittance ($W/(m^2 \cdot K)$), A is outer wall area of refrigerator (m^2), T_{in} is inside temperature of refrigerator ($^{\circ}C$) and T_{out} is outside temperature of refrigerator ($^{\circ}C$).

The test involves heating inside above ambient conditions with auxiliary heaters. The inside of the cabinet is normally heated up to $40^{\circ}C$, and then checks the rate of heat transfer through the cabinet to outside maintained at $15 \sim 20^{\circ}C$, after steady-state conditions have been reached. [6].

Tab. 1 Comparison of the results between the center-of-panel thermal conductivity and the energy efficiency

RHL test	Center of panel of thermal conductivity/ ($mW/m \cdot K$)	Improvement of energy saving/(%)
Fumed silica+metalize film	5.0	14
Glassfiber+Al foil	3.0	14

As described in equation(1), the size and thickness

of a VIP influences on the total heat flux through the insulation materials. Actually, the effective thermal conductivity was changed with the size and thickness in real measurement, as shown Tab. 2.

Tab. 2 Effect of the size of thickness of a VIP

Sample	1	2
VIP size ($W \times L \times H$)	$400mm \times 900mm \times 15mm$	$425mm \times 1060mm \times 20mm$
Thermal conductivity ($mW/m \cdot K$)	7.0	10.3

2.3 Modified heat flow meter (M-HMF) test

For the measurement of ETC, the special instruments and complicated apparatus are essential. Thus, the simplest way is required. Generally, ETC is directly calculated by the compensation of area ratio to the center-of-panel and edge value of thermal conductivity measured by heat flow meter. This method is becoming to be confirmed by the comparison of ETC value obtained from RHL test, as shown in Tab. 3.

Tab. 3 Comparison of ETC derived from M-HFM and RHL method

Envelope type	Effective thermal conductivity/($mW/(m \cdot K)$)	
	M-HFM test	RHL test
AL foil ($7\mu m$)	6.6	6.5
VM-PET (3layer)	4.2	4.0

* (VIP size : $425mm \times 1350mm \times 12mm$)

2.4 Numerical analysis (Calculating from literatures)

In the market, the most of VIP supplier used the typical envelope which is layered by $6 \sim 8$ micron Al film and/or the Al metalized PET film with 100nm Al thickness. Thus, the common calculation method published in the reference of [3] and [7].

3. Enhancement of effective thermal conductivity

$$\lambda_{eff} = \lambda_{cop} + \psi(d)dp/A \quad (1)$$

λ_{cop} and $\psi(d)$ are minimized to result in a low effective thermal conductivity (λ_{eff}). λ_{cop} is not only a function of the applied pressure but also from the core materials characteristics. On refrigerator industry, the glass fiber is the most valid core material because of the low price and the lowest λ_{cop} , although the least inner pressure of a VIP is below a few Pascals. The details such as diameter, length and orientation of fiber as well

as evacuated pressure have been reported as a variable of λ_{cop} . Especially, the influence of the inner pressure on glass fiber core materials is bigger than other materials due to the large pore diameter. Thus, the high performance of the barrier film should be chosen in the case of fiber core material.

The high heat flux through an envelope is caused by the inclusion of metal in the barrier film. Al foil film showed around $17\text{mW}/(\text{m} \cdot \text{K})$, whereas Al coated polymer film type has only $7\text{mW}/(\text{m} \cdot \text{K})$ [8]. The lowest $\psi(d)$ can be realized by use of polymeric barrier film that is no longer needs metal layers to maintain the inner lower pressure. But because the metalized polymeric barrier film has the higher permeation rate of gas and water than Al foil film, the barrier property of metalized polymeric film should be improved crucially to apply on fiber core materials.

Simply low λ_{cop} and low $\psi(d)$ can be brought by the use of glass fiber as a core material and metalized polymeric barrier film as an envelope with a low inner pressure. However, this combination could lead the worst performance in terms of long-term stability. When the inner pressure is increasing, the λ_{cop} is increased rapidly due to the large pore diameter of a fiber core material.

Among gas and water vapor permission, the manufactures of refrigerator strongly control the influence of water vapor, because the moisture increase in a VIP brings more negative effect on λ_{eff} due to three heat fluxes: (1) heat conduction via water vapor, (2) heat conduction by adsorbed water at the inner surface of the core, (3) heat transfer via evaporation of adsorbed water, diffusion and condensation of water vapor [3]. They have set up the severe testing procedures and thoroughly qualify the long-term stability under their own conditions.

Some researchers have done and proposed new barrier materials and laminated layered structure [7,9]. Main approaching ways are the decrease of defects on the barrier film. Still the development of the barrier layer for water vapor has been a challenging issue.

Thus, the authores have attempted another direction with "capture concept". Two approaches for capturing water vapor have been done. Firstly, the

integration of the active material into the polymeric matrix was performed via the compounding process. In this work, two different polymeric materials were used as the polymer matrix; Polyethylene and Polypropylene. Molecular sieve with a pore size of 4\AA was used as the active material for the adsorption of water vapor. The compounding was performed by the extruder. Secondly, the polymer matrix was modified via the physical treatment. Both approaches applied simultaneously at some cases.

Tab. 4 Enhancement of effective thermal conductivity by the application of the developed envelope on a VIP

VIP size ($W \times L \times H$)	190mm \times 250mm \times 8mm	
Envelope type	AL foil ($7\mu\text{m}$)	Developed
Center of thermal conductivity/ $(\text{mW}/(\text{m} \cdot \text{K}))$	3.0	2.8
Effective thermal conductivity/ $(\text{mW}/(\text{m} \cdot \text{K}))$	10.1	3.1

The VIP prepared by the glass fiber and the envelope laminated with water-capturing film layer (developed) was measured λ_{cop} and λ_{eff} . The results are shown in Table 4, λ_{cop} decreased by $0.2\text{mW}/(\text{m} \cdot \text{K})$, while about 70% reduction of λ_{eff} achieved through the decrease of λ_{eff} from $10.1\text{mW}/(\text{m} \cdot \text{K})$ to $3.1\text{mW}/(\text{m} \cdot \text{K})$. The contribution of heat flux due to the edge effect is only $0.3\text{mW}/(\text{m} \cdot \text{K})$ in the case of the VIP prepared by the developed envelope.

To confirm the long-term stability, the samples with the size of $300\text{mm} \times 300\text{mm} \times 20\text{mm}$ and $260\text{mm} \times 460\text{mm} \times 12\text{mm}$ tested under the condition of 70°C and 90% RH for 1 week and 2 month. After 1 week, the samples ($260\text{mm} \times 460\text{mm} \times 12\text{mm}$) showed 39% λ_{cop} increment to the initial λ_{cop} . After 2 month later, λ_{cop} ($300\text{mm} \times 300\text{mm} \times 20\text{mm}$) was increased by 168% compared to the initial λ_{cop} . These increase of values of λ_{cop} is about 33% ~ 83% lower than the guideline of customers. The samples composing of the developed envelope and the glass fiber core materials satisfy for customer's specification of the long term stability.

The further expansions to the other application markets such as building industry, transportation and water heater are still being retarded because of the

limitation of service life due to the drawback of the long term stability. Thus, the improvement of the barrier performance of the envelope by the application of new barrier layer with “capture concept” can be one of effective ways to overcome and breakthrough to the bottleneck of the service life of a VIP.

References

- [1] <http://www.gpo.gov/fdsys/pkg/CFR-2012-title10-vol3/pdf/CFR-2012-title10-vol3-sec431-304.pdf>
- [2] Official Journal of the European Union (2010) 17 – 46.
- [3] R. Baetens et al. , *Energy & Buildings* 42 (2010) 147 – 172.
- [4] J. Fricke et al. , *Vacuum* 82 (2008) 680 – 690.
- [5] K. Ghazi Wakili et al. , *Building Research & Information* 32 (2004) 293 – 299.
- [6] D. M. Staley et al. , *ACRC TR-22* (1992) 103 – 106.
- [7] Martin Tenpierik et al. , *Journal of Building Physics* (2007) 185 – 215.
- [8] S. M. Jung, *International Vacuum Insulation Symposium* (2013) 31 – 32.
- [9] Hans Simmler et al. , *IEA/ECBCS Annex 39* (2005).

Vacuum Insulation Panel (VIP) Integrated Vaccine Storage Device

Harjit Singh^{a*}, Homan Hadavinia^a, Duncan Kerridge^b, Jillian Henderson^b, Damodaran Ranga^b

a. Institute of Future Energy, Brunel University London, Uxbridge, UB8 3PH, UK

b. The Sure Chill Company, Tywyn, Gwynedd LL36 9LW, UK

Abstract

We report the development of an optimised vacuum panel insulated vaccine storage device (VSD) intended for storing vaccines at 4~8°C for up to 35 days without any active means of cooling. The vaccine chamber performance relies on an innovative arrangement of an ice container and vacuum insulation panels (VIPs) in conjunction with Sure Chill's patented heat transfer element. The development and optimisation of the vaccine chamber design involved complex COMSOL finite element analysis modelling coupled with an extensive experimental programme to collect performance data under realistic operating and boundary conditions. Simulations have shown that the optimised vaccine chamber reported here is able to maintain ice at <10 °C for over 30 days.

Keywords Vacuum insulation panels (VIPs); COMSOL modelling; Phase change; Vaccine cold chain; Sure Chill element

1. Introduction

Currently, worldwide 1.3 billion people, equivalent to 18% of the global population, have no access to electricity [1]. Vaccines for the prevention of many life-threatening childhood diseases must be stored at a temperature of 2-8 °C to avoid any degradation. This is a steep challenge in the absence of active chilling facilities, which run on electric power. The vaccine storage device (VSD) described in this paper (see Fig. 1 and Fig. 2) employs an innovative arrangement of VIPs to insulate vaccine compartment from the ambient environment. The patented Sure Chill element transfers heat from the vaccine compartment to a store of ice packs, using the anomalous expansion behaviour of water to maintain a temperature of 2 ~ 8 °C. The element works on the principle that water is most dense at 4°C, thus creating convection currents throughout the Sure Chill element to self-regulate the temperature of the vaccine compartment. Critically, the Sure Chill element prevents the vaccine chamber from getting too cold, as freezing will irreparably damage many vaccines.

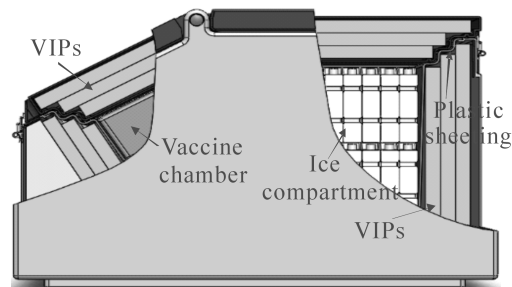


Fig. 1 Construction details of the vaccine storage chamber developed

The ice is loaded into the vaccine chamber at an initial temperature of -25 °C. The 'cold holdover' life of the device is the time it takes for the temperature of the vaccine compartment to rise to 10°C. To simplify the modelling, this point was taken as the point where the volume average ice compartment temperature exceeds 10 °C. The thermo-physical design of the VSD was accomplished employing COMSOL-Multiphysics, which was validated against experimental data collected in controlled lab testing of the vaccine chamber using an environment chamber. A range of VIP types and sizes and different materials for parts of the device were tested

* Corresponding author, Tel : 44-1895-265468, E-mail: Harjit.singh@brunel.ac.uk

in order to identify the best combination to achieve the intended useful cold holdover life. During experiments, the temperature inside the environment chamber was varied according to the day-night temperature cycle prescribed by the World Health Organisation's Performance, Quality and Safety standard (WHO PQS) of 43 °C and 25 °C with a ramp of three hours on either side.

2. Details of the Computer Model and Physical Domain

The performance of the vaccine storage device in maintaining vaccine temperature within the prescribed limits is directly influenced by the complex, multi-mode, transient and simultaneously occurring heat exchanges summarised as follows:

(i) Convective heat transfer between the room air and the outer surfaces (vertical walls and the top) of the vaccine storage device

(ii) Radiative heat transfer between the room and the outer surfaces (vertical walls and the top) of the vaccine storage device

(iii) Conductive and radiative heat transfer between the bottom surface of the vaccine storage device and the room floor

(iv) Heat transfer caused by the warm room air infiltration to the interior of the vaccine storage device.

(v) Heat transfer caused by the warm room air entering the vaccine chamber when the door is opened to remove vaccine vials

(vi) Convective heat transfer as the infiltrating air circulates inside the vaccine storage device through gaps between adjacent VIPs and the storage device surfaces. VIP envelopes are folded on the edges which leave unwanted gaps between them and neighbouring surfaces.

(vii) Conductive heat transfer through the VIPs

(viii) Radiative heat transfer among components of the vaccine chamber such as VIPs and ice compartment.

(ix) Conductive heat transfer through the solid surfaces such as PU foam insulation and the plastic casing (see Fig. 1, Fig. 2)

(x) Sensible and latent heat transfer phenomena in the ice

(xi) Convective heat transfer phenomena taking place inside the Sure Chill element driven by the

anomalous expansion of water



Fig. 2 Assembled Vaccine storage device (VSD)

Further, complexity is added by the geometry (shape and size) of the vaccine storage device, which significantly affects all modes of heat transfer and the infiltration of air and its circulation inside the device. The VSD is expected to be opened several times a day for removal and replacement of vaccine vials. The opening of the lid was assumed to completely replace the inside air with the room air at 43 °C. In reality, the opening of the lid will additionally result in convective loss as the room air will rush into and out of the vaccine chamber when the lid is open. This will create a significant heat gain to the device.

In general, heat transferred between any two arbitrary surfaces and neighbouring fluid can be mathematically calculated as:

$$\text{Convective: } hA(T_a - T_s) \quad (1)$$

$$\text{Conductive: } kA(T_{s1} - T_{s2})/x \quad (2)$$

$$\text{Radiative: } A \frac{\sigma}{1/\epsilon_1 + 1/\epsilon_2 - 1} (T_1^4 - T_2^4) \quad (3)$$

Where

h is the convective heat exchange coefficient between fluid at temperature T_a and a surface at temperature T_s ,

A is the heat transfer area,

k is the thermal conductivity of any material whose surfaces, x distance apart, are held at temperatures T_{s1} and T_{s2} ,

σ is the Stefan Boltzmann's constant,

ϵ_1 and ϵ_2 are the emissivities of the surfaces,

T_1 and T_2 are the temperatures of the surfaces (K).

During operation after charging the device with ice and vaccines, temperatures of the various components of the vaccine storage device are unknown. Predicting these temperatures to analyse the device performance involves solving these equations for each component, which is complicated by the fourth power temperature terms introduced by equation (3). The authors adopted ice temperature as an indicator of device “state of charge” (remaining cold life) and employed COMSOL Multiphysics software to solve these equations to predict the time dependent temperature of various components over the full duration of the storage. A series of CAD models of the VSD were used to simulate the performance under a range of insulation level, geometric and shape features. Because of the complexity of physical shape (Fig. 1) an iterative procedure was employed to avoid the problems associated with Boolean geometry operation due to overlapping features, intersecting features and tiny gaps within the model that caused meshing problems for COMSOL multi-physics analysis.

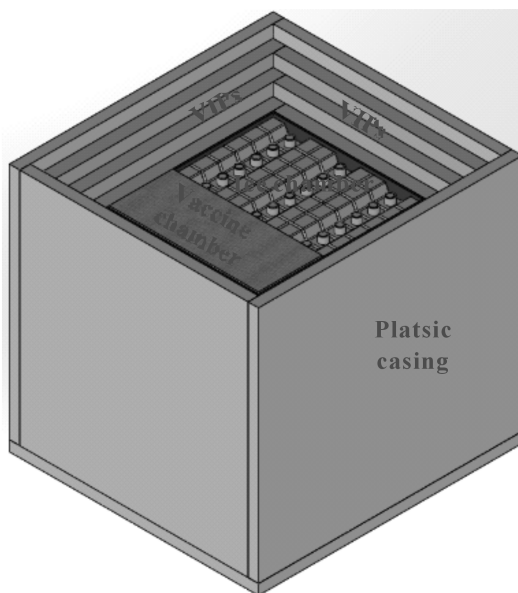


Fig. 3 Cuboid shaped VSD

COMSOL provides a set of direct solvers and iterative solvers. The iterative solver, which despite being a slower solver takes less memory was used. It is

an ideal solver for large projects or distributed computing and is more stable to bad problem set-ups. Solution convergence was achieved within 50 time steps due to the quality of mesh, setup and solver employed. Convergence was affected by the quality of the mesh, the addition of a day/night cycle, temperature discrepancy between the ice and neighbouring VIPs set at ambient and latent heat modelling method.

The analysis began with simulating a simpler cuboid vaccine storage device (see Fig. 3) which had all sides insulated with square cross section VIPs with an outer plastic shell and an inner ice block core. The VIPs were assumed as one VIP panel of thickness equal to the sum of the individual VIPs normal to the direction of heat flow on any assembly section. The aim was to determine the number of days needed for a combination of ice packs to melt and to analyse the factors that could have a long term effect on the performance of the system. The plastic casing had a significantly higher thermal conductivity and as such it was a major source of heat gain from the room environment. The results of the COMSOL model were validated with those obtained from a parallel conducted experiment and an acceptable agreement between the results was obtained. The model was then extended to add extra geometrical features, such as outer shell, separate VIP panels, merged shell, shell extension to outer surface, vaccine chamber and the Sure Chill element. The operational features such as the day-night cyclic temperature variation, heat flux due to opening and the closing of the vaccine chamber lid were added as well. Thin layer ramping of temperature gradient at nodes next to ice were added as well.

The initial condition at the ice block was set at $-25\text{ }^{\circ}\text{C}$ and the adjacent VIP surface $43\text{ }^{\circ}\text{C}$. Even though ice was originally set at $-25\text{ }^{\circ}\text{C}$, it was found in the results the initial temperature was always different. The problem was posed by the hugely different temperatures on the nodes which were at the interface of the ice block and VIP/ambient. This was due to the model not converging with the boundary being at both $-25\text{ }^{\circ}\text{C}$ (initial ice temperature) and $43\text{ }^{\circ}\text{C}$ (VIP initial temperature and ambient day temperature). This issue was resolved using a thin layer feature to gradually “turn on” the surface conductivity. This

improved convergence as well. The phase change process of ice (from ice to water) was simulated using stepped specific heat function. This simulated the phase change from ice to water. The energy required to melt ice at 0 °C at 1 atmospheric pressure is 334 kJ/kg, therefore when simulating the exchange of latent heat to allow melting over 2°C, we created a piecewise rectangular function from -1°C to 1°C set to 1.6×10^5 J/kg to get the values of specific heat shown in Fig. 4.

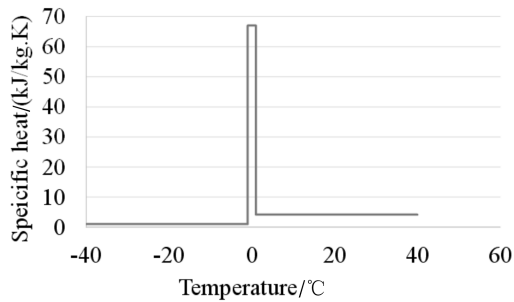


Fig. 4 Specific heat variation adopted time

An alternative was to use the phase change physics available in COMSOL. Here two separate materials with individual properties are defined and selected for phase 1 and phase 2. Three parameters would then be set: the phase change temperature (0°C in the case of ice), the transition temperature interval between phase 1 and phase 2 and the latent heat exchanged to facilitate change from phase 1 to phase 2. In practice, for a complex physical problem like the vaccine chamber being investigated in this project, the COMSOL phase change physics affected the convergence and the accuracy of the results. The more customizable specific heat function described above gave better results as the physical domain became more complex.

A constant heat flux input factor was adopted to account for opening/closing of vaccine chamber lid and heat gain due to manufacturing tolerances, such as imperfect contact between adjacent VIP surfaces and between VIPs and the plastic shell. The heat flux from 0.5 ~ 10W was applied directly on the base of the vaccine chamber. The effect of the heat flux on the time required to melt the ice is shown in Fig 5. As expected, an increase in the heat flux decreased the ice holdover duration of the vaccine chamber. A heat flux input factor of 3 W was adopted as the modelling results

obtained on its use matched with the experimental data. This factor will change as the design features of the vaccine storage device change.

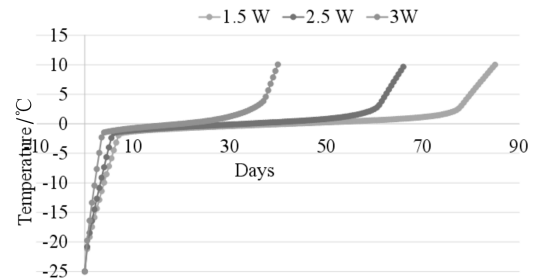


Fig. 5 Effect of heat flux on the ice temperature

3. Boundary Conditions Employed and Results

The following boundary and operating conditions were employed in the computer model:

(i) Room conditions were simulated assuming either a fixed temperature of day (43 °C) and night (25 °C) or by assuming a ramp of three hours in the morning and evening each to allow a smooth transitions of day temperature to night temperature and vice versa. Day and night each was assumed to be 9 hrs long.

(ii) The ice load comprising 54, 0.6 litre ice packs was simplified for the model to a single block of ice of volume 32.8 litres and was assumed to be at -25°C at the start of operation.

(iii) Heat was allowed to be exchanged between room environment and the vaccine chamber sides and top surface through convection and radiation. For the purpose of convection, the air velocity in the room was assumed to be <1m/s.

(iv) Different thicknesses of plastic casing were employed in the model ranging from 1.2 mm to 8mm to see their effect on the ice temperature. This was mainly to identify and evaluate the thermal bridge effect of the plastic casing. During experiments plastic cased field trial models were found to suffer a 60% ~ 70% reduction in holdover life compared to the VIP-only test models. The challenge here is to identify and evaluate the relative (and absolute) effects of simultaneously occurring factors such as thermal bridging due to plastic sheeting (casing), air infiltration and door opening on ice temperature.

The model was run to estimate the effects of VIP

thermal conductivity, manufacturing defects (in terms of air infiltration and circulation of air) and heat exchange with the room environment on the ice temperature. A threshold of 10 °C for the volume average temperature of ice was adopted to indicate the need for recharging the vaccine chamber with fresh supply of ice. This indicated the longest duration for which vaccine can be stored by the vaccine chamber without causing any degradation. The effect of VIP thermal conductivity is shown in Fig. 6 whereby it can be seen that an increase in the thermal conductivity directly reduced the ice holdover time.

To identify and evaluate the thermal bridge effect of the plastic casing a range of thicknesses of plastic sheeting, from 1.2 mm to 8mm, were employed in the model. The model results giving the effect of plastic casing thickness are shown in Fig 7. Clearly a thinner plastic casing would yield a longer holdover period due. Similar results were obtained through experiments as well. Fig. 8 shows the volume-average temperature of ice block during the period of 25 ~ 35 days for varying plastic thickness.

(V) Heat was assumed to be exchanged between the bottom face of the vaccine chamber and the floor through conduction with the floor assumed to be at room condition at any instant.

(vi) The thermal conductivity of the VIP panels was varied from 3 ~ 6 mW/(m · K). It was felt that the conductivity of 6 mW/(m · K) would compensate for the effect of thermal bridging through the envelope material. This value is representative of the overall thermal conductivity of commonly available commercial VIPs. The effect of the varying VIP thermal conductivity on ice temperature is shown in Fig. 6.

A continuous heat flux input factor (thermal gain) was employed to simulate the manufacturing and operational factors (e. g. air gaps, door opening) that add to the heat transfer from the ambient to inside of the ice chamber. The challenge here is to get one unique value for the thermal gain to represent one specific set of geometric, boundary and working conditions of the vaccine chamber. For example, a lower value of thermal gain factor will mean conductive paths other than VIPs (such as plastic casing or PU foam parts) will have a

greater impact.

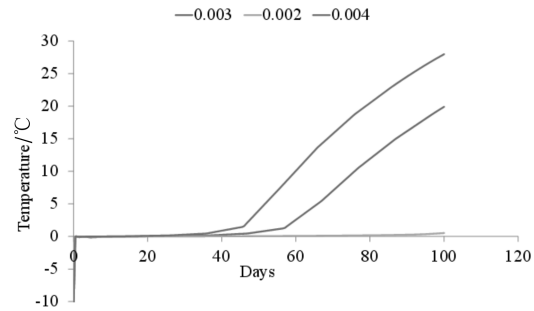


Fig. 6 Effect of VIP thermal conductivity (W/(m · K)) on ice temperature

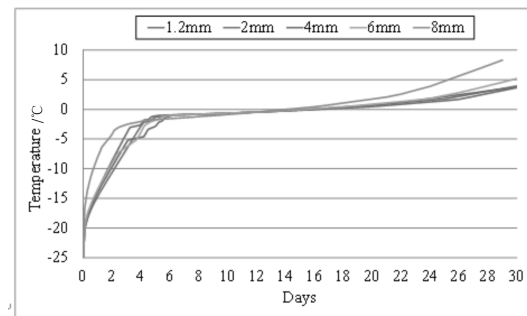


Fig. 7 Ice temperature with the thickness of the plastic casing

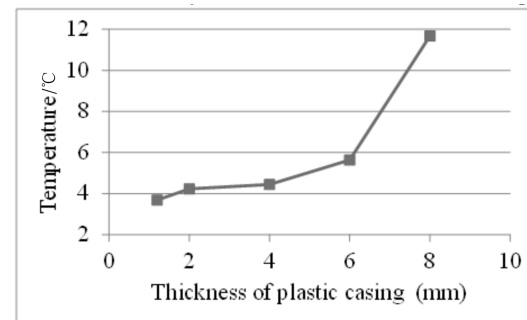


Fig. 8 Average ice temperature during the period of 25 ~ 35 days for varying plastic casing thickness

4. Conclusions

A COMSOL-Multiphysics model has been developed to simulate the performance of a vaccine storage device in holding temperature of 4 to 8 °C in the vaccine storage compartment. The performance has been simulated in a range of scenarios including variation of VIP thermal conductivity, ambient conditions and manufacturing details such as plastic shell thickness. The model was validated against the experimental data

collected. We plan to publish the experimental results along with more details of the computer model developed in a technical paper which is being submitted to a high impact scientific journal. It has been found that with the proposed VIP and geometric configuration the vaccine can be stored in the chamber for up to 30 days without causing any degradation. To extend the cold holdover life, it is strongly felt that the plastic casing will require reducing in thickness to minimise heat flux from the surroundings. Prototypes are under test to demonstrate practical ways of achieving this. Further, avoidable heat flux is presumed to occur along the VIP edges where spare envelope material is folded preventing full surface to surface contact between adjacent VIPs. The gap between any two adjacent VIPs has been found to be a path for circulation of air inside the vaccine storage device.

Acknowledgements

The authors would like to thank the Bill and

Melinda Gate Foundation for funding for developing the vaccine storage chamber.

References

- [1] IEA, International Energy Agency, 2014, World Energy Outlook 2014, Available from www.worldenergyoutlook.org; accessed 01/07/2015.
- [2] H Singh, M Geisler, F Menzel, 2015, Experimental investigations into thermal transport phenomena in vacuum insulation panels (VIPs) using fumed silica cores, Energy and Buildings, Under Review (manuscript number ENB-D-15-00704R1).
- [3] M. Alam, H. Singh, 2014, Experimental characterisation and evaluation of the thermo-physical properties of expanded perlite—Fumed silica composite for effective vacuum insulation panel (VIP) core, Energy and Buildings 69, 442 – 450.
- [4] M. Alam, H. Singh, M. C. Limbachiya, 2011, Vacuum Insulation Panels (VIPs) for building construction industry - A review of the contemporary developments and future directions, Applied Energy 88 (11), 3592 – 3602.